REPUBLIQUE DU CAMEROUN

****

Paix-Travail-Patrie

****

REPUBLIC OF CAMEROON

****

Peace-Work-Fatherland

****

UNIVERSITÀ
DEGLI STUDI
DI PADOVA

****

DEPARTMENT OF CIVIL ENGINEERING

DEPARTEMENT DE GENIE CIVIL

****

****

DEPARTMENT OF CIVIL, ARCHITECTURAL AND ENVIRONMENTAL ENGINEERING

****

FOUNDATION DESIGN FOR A COMMERCIAL BUILDING IN VICENZA (ITALY)

A thesis submitted in partial fulfilment of the requirements for the degree of Master of Engineering (Meng) in Civil Engineering

Curriculum: Geotechnical Engineering

Presented by

BASSOM BITA CHRISTIAN T.

Student number: **16TP21123**

Supervised by

Prof. Simonetta COLA

Co-Supervised by

Dr. Lorenzo BREZZI

Defended on October 3, 2022 in front of the jury composed of:

President: **Prof. NKENG George Elambo**

Examiner: **Dr. WOUNBA Jean François**

Reporter: **Prof. Simonetta COLA**

Academic year: 2020/2021

DEDICATION

I dedicate this thesis

To my family

Who offered unconditional love, invaluable educational facilities, guidance and support

Throughout this journey.

Thank you so much.

AKNOWNLEDGEMENT

I wish to thank:

- The **President of the jury Prof. NKENG GEORGES ELAMBO** for the honour he gave me in being the president of the jury in my thesis presentation;

- The **Examiner** of this jury **Dr. WOUNBA JEAN FRANÇOIS** for accepting to bring his criticisms and observations to ameliorate this work;

- My supervisors **Prof. Simonetta COLA** and **Dr. Eng. Lorenzo BREZZI** who took patience and know-how to accompany me for important orientation, leading to a right achievement of my thesis.

- The Director of the National Advanced School of Public Works **Prof. NKENG GEORGES ELAMBO** for all his academic and administrative support towards our formation during these five years, and during elaboration of this thesis.

- **Prof. Eng. Carmelo MAJORANA and ESOH ELAME**, who are the principal initiators of the new Engineering curricula at the NASPW.

- **Prof. MBESSA Michel**, the head of department of Civil Engineering for his tutoring and valuable advices.

- **All the teaching staff** of NASPW and University of Padova for their good quality teaching and their motivation but also **the administrative staff** of NASPW.

- To my dear family and especially my parents for their advices which led me through here.

- Finally, I wish to thank all my dear classmates who constituted a friendly and joyful motivation during these years. I really enjoyed our collaboration and hope it will continue in the future.

LIST OF ABBREVIATIONS

$(N_1)_{60}$	Normalized value of N_{SPT}
Ø	Friction angle
a_{max}	Maximum horizontal acceleration
B	Width of footing
B’	Effective footing width
c	Cohesion
c’	Effective cohesion
C_A	Limiting settlement
CFA	Continuous Fligth Auger
C_N	Correction coefficient dependent on the effective pressure
CPT	Mechanical tip static Cone Penetrometer Test
CRR	Cyclic Resistance Ratio
CSR	Cyclic Stress Ratio
c_u	Undrained cohesion
d	Pile diameter
DA1	Design Approach 1
DA1a	Design Approach 1a
DA1b	Design Approach 1b
DA2	Design Approach 2
DA3	Design Approach 3
e	Eccentricity
E	Young's modulus

E_A	Action effect
EC7	Eurocode 7
E_d	Oedometric modulus
ER	Average efficiency of the driving device
E_u	Undrained modulus
FDP	Full Displacement Pile
H	Depth substrate
h_i	Thickness of i-th layer
I_s	Influence factor
L	Length of footing
LRFD	Load and Resistance Factor Design
m	Intercept on the vertical axis
MASW	Multi-channel Analysis of Surface Waves
M_w	Reference magnitude
n	Inclination over the horizontal
N	Number of influence areas
N_c	Bearing capacity factor
N_q	Bearing capacity factor
N_{SPT}	Resistance to the penetration
NTC18	Italian norm
N_γ	Bearing capacity factor
Q	Action load
q	Uniform pressure
Q_b	Base bearing capacity

q_b	Ultimate tip resistance
$q_{c,p}$	Average value of the cpt tip resistance
q_c	Tip resistance
q_f	Ultimate bearing capacity
Q_{lim}	Limit load
$q_{s,p}$	Average value of the cpt shaft resistance
q_s	Limit unit shaft resistance
Q_s	Shaft bearing capacity
R	Resistance factor
$R_{c,k}$	Characteristic value of the bearing capacity for pile in compression
$R_{c,m}$	Correspondent value of the bearing capacity for pile in compression
R_d	Ground resistance
$R_{l\,tot}$	Overall resistance of the tip and sleeve
R_l	Resistance to the advancement of the sleeve
R_p	Resistance to advancement of the tip
$R_{t,k}$	Characteristic value of the bearing capacity for pile in tension
$R_{t,m}$	Correspondent value of the bearing capacity for pile in tension
S.C.P.T.	Seismic Cone Penetration Test
S.P.T	Standard Penetration Test
s_c	Shape factor
s_i	Vertical displacement
SLD	Damage Limit State
SLO	Operatively Limit State
SLS	Serviceability Limit State

SLV	Life-Saving Limit State
s_q	Shape factor
s_γ	Shape factor
ULS	Ultimate Limit State
V_N	Nominal life of the structure
V_R	Reference period for the seismic action
$V_{s,30}$	Equivalent speed of shear waves at depth H = 30 m
$V_{s,eq}$	Equivalent speed of propagation of surface waves
$V_{s,i}$	Speed of the shear waves of the i-th layer
V_s	Shear waves speed
w	Settlement of pile
X	Material properties
z	Depth
α	Penetration resistance
γ	Unit weigth of soil
γ_1	Average volume weight above the laying surface
γ_2	Average volume weight below the laying surface
γ_A	Partial factor applied to actions
γ_n	Natural unit weigth
γ_R	Partial factor applied to resistance
γ_x	Partial factor applied to material properties
λ	Energy loss for the length of the rods
μ_0	Parameter function on D/B
μ_1	Parameter function on H/B and L/B

ξ_i	Parameter function on the number of load tests
ξ_j	Parameter function on the number of load tests
σ'_v	Effective vertical stress
σ'_{v0}	Effective pressure at the test execution heigth
σ_z	Total vertical stress
Φ’	Effective friction angle

ABSTRACT

The purpose of this study was to evaluate the bearing capacity of a pile foundation after its construction based on the resistance to penetration of the drilling tool through the ground. This study was carried out on three full displacement piles of a commercial building in the municipality of Lonigo located in the region of Vicenza in Italy. To achieve this objective, we started with a review of the literature on foundations and then we determined the characteristics of our land using the data provided by the company GEOLAMBDA Engineering. The bearing capacity of our foundation was first evaluated using the analytical formulation and the results of the in-situ tests carried out by GEOLAMBDA Engineering. We obtained a value of 1033.97 KN then the bearing capacity of our foundation was also evaluate using the results of the load tests carried out on three test piles by the company RGM PROVE. We obtained a value of 1224.49 kN, since the two values of the bearing capacity were not far apart we were confident in our design. We completed our design by evaluating the resistances to drill bit penetration for the three test piles and compared them with the stratigraphy given by the cone penetrometer tests, the corer penetrometer tests and the continuous coring. We observed some similarities in terms of identification of different layers between the stratigraphy given by the penetration resistances and those given by the cone penetrometer tests, which was not the case with the stratigraphy of the standard penetrometer tests and continuous coring. In order to have precise and reliable data of the resistance to the penetration of the drilling tool by the ground, we suggested, for the future, to consider during the calculation the speed of rotation of the drilling tool, the pushing force of the drilling tool and the depth of penetration of the drilling tool.

Key words: full displacement pile, penetration resistance, cone penetrometer test, standard penetrometer test, load test.

RESUMÉ

Le but de cette étude était d'évaluer la capacité portante d'une fondation sur pieux après sa réalisation en se basant sur la résistance à la pénétration de l'outil de forage par le sol. Cette étude a été réalisée sur trois pieux à déplacement latéral total d'un bâtiment à usage commerciale dans la municipalité de Lonigo située dans la région de Vicence en Italie. Pour atteindre cet objectif, nous avons commencé par une revue de la littérature sur les fondations puis nous avons déterminer les caractéristiques de notre terrain grâce au données fournit par l'entreprise GEOLAMBDA Engineering. La capacité portante de notre fondation a d'abord été évaluer en utilisant la formulation analytique et les résultats des essais in-situ effectués par GEOLAMBDA Engineering. Nous avons obtenu une valeur de 1033,97 KN puis la capacité portante de notre fondation a été aussi évaluer en utilisant les résultats des essais de charge menés sur trois pieux tests par la société RGM PROVE. Nous avons obtenu une valeur de 1224,49 kN, puisque les deux valeurs de la capacité portante n'étaient pas éloignées nous étions confiants dans notre conception. Nous avons terminé notre conception en évaluant les résistances à la pénétration de l'outil de forage pour les trois pieux tests et nous les avons comparées avec les stratigraphies données par les essais au pénétromètre à cône, les essais au pénétromètre au carottier et les carottages continus. Nous avons observé quelques similitudes en termes d'identification de différentes couches entre les stratigraphies données par les résistances à la pénétration et celles données par les essais au pénétromètre à cône ce qui n'était pas le cas avec les stratigraphies des essais au pénétromètre au carottier et des carottages continus. Afin d'avoir des données précises et fiables de la résistance à la pénétration de l'outil de forage par le sol, nous avons suggéré, pour le futur, de considérer lors du calcul la vitesse de rotation de l'outil de forage, la force de poussée de l'outil de forage et la profondeur de pénétration de l'outil de forage.

Mots clés : pieu à déplacement latéral total, résistance à la pénétration, essai au pénétromètre à cône, essai au pénétromètre au carottier, essai de charge.

LIST OF FIGURES

LIST OF TABLES

TABLE OF CONTENT

GENERAL INTRODUCTION

Structures such as buildings, bridges and dams generally take their stability from their foundations. Therefore, a well design foundation plays an important role in the ability of a structure to resist external loads due for example to wind, snow or even seismic actions.

Before the dimensioning phase of the work, a geological survey is carried out in order to determine the structural characteristics of the soil at different depths. This is necessary to determine its bearing capacity to the different substrates, and therefore to understand at what depth it is necessary to go down to be sure that the foundation structure has the desired capacity. In most cases, however, this geological survey is incomplete for several reasons, the vastness of the area in which to carry out the work and the limited number of surveys do not provide reliable data on the entire plot of land, the investigations stop at modest depths, and the characteristics of the rest of the substrates are often estimated. This leads the designers to use, at the time of the calculation, important safety factors and therefore to oversize the foundation structures in an important way, resulting in increase in the total cost of the work, increase of the environmental impact of the work, increase in the material used and the resources used, lengthening of production times.

In accord to this, the choice of the thesis subject is selected on foundation design for a commercial building in Vicenza (Italy). Several researches have been carried out to analyze the design methods of foundations using analytical formulations, empirical formulations (CPT and SPT) and load test. In this analysis, a design method using information on the pile installation parameters will be set up by, taking soil parameters of a site in the municipality of Lonigo in Vicenza (Italy), using the drilling data retrieve by a software installed in the drilling machine.

Three main chapters composed this thesis; the first chapter is a literature review on foundations. The second chapter presents the methodology used to design our foundation structure and the last chapter focuses on the presentation and interpretation of the results obtained.

CHAPTER 1: LITTERATURE REVIEW

Introduction

This chapter will consist in first presenting shallow foundations and their design according to Eurocode 7 then we will continue with deep foundations and some methods of evaluation of their bearing capacities finally a complete design procedure of a foundation will be set up.

1.1 Shallow foundations

Shallow foundations transfer structural loads to relatively small depths into the ground. They range from isolated foundations, each carrying its own column load, to elements carrying several columns, walls or even all the loads for a given structure or building. Shallow foundations are easy to build, requiring little to no specialized equipment (Salgado, 2006). Depending on the situation, a particular type of shallow foundation is chosen then the stresses and the displacement due to that type of foundation have to be known. After having evaluated the bearing capacity, we have to make sure that the limit states are respected.

1.1.1 Types of shallow foundations

The main types of shallow foundations are summarized in Table 1.1. For very lightly loaded foundations, unreinforced concrete or masonry footings are possible; however, shallow foundations are most of the time built of reinforced concrete. When a foundation element supports a single column load, it is referred to as an isolated footing. When it supports two columns, it is called a combined footing. When supporting a line of columns or a load-bearing wall, it is called a strip footing. If it supports a large number of columns that are not aligned, it is referred to as a mat or raft. When two isolated footings are connected by a beam, so they work as a unit, the term strap footing is used to refer to them (Salgado 2006)

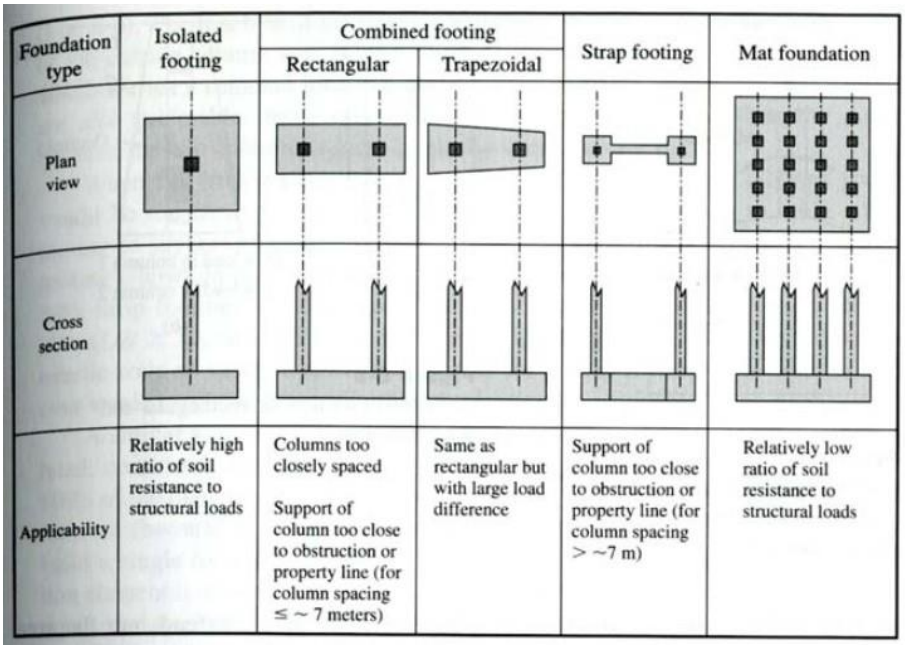

Foundation type	Isolated footing	Combined footing: Rectangular	Combined footing: Trapezoidal	Strap footing	Mat foundation
Plan view					
Cross section					
Applicability	Relatively high ratio of soil resistance to structural loads	Columns too closely spaced Support of column too close to obstruction or property line (for column spacing ≤ ~ 7 meters)	Same as rectangular but with large load difference	Support of column too close to obstruction or property line (for column spacing > ~7 m)	Relatively low ratio of soil resistance to structural loads

Table 1.1. Summary of types of shallow foundations (Salgado, 2006)

1.1.2 Stresses and displacement of a shallow foundation

This part will talk about the evaluation of the vertical stress and the settlement from the elastic theory.

1.1.2.1 Stresses from elastic theory

Newmark constructed an influence chart, based on the Boussinesq solution, enabling the vertical stress to be determined at any point below an area of any shape carrying a uniform pressure q. the chart, shown in Figure 1.1, consists of influence areas, the boundaries of which are two radial lines and two circular arcs. The loaded area is drawn on tracing paper to a scale such that the length of the scale line on the chart represents the depth z at which the vertical stresses is required. The position of the loaded area on the chart is such that the point at which the vertical stresses is required is at the centre of the chart. For the chart shown in Figure 1.2 the influence value is 0.005, i.e. each influence area represents a vertical stress of 0.005q. Hence, if the number of influence areas covered by the scale drawing of the loaded area is N, the required vertical stress is given by the Equation 1.1 (Craig, 2004)

$$\sigma_z = 0.005Nq \qquad (1.1)$$

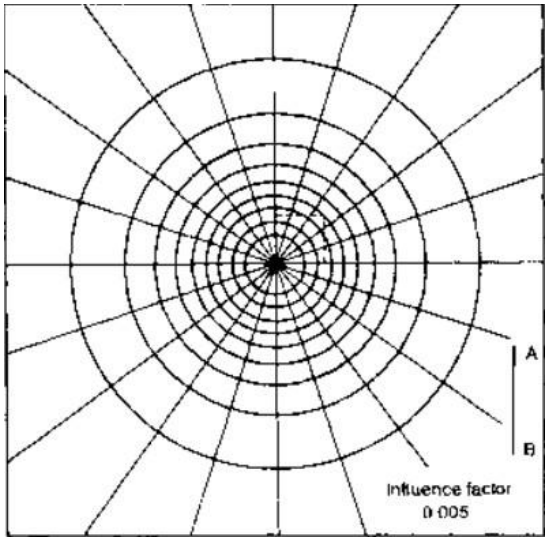

Figure 1.1. Newmark's influence chart for vertical stress under a foundation (www.euroguide.org/soil-mechanics/influence-charts-for-vertical-stress-increments.html, 2021)

1.1.2.2 Displacement from elastic theory

The vertical displacement (s_i) under an area carrying a uniform pressure q on the surface of a semi-infinite, homogeneous, isotropic mass, with a linear stress-strain relationship, can be expressed as

$$s_i = \frac{qB}{E}(1 - \nu^2)I_s \qquad (1.2)$$

Where I_s is an influence factor depending on the shape of the loaded area, In the case of a rectangular area, B is the lesser dimension (the greater dimension being L) and in the case of a circular area, B is the diameter. The loaded area is assumed to be flexible and the values of the influence factors are given in Table 1.2 for displacements under the centre, the corner (the edge in the case of a circle) of the area and for the average displacement under the area as a whole.

Table 1.2. Influence factors for vertical displacement under flexible area carrying uniform pressure (Craig, 2004)

Shape of area	I_s		
	Centre	*Corner*	*Average*
Square	1.12	0.56	0.95
Rectangle, $L/B = 2$	1.52	0.76	1.30
Rectangle, $L/B = 5$	2.10	1.05	1.83
Circle	1.00	0.64	0.85

In most cases in practice, the soil deposit will be of limited thickness and will be underlain by a hard stratum. Christian and Carrier proposed the use of results made by Giroud and Burland in such cases. Equation 1.3 gives the average vertical displacement under a flexible area carrying a uniform pressure$q$.

$$s_i = \mu_0 \mu_1 \frac{qB}{E} \tag{1.3}$$

Where μ_0 depends on the depth of embedment and μ_1 depends on the layer thickness and the shape of the loaded area. Values of μ_0 and μ_1 for Poisson's ratio equal to 0.5 are given in Figure 1.2. The principle of superposition can be used in cases of a number of soil layers each having a different value of E (Craig, 2004).

The above solutions for vertical displacement are used mainly to estimate the immediate settlement of foundations on saturated clays; such settlement occurs under the undrained conditions, the appropriate value of Poisson's ratio being 0.5. The value of the undrained modulus E_u is therefore required and the main difficulty in predicting immediate settlement is in the determination of this parameter. For particular clays, correlations can be established between E_u and the undrained shear strength parameter c_u (Craig, 2004).

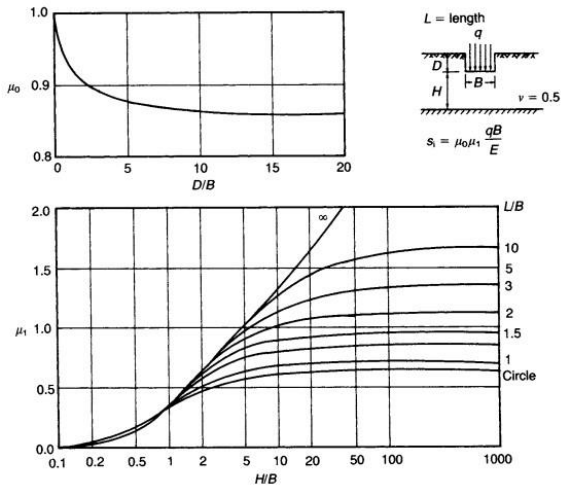

Figure 1.2. Coefficients for vertical displacement (Craig, 2004)

1.1.3 Bearing capacity of shallow foundations

The ultimate bearing capacity (q_f) is defined as the pressure which would cause shear failure of the supporting soil immediately below and adjacent to a foundation (Craig, 2004)).

Equation 1.4 can express the ultimate bearing capacity of a soil, in drained condition, under a shallow strip footing.

$$q_f = cN_c + \gamma D N_q + \frac{1}{2}\gamma B N_\gamma \tag{1.4.}$$

Where N_c, N_q, N_γ are bearing capacity factors depending only on the value of the shear strength parameter ∅. The first term in Equation 1.4. is the contribution to the bearing capacity due to the shear strength component represented by parameter c, the second term is the contribution due to the surcharge pressure and the third term is due to the weight of the soil below foundation level. The superposition of components of bearing capacity is theoretically incorrect for a plastic material but the resulting error is considered to be on the safe side (Craig, 2004).

The values of N_q and N_c is calculated as shown in Equation 1.5 and 1.6 i.e.

$$N_q = \exp(\pi \tan \emptyset) \tan^2(45° + \frac{\emptyset}{2}) \quad (1.5.)$$

$$N_c = (N_q - 1) \cot \emptyset \quad (1.6.)$$

Hansen and Meyerhof has obtained values for Nγ represented by the Equation 1.7 and 1.8:

$$N_\gamma = 1.8(N_q - 1) \tan \emptyset \quad \text{(Hansen)} \quad (1.7.)$$

$$N_\gamma = (N_q - 1) \tan(1.4\emptyset) \quad \text{(Meyerhof)} \quad (1.8.)$$

In Eurocode 7 the Equation 1.9 is proposed for Nγ

$$N_\gamma = 2.0(N_q - 1) \tan(\emptyset) \quad (1.9.)$$

The problem involved in extending the two-dimensional solution for a strip footing to three dimensions would be considerable. Accordingly, the bearing capacities of square, rectangular and circular footings are determined by means of semi-empirical shape factors applied to the solution for a strip footing. The bearing capacity factors N_c, N_q and N_γ should be multiplied by the respective shape factors, s_c, s_q, and s_γ. Various proposals for shape factors have been published. The following simplified values are sufficiently accurate for most cases in practice: $s_c = s_q = 1.2$ for both square and circular footings; $s_\gamma = 0.8$ for a square footing or 0.6 for a circular footing (i.e. the third term Equation 1.4 becomes $0.4\gamma B N_\gamma$ or $0.3\gamma B N_\gamma$, respectively). For a rectangular footing of breadth B and length L, the shape factors are obtained by linear interpolation between the values for a strip footing ($B/L = 0$) and a square footing ($B/L = 1$) (as we can see in Equation 1.10 and Equation 1.11).

$$s_c = s_q = 1 + 0.2\, B/L \quad (1.10)$$

$$s_\gamma = 1 - 0.2\, B/L \quad (1.11).$$

Hansen and DeBeer have given more detailed proposals for shape factors, as functions of ∅. Detailed expressions are also given in Eurocode 7 (Craig, 2004).

According to Craig (2004), the bearing capacity equation can be written in a general form, as show in equation 1.12, by including the shape and inclination factors, due to the inclination of the load, (plus depth factors if appropriate). thus

$$q_f = cN_c s_c i_c + \gamma D N_q s_q i_q + \frac{1}{2}\gamma B N_\gamma s_\gamma i_\gamma \qquad (1.12)$$

Footings may be subjected to eccentric and inclined loading resulting in a reduction in bearing capacity. If e is the eccentricity of the resultant load on the base of a footing of width B, an effective foundation width B' should be computed from equation 1.13.

$$B' = B - 2e \qquad (1.13)$$

The resultant load is assumed to be uniformly distributed over the effective width B'. if the resultant load is also eccentric in the length direction of a rectangular footing, a similar expression is used for the effective length L'.

In a review of bearing capacity theory, Skempton concluded that in the case of saturated clays under undrained conditions ($\emptyset_u = 0$) equation 1.14 could be used to express the ultimate bearing capacity of a footing.

$$q_f = c_u N_c + \gamma D \qquad (1.14)$$

The factor N_c being a function of the shape of the footing and the depth/breadth ratio. Skempton's values of N_c are given in Figure 1.3.

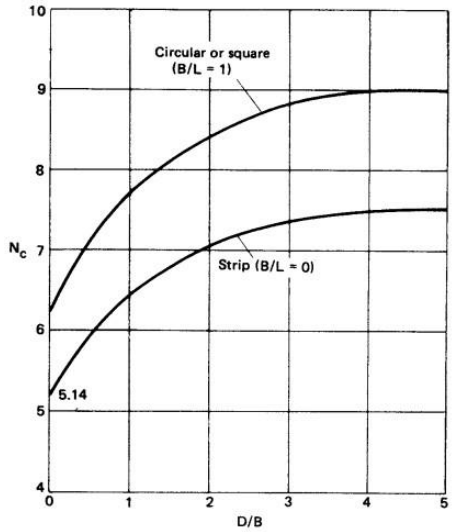

Figure 1.3. Skempton's values of N_c for $\emptyset_u = 0$ (reproduce from A.W. Skempton (1957))

1.1.4 Limit state design based on Eurocode 7

According to Salgado (2006), << A limit states is a set of conditions or outcomes that must not be reached>>. A geotechnical engineer must ensure that a foundation satisfies the following two stability conditions:

- Ultimate Limit State (ULS): the foundation must not collapse or become unstable under any conceivable loading.
- Serviceability Limit State (SLS): settlement of the structure must be within tolerable limits.

Both requirements must be satisfied. Often, it is the settlement that governs the design of a shallow foundation.

1.1.4.1 Design at ultimate limit stress

According to S. Cola (lesson 6, 2021), at ultimate limit state, the sum of the applied actions (loads) on the structure must be less than or equal to the available resistance of the system.

For instance, the resistance (R) of a shallow foundation is the bearing capacity of the soil below the footing. It is a function of various mechanical and physical properties of the foundation soil (unit weight γ, material strength c_u for undrained conditions; $\emptyset'$ and c' for drained conditions).

Equation 1.15 may express defining the actions by Q and the material properties by X, the criterion that must be satisfied in design:

$$\sum Q \leq R(X) \tag{1.15}$$

In order to consider, the uncertainties associated with the determination of parameters involved in the design, partial (safety) factors are used to modify the three terms to give the design as expressed in Equation 1.16.

$$\sum \gamma_A Q \leq \frac{R\left(\frac{X}{\gamma_X}\right)}{\gamma_R} \tag{1.16}$$

Where:

- γ_A, γ_X and γ_R are partial factors applied respectively to the actions Q, the material properties X and the resistance R. Each of these factors are greater than one (γ_A, γ_X, γ_R >1).

- Q, R, and X represent the best estimations of actions, material properties and resistances (known as characteristic values).

A characteristic value that has been modified by a partial factor is known as design value.

The three sets of partial factors are not necessarily all applied at the same time. It depends on the limit state design code being followed (as presented in Table 1.3, Table 1.4 and Table 1.5).

In Eurocode 7, three (four possible) design approaches are proposed.

- Design Approach 1 (DA1) made of
  - DA1a, factoring actions only
  - DA1b, factoring materials only
- Design Approach 2 (DA2)

  Factoring actions and overall resistance (not materials). It is similar to LRFD method of US standards.
- Design Approach 3 (DA3)

  Factoring structural actions and materials (no geotechnical actions).

Table 1.3. Partial action factors (Cola, Lesson on Euro code 2021)

	Partial factors to be taken from set…		
	Actions (γ_A)	*Resistances (γ_R)*	*Material properties (γ_M)*
Design Approach 1a	A1	R1	M1
Design Approach 1b	A2	R1 (R4 for piles)	M2 (M1 for piles)
Design Approach 2	A1	R2	M1
Design Approach 3	A2	R3	M2

Action (Q)	*Symbol*	*Set*	
		A1	*A2*
Permanent unfavourable action	γ_A	1.35	1.00
Variable unfavourable action		1.50	1.30
Permanent favourable action		1.00	1.00
Variable favourable action		0	0
Accidental action		1.00	1.00

***NOTE:** in DA3 the partial factors are A1 for structural actions and A2 for geotechnical actions.

Table 1.4. Partial material factors (Cola, lesson on Eurocode, 2021)

	Partial factors to be taken from set…		
	Actions (γ_A)	*Resistances (γ_R)*	*Material properties (γ_X)*
Design Approach 1a	A1	R1	M1
Design Approach 1b	A2	R1 (R4 for piles)	M2 (M1 for piles)
Design Approach 2	A1	R2	M1
Design Approach 3	A2	R3	M2

Material property (X)	*Symbol*	*Set*	
		M1	*M2*
tan ϕ'	$\gamma_{\tan\phi}$	*1.00*	*1.25*
Cohesion intercept, c'	γ_c	1.00	1.25
Undrained shear strength, c_u	γ_{cu}	1.00	1.40
Unit weight*, γ	γ_γ	1.00	1.00

Table 1.5. Partial resistance factors for shallow foundation (Cola, lesson on Eurocode, 2021)

Resistance	Symbol	Set		
		R1	*R2*	*R3*
Bearing	$\gamma_{R;v}$	1,0	1,4	1,0
Sliding	$\gamma_{R;h}$	1,0	1,1	1,0

1.1.4.2 Design at serviceability limit state

To satisfy the serviceability limit state (SLS), the effect of the applied actions, E_A (also called an action effect) must be less than or equal to a limiting value of the action effect, C_A (i.e. a limiting settlement).This may be expressed by equation 1.17.

$$E_A < C_A \tag{1.17}$$

For the evaluation of E_A the characteristic values are used without considering partial factors, as this limit state does not relate to the safety of the foundation, but to maintain its performance under working load. The limiting value C_A shall be chosen in relation to the behaviour of the over structure and all other structure interacting with the geotechnical work and in relation with the load duration. In seismic analysis SLE are the Operatively Limit State (SLO) and the Damage Limit State (SLD) (Cola, lesson on Eurocode, 2021).

Considering the Serviceability Limit States of shallow foundation means according to Cola (lesson 6, 2021) limiting the settlements:

- For normal structure with isolated foundations, total (gross) settlements up to 50 mm are often acceptable, though in sands this may be reduced to 25 mm.

- Larger settlements may be acceptable. It should be proved that the total settlements do not cause problems with the services entering the structure, or cause tilting, etc.

1.2 Deep foundations

When the term deep foundation is used, it invariably means pile foundation. << A pile is a slender, structural member installed in the ground to transfer the structural loads to soils at some significant depth below the base of the structure>> (Muni Budhu, 2010, P.368). Pile foundation are use when it is not possible to use shallow foundation and so the type of pile that is chosen have to be satisfactory and the bearing capacity able to support the design load.

1.2.1 Types of deep foundation

Foundation piles can be classified following different criteria: the size, the material used and the installation technique.

1.2.1.1 Classification based on the size.

Referring to their size, pile can be subdivided into small (diameter $d \leq 250$ mm), medium (300 mm$\leq d \leq$600 mm) and large diameter ($d \leq 800$ mm) (Viggiani & al., 2012).

1.2.1.2 Classification based on material

The selection of the type of pile required for a project depends on what type is readily available, the magnitude of the loading, the soil type, and the environment in which the pile will be installed, for example, a corrosive environment or a marine environment. So, we can distinguish:

a. Concrete piles

There are several types of concrete piles that are commonly used. These include cast-in-place concrete piles, precast concrete piles, and drilled shafts. Cast-in-place concrete piles are formed by driving a cylindrical steel shell into the ground to the desired depth and then filling the cavity of the shell with fluid concrete. The steel shell is for construction convenience and does not contribute to the load transfer capacity of the pile. Its purpose is to open a hole in the ground and keep it open to facilitate the construction of the concrete pile. Plain concrete is used when the structural load is only compressive. If moments and lateral loads are to be transferred, then a steel reinforcement cage is used in the upper part of the pile. Vigilant quality control and

good construction practice are necessary to ensure the integrity of cast-in-place piles (Budhu, 2012). Figure 1.4 presents some concrete piles.

Precast concrete piles usually have square or circular or octagonal cross sections and are fabricated in a construction yard from reinforced or prestressed concrete. They are preferred when the pile length is known in advance. The disadvantages of precast piles are problems in transporting long piles, cutting, and lengthening. A very popular type of precast concrete pile is the Raymond cylindrical prestressed pile. This pile comes in sections, and lengths up to 70 m can be obtained by stacking the sections. Typical design loads are greater than 2 MN (Budhu, 2012).

Figure 1.4. Concrete piles (www.nationalpilecroppers.com ,2021)

b. Steel piles

Steel piles come in various shapes and sizes and include cylindrical, tapered, and H-piles. Steel H-piles are rolled steel sections. Steel pipe piles are seamless pipes that can be welded to yield lengths up to 70 m. they are usually driven with open ends into the soil. A conical tip is used where the piles have to penetrate boulders and rocks. To increase the load capacity of steel pipe piles, the soil plug is excavated and replaced by concrete. These piles are called concrete-filled steel piles. Figure 1.5 presents H-Steel piles.

Figure 1.5. H-Steel piles (foundation blogspot.com, 24 April 2014)

c. Timber piles

Timber piles have been used since ancient times. The lengths of timber piles depend on the types of trees used to harvest the piles, but common lengths are about 12 m. longer lengths can be obtained by splicing several piles. Timber piles are susceptible to termites, marine organisms, and rot within zones exposed to seasonal changes. Figure 1.6 presents some timber piles

Figure 1.6. Timber piles (JICA, 2019)

1.2.1.3 Classification based on the installation technique

The installation technique, however, is by far the most important differentiating factor among piles. The fundamental difference in installation techniques is that between displacement (or driven, pushed or screwed) piles and replacement (bored or drilled) piles. In the former, there is no removal of soil the pile is driven in the ground using a driving equipment, while in the latter a hole is previously bored, and the removed soil is replaced by concrete.

a. Displacement piles

The methods for installing displacement piles are jacking, vibration and driving. Jacking and vibratory installation is comparatively rare. Among displacement pile we distinguish:

i. Franki piles (Pressure-injected Footings)

Franki piles are cast-in-place concrete piles that may or may not be reinforced. They are installed with the aid of a steel casing. The casing is positioned vertically, a plug of dry concrete is introduced near the lower end of the casing, and a drop hammer is used to pound on the concrete. Because the concrete is quite dry, its friction with the steel casing is sufficient for the blows to drag the casing down into the ground. This continues until the desired depth is reached. If necessary, more dry concrete is placed along the way, so that there is sufficient concrete within the casing at all times. When the desired depth is reached, concrete with a much wetter mix is introduced and the casing is pulled up as the concrete is driven out of the casing by the hammer blows. As the casing is pulled up, the level of concrete within the casing must be kept above the lower end of the casing at all times to guarantee a continuous pile. The process is illustrated in Figure 1.7

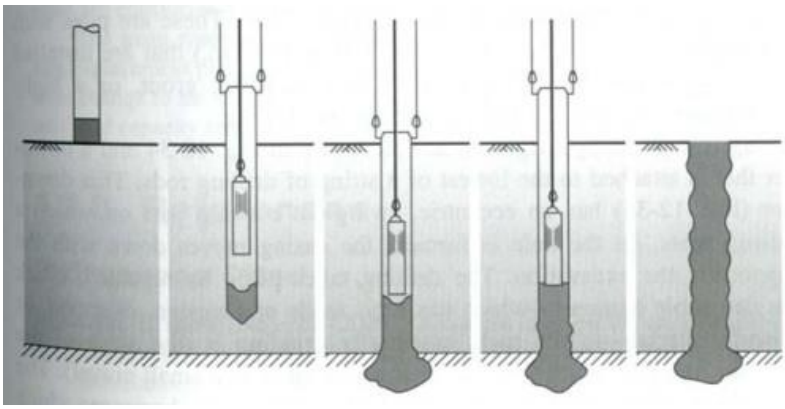

Figure 1.7. Installation sequence of a Franki pile (Salgado, 2006)

ii. Raymond piles

Raymond piles (Figure 1.8) are cast-in-place concrete piles installed by the driving of a thin, corrugated, usually tapered shell into the ground with a closed end, followed by concrete placement. These piles were common in the past, but they are less used today, given the many new types of piles that have been developed. The shells are available in lengths up to 12 m or so (Salgado, 2006).

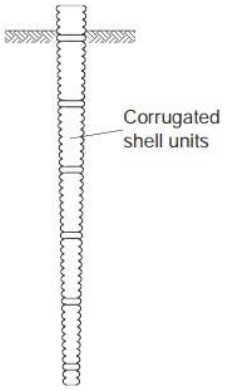

Figure 1.8. Raymond piles (Viggiani & al., 2012)

b. Replacement piles

Among replacement piles, we distinguish

i. Continuous flight auger piles (CFA piles)

They are installed by inserting into the soil a continuous flight auger by the combined action of a torque and an axial thrust (Figure 1.9.). The auger has a hollow stem with an inner diameter of 60 to 100 mm provide with seal at the lower end. Once the desired depth is attained, a fairly fluid concrete is pumped down the stem releasing the bottom seal whose function is to prevent the soil from entering. As concrete is pumped, the auger is pulled up without rotation removing the soil within the spiral flights; the rate of raising the auger must be compatible with the volume of concrete pumped. With this technique there is no need of temporary support, since the wall of the borehole is continually supported by the spiral flights and the soil within them, or by the concrete as it is pumped. Piles with a diameter up to 1200 mm have been installed, but the typical range of diameters is between 400 mm to 800 mm.

CFA piles offer considerable advantages: vibration is minimal and noise is the lowest for any pile of comparable size; productivity is high. The insertion of the auger involves a slight displacement of the soil; for this reason, some authors classify CFA piles among the partial displacement piles. Since the effects of the displacement are substantially cancelled by the removal of the soil-filled auger, it is believed that this pile type is included more properly among the replacement piles.

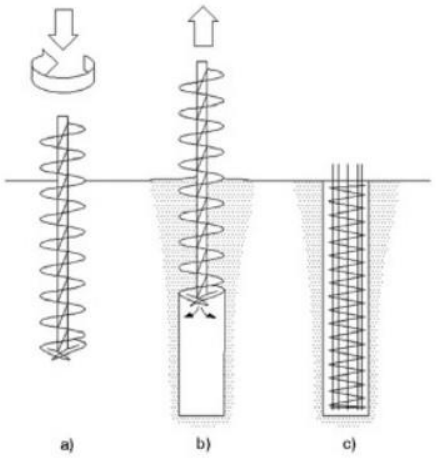

Figure 1.9. Continuous flight auger (CFA) piles: a) insertion of the auger; b) auger withdrawal and concrete casting; c) insertion of the reinforcement cage into the fresh concrete (Viggiani & al., 2012)

ii. Full Displacement Pile

Full Displacement Pile (FDP) also known as "total lateral displacement", are generally used as foundation piles of medium diameter (360 mm to 720 mm).

This technology was first developed by Bauer Maschinen GmbH in the 18th and 19th centuries to increase the bearing capacity of wooden posts.

However, the use was limited to loamy and clayey soils, due to the considerable torque value required to drive the pile into the sandy layers and in the presence of medium-density gravels. The development of ever more powerful machines, capable of providing high torque overhead, made it possible to spread the FDP technology which was then recently introduced in Italy.

This type of pile drastically reduces the volume of soil removed, since the resulting material is compressed against the side walls, this feature allows the FDP pile a greater lateral capacity than other available technologies.

The characteristics of the tool (Figure 1.10) are:

- variable length, from a minimum of 3 meters approximately to a maximum standard of 6-7 meters;
- variable diameters (for Negropal 420 mm, 520 mm and 620 mm);

interchangeable drill bits and prepared for different types of teeth and configuration of the flanges in order to maximize performance.

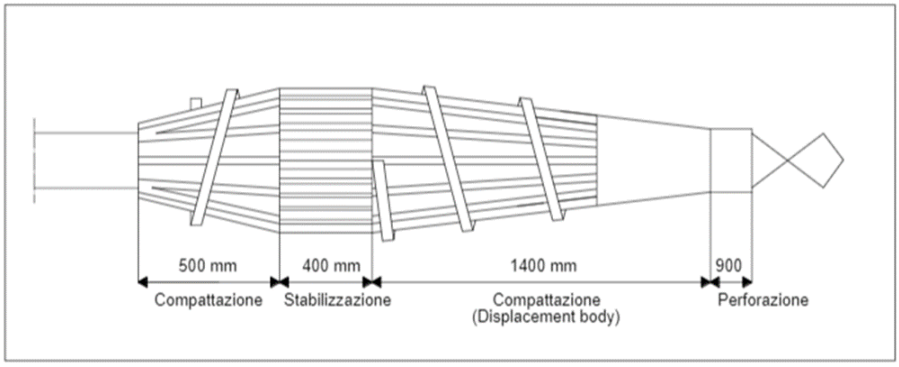

Figure 1.10. FDP tool (Negropal, 2021)

PHASE 1: Drilling with lateral displacement of the ground

During the first phase (Figure 1.11) a displacer tool connected to a hollow rod is used. At the lower end of the rod there is a device that prevents the passage of both water and soil. In this way the excavation causes a lateral displacement of the ground itself, with relative compression of the material, increasing its mechanical resistance characteristics, both for lateral friction and for tip resistance.

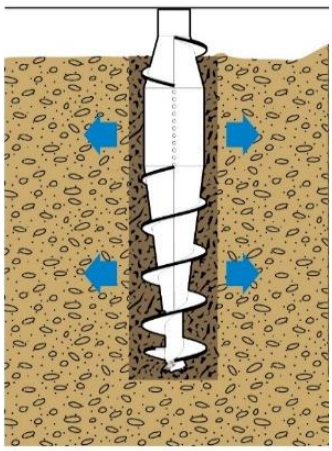

Figure1.11. Drilling phase (Negropal, 2021)

PHASE 2: Extraction of the tool and simultaneous casting of the concrete

Once the depth decided in the project has been reached, the tool is extracted from the ground, without removing the ground (Figure 1.12). During this phase, the hole is also filled, starting from the bottom, with a highly workable mixture (SCC) which is pumped under pressure.

The casting is electronically controlled by means of a LUTZ device installed on board the drilling machine, which records the quantity and pressures of the injected concrete, with the

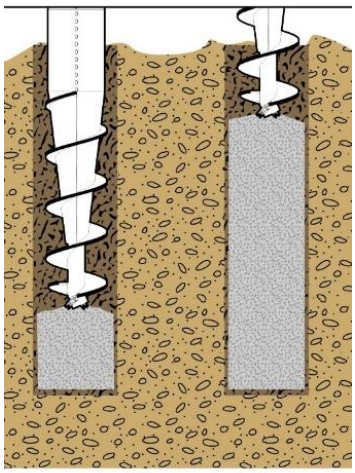

Figure 1.12. Extraction and casting (Negropal, 2021)

PHASE 3: Installation of the reinforcement

Once the hole has been filled with concrete up to the work surface of the equipment, proceed with the insertion of the metal reinforcement which will be left in place, thus completing the medium diameter FDP foundation pile (Figure 1.13).

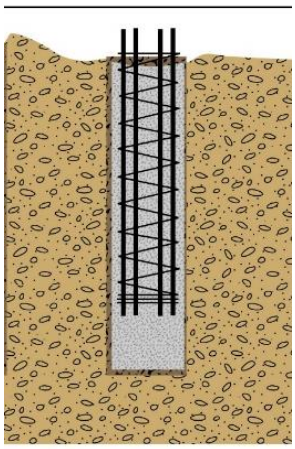

Figure 1.13. Armature of the pole (Negropal, 2021)

There are many advantages of an "FDP" pile:

- Reduced soil removal, with consequent savings in the costs of transport and disposal of the waste material

- High bearing capacity of the pile, greater than CFA technology or traditional bored piles with the same diameter, due to the densification of the soil induced during the execution phase
- Absence of induced vibrations
- Possibility of optimizing the drilling by analysing the excavation parameters
- Reduced consumption of concrete compared to traditional techniques that involve the removal of material

Fields of application**:**

- Indirect foundations
- Piling
- The low production of waste material makes the use of FDP poles optimal even in contaminated sites

Land suitable for this technique:

- strongly cohesive soils (clay, silty clay, peat)
- Degraded or fractured rock

NOT suitable soils, as you may encounter problems in drilling because the tool does not have sufficient torque and thrust:

- Hard rocks
- Very consistent clays
- Incoherent even dense soils (Sand, Gravel)
- Cemented sands

1.2.2 Bearing capacity of a pile

The bearing capacity can be evaluated before the pile realization from fundamental soil properties or from correlation with penetrometer data (CPT, SPT) but it can also be obtained just after the pile realization from the load test realized on the pile or basing on the information of the pile installation (pressure, velocity, volume of concrete…).

1.2.2.1 Bearing capacity from load tests

a. Aim of the tests

According to their purpose, load tests on piles can be subdivided into design load tests and proof load tests.

The aim of a design load test is to determine, at the design stage, the bearing capacity of the pile and its load-settlement relationship.

The proof load test is aimed at verifying the correct installation of the piles, but indications on the load-settlement behavior and, by extrapolation, on the bearing capacity may be also obtained.

b. Tests principle

The design test is usually kept to failure, or at least to a maximum load not less than three times the intended service load. It is a destructive test, and has to be carried out on a purposely installed test pile, which does not belong to the foundation. The installation of the test pile must reproduce as closely as possible that of the production piles in order to obtain representative results; if possible, the same specialized contractor should install the test pile and the production piles. For the same reason the test pile has to be installed as close as possible to the location of the foundation. A borehole or CPT is carried out in the vicinity of the test pile, in order to know the exact subsoil profile at the test site.

The proof load test, on the contrary, is carried out on piles selected among the piles of the foundation, after they have been all installed. The test cannot be destructive, and hence the maximum test load is usually limited to 1.5 times the intended service load. The number of piles to be proof tested is generally specified in the tender documents; in Italy it ranges usually between 1% and 2% of the total number of piles, with a minimum of two. The piles to be proof tested are selected only after all the piles have been installed, in order to prevent a particularly careful installation of the intended test pile and to obtain an equal care for all the piles.

c. Test equipment

The test equipment and procedures are essentially the same for design and proof load tests. The load is applied by means of a hydraulic jack, resting on the pile head; to this aim the pile head must be plane and horizontal. For cast in situ piles, additional hoop reinforcement or a steel tube casing about two diameters long is provided at the pile head.

The reaction to the jack is provided either by a kentledge or by a reaction beam anchored to the ground by tension piles or ground anchors. The kentledge rests on two lateral support walls through a bed of steel beams (Figure 1.14); in order not to influence the behaviour of the test pile, the spacing between the supports and the test pile should be not less than 2m or two times the pile diameter. The total weight of the kentledge should be 10% more than the maximum test load, and carefully centred over the test pile. If an anchored beam is used as reaction system (Figure 1.15), the tension piles should also be sufficiently spaced;

The hydraulic jack is pressurized by an oil pump; the load can be kept constant either by continuous manual regulations or by providing the pump with an automatic adjustment controlled by the load measurement.

In principle, the applied load could be obtained by the oil pressure multiplied by the area of the jack ram; such a measurement, unfortunately still in use, is very rough due to the inevitable and somewhat random friction in the jack. A correct practice requires the use of a load cell, interposed between the jack piston and the reaction system.

The settlement of the head of the test pile is measured by dial gauges or displacement transducers (or both), fixed to the pile head and contrasting on one or two reference beams, anchored to supports sufficiently spaced from the test pile (Figure 1.16).

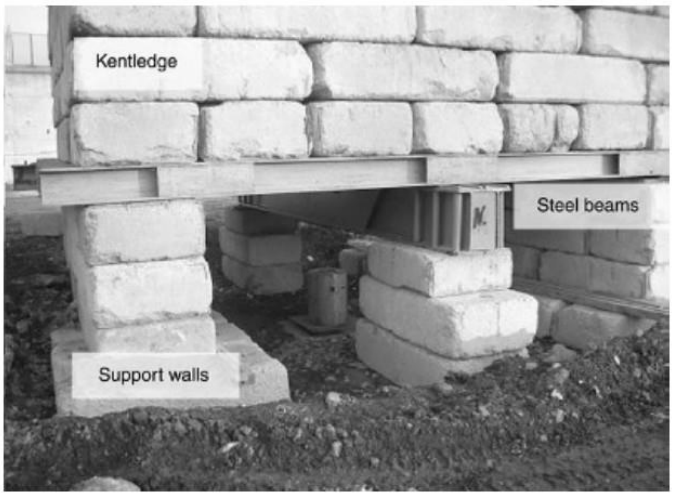

Figure 1.14. Load test setup with kentledge (Viggiani & al., 2012)

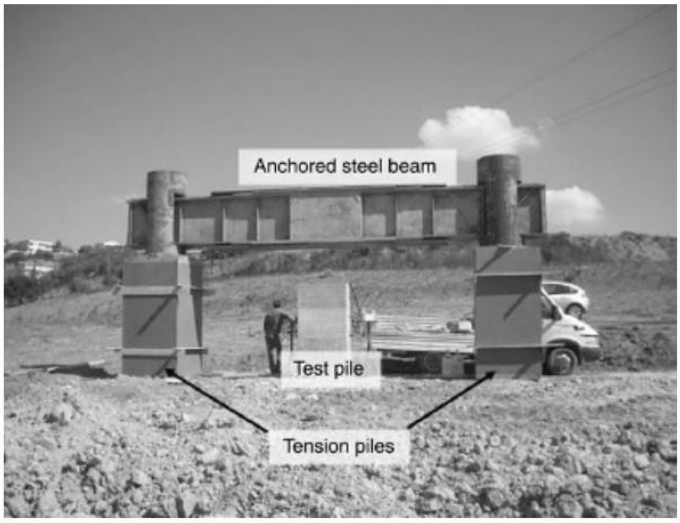

Figure 1.15. Load test setup with tension piles and spreader beam (Viggiani & al., 2012)

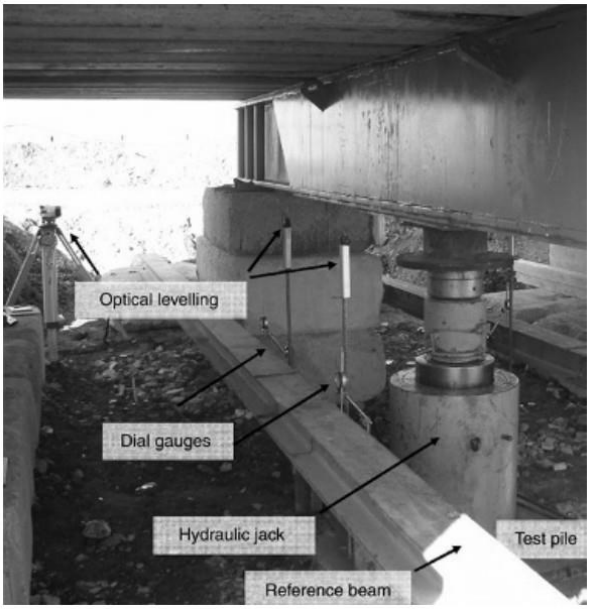

Figure 1.16. Dial gauges for measuring pile head settlement (Viggiani & al., 2012)

Dial gauges or displacement transducers allow settlement to be read to the approximation of 0.01 mm or better, but are influenced by the possible movement of the reference beams and their support and by temperature variations; optical levelling guarantees an approximation of 0.1 mm but is more stable and reliable.

The results of a typical load test are reported in Figure 1.17.

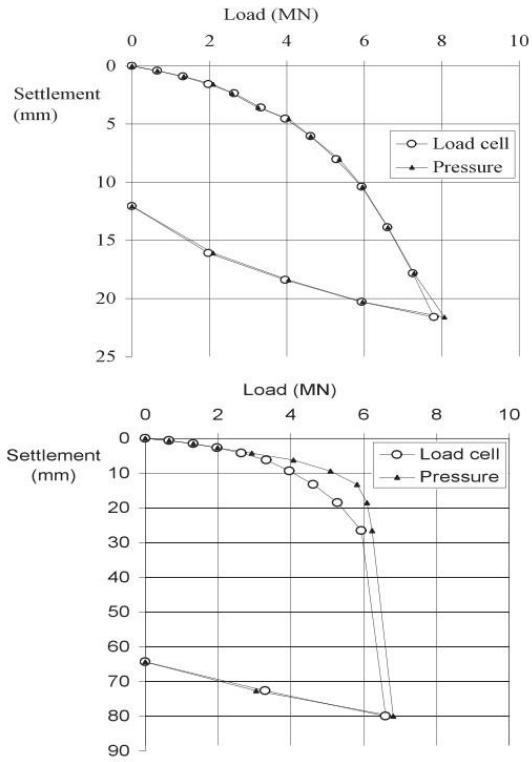

Figure 1.17. Typical results of a pile load test (Viggiani & al., 2012)

d. Test procedure

The most common test procedure is the so-called maintained load test, in which the load is applied in steps and each load step is kept constant for a certain time while the settlement is measured. Each load increment should be around 25% of the intended design load or smaller; so, doing, at least six increments are obtained in a proof test and 12 in a design test, which allow a good definition of the load-settlement relationship. The duration of each increment may be fixed prescribing that the next load step may be applied when the settlement has attained its final value. It is assumed that the settlement has reached its final value when two readings, taken at an interval of 20 minutes, do not differ more than 0.01 to 0.03 mm.

It is suggested to adopt a load history consisting in a single loading cycle from zero to the maximum test load, followed by unloading to zero. In the unloading stage, unloading steps larger and duration shorter than those in the loading stage may be adopted.

e. Expression of the bearing capacity

Chin (1970) noted that in most cases the load-settlement curve is well approximated by a hyperbola (Equation 1.18):

$$Q = \frac{w}{m+nw} \qquad (1.18)$$

Where w is the settlement under the load Q and m, n are two constants to be determined by fitting the curve to the experimental results. Equation 1.19 may be written:

$$\frac{w}{Q} = m + nw \tag{1.19}$$

Suggesting plotting the experimental result in a graph (w/Q, w) and to interpolate a straight line among them (Figure 1.18). the intercept on the vertical axis is equal to m, while the inclination over horizontal is equal to m. Once m and n have been determined, Equation 1.18 may be used to calculate the bearing capacity:

$$Q_{lim} = \frac{0.9}{n} \tag{1.20}$$

If the test has been kept to a sufficiently high maximum test load, the extrapolation is very reliable.

The same technique may be employed to extrapolate a proof test to estimate the bearing capacity.

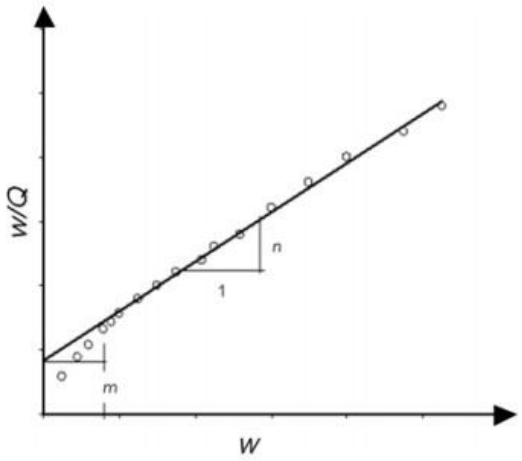

Figure 1.18. The procedure suggested by Chin (1970) to interpolate a hyperbola through the experimental results of a load test (Viggiani & al., 2012)

f. Prescriptions for pile load tests in NTC2018

According to NTC2018 the characteristic value $R_{c,k}$ of bearing capacity for a pile in compression, $R_{c,k,}$ or in traction $R_{t,k}$ is obtained from the correspondent values $R_{c,m}$ or $R_{t,m}$, determined by elaborating the results of:

a) One or more static design load tests;

b) One or more dynamic design test.

$$R_{c,k} = min\left\{\frac{(R_{c,m})_{mean}}{\xi_i}; \frac{(R_{c,m})_{min}}{\xi_j}\right\} \tag{1.21}$$

$$\text{or } R_{t,k} = min\left\{\frac{(R_{t,m})_{mean}}{\xi_i}; \frac{(R_{t,m})_{min}}{\xi_j}\right\} \quad (1.22)$$

i equal to 1,5 and j equal to 2,6. Values of ξ_i and ξ_j are given in Table 1.6

Table 1.6. Values of ξ_i and ξ_j (Cola,lesson 12, 2022)

Number of load tests	1	2	3	4	≥ 5
ξ_1	1.40	1.30	1.20	1.10	1.0
ξ_2	1.40	1.20	1.05	1.00	1.0

Number of load tests	≥ 2	≥ 5	≥ 10	≥ 15	≥ 20
ξ_5	1.60	1.50	1.45	1.42	1.40
ξ_6	1.50	1.35	1.30	1.25	1.25

1.2.2.2 Bearing capacity from the information on the pile installation

a. Control and modulation with electronic "assistants"

Drilling rigs can be equipped with electronic software programmes for use with the FDP Soil Displacement Pile System ("Drilling Assistant"), which modulate the optimal rate of penetration and crowd force during the drilling process for an optimal speed of rotation of the displacement tool. The desired initial parameters can be input by the rig operator with the help of simple onscreen menus.

By using a programmable "extraction assistant", the speed of extraction and volume of concrete can be modulated. This involves measuring the volume of concrete continuously throughout the concreting process and automatically adjusting the speed of extraction based on the flow rate of the concrete.

The "Assistants" are integrated into the monitoring and control system (for example Lutz SW). They ensure the piles are installed to a high and consistent quality standard.

Figure 1.19 illustrates the data extracted from the “Lutz” SW currently installed on the B175 drilling rig presented in figure 1.20 relating to the construction of one of the piles of the test field n ° 1 in Meledo di Sarego (VI).

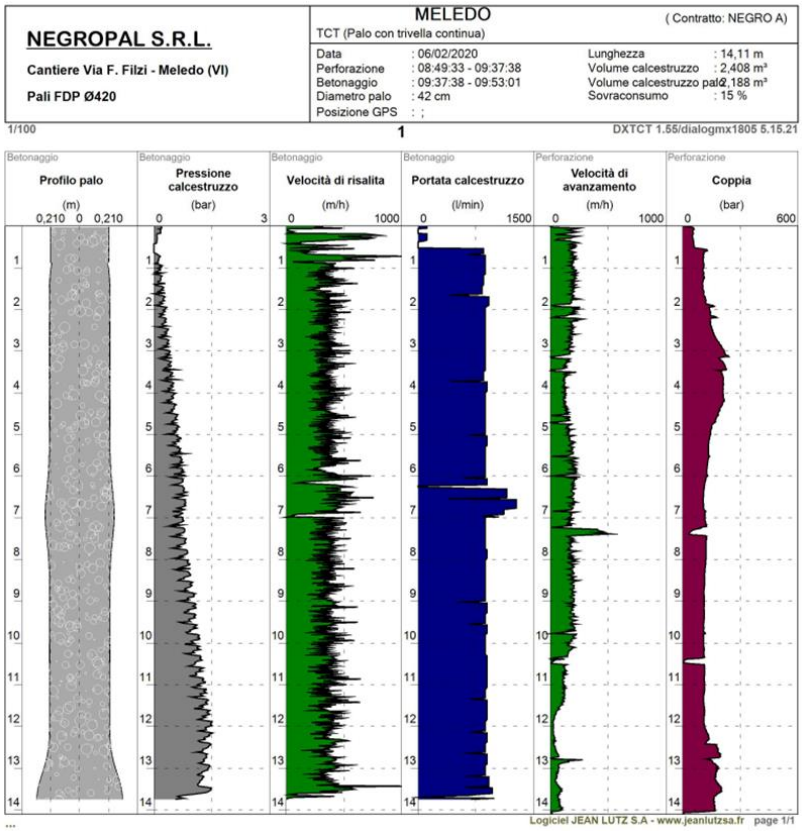

Figure 1.19. Sw Lutz graphic report on an FDP pile made in the Meledo (VI) construction site (Negropal , 2021)

Figure 1.20. Casagrande drilling rig mod. B175XP-2 supplied with Negropal (Negropal, 2021)

The same data are obviously available in other formats (table 1.7 and table 1.8), for example Excel, and supplied to the geotechnical engineer for the subsequent phase of analysis and realization of the mathematical model.

Table 1.7. Extract of the excel file with the data recorded by the Lutz software relating to the test pile n.1 of the Meledo (VI) construction site: general data of the pile (Negropal, 2021)

Record's information:	
Name1	PALO P 1
Name2	
Name3	
Recorder	dialogmx1805
Process	TCT (Palo con trivella continua)
Site	MELEDO
ContractNumber	NEGRO A
StartDate	10/02/2020
DrillStartH	15:54:40
DrillEndH	16:27:14
ConcrStartH	16:27:14
ConcrEndH	16:33:26
PileDiam	0,420 m
PileLength	13,71 m
ConcrVol	1,976 m³
ConcrPileVol	
VolTheoric	1,900 m³
Overcons	1 %
OverconsConcrVol	7 %
XSlope	0,1 °
YSlope	0,1 °
MaxLength	13,71 m
MachineName	
GeoPosRec	45°25'56,1882"N/011°25'05,8758"E/28,30 m
LocalPosRec	0,00/0,00/9,00 m
GeoPosTarget	00°00'00,0000"N/000°00'00,0000"E/0,00 m
LocalPosTarget	0,00/0,00/0,00 m
DeviationRecTarget	0,00/0,00 m

Table 1.8. Extract of the excel file with the data recorded by the Lutz software relating to the test pile n.1 of the Meledo (VI) site: data collected during drilling (Negropal, 2021)

Measures:	Tempo	s	0	0	0,107	1757,957	1757,957	1757,957	1764,618	1764,874
Perforazione	Tempo attivo	s	0	0	0	0	0	0	6,661	6,917
	Phase Time	s	0	0	0	0	0	0	6,661	6,917
	Profondità	m	0	0	0	0	0	0	0,021	0,043
	Velocità di avanzamento	m/h	0,4648	0,4648	0,4648	0,3254	0,3254	0,3254	10,2953	309,3748
	Tube depth	m	0	0	0	0	0	0	0	0
	STOJU		0	0	0	0	0	0	0	0
	Plot	s	-25639,1	-25639,1	-25639,1	-25639,1	-25639,1	-25639,1	-25639,1	-25639,1
	Coppia	bar	5	5	5	2,0459	2,0459	2,0459	9,8462	32
	Rapporto della zoppica di velocità		0	0	0	0	0	0	0	0
	Spinta	bar	-98,6133	-98,6133	-98,6343	-98,6236	-98,6236	-98,6236	-98,6256	-98,6305
	Thrust Force	N	0	0	0	0	0	0	0	0
	Ritenzione	bar	0	0	0	0	0	0	0	0
	Retaining Force	N	0	0	0	0	0	0	0	0
	Velocità rotazione	tr/min	0	0	0	0	0	0	3,4288	6,6
	Nessuna vite	m/rad	0	0	0	0	0	0	0,0041	0,1243
	Smoothed rotation	rad	0	0	0	0	0	0	4,7692	5,1148
	Pump Pressure	bar	0	0	0	0	0	0	0	0
	Pressione calcestruzzo	bar	0,0898	0,0898	0,0865	0,1017	0,1017	0,1017	0,0996	0,1013
	Volume	l	0	0	0	0	0	0	0	0
	Volume lisciato calcestruzzo	m3	0	0	0	0	0	0	0	0
	Portata calcestruzzo	l/min	0	0	0	0	0	0	0	0
	SGVTW	l	0	0	0	0	0	0	0	0
	SAPNN	bar	0	0	0	0	0	0	0	0
	SAPND	Pa	0	0	0	0	0	0	0	0
	Inclinazione X	°	0	0	0	0	0	0	-0,001	0
	Inclinazione Y	°	0	0	0	0,0001	0,0001	0,0001	-0,0019	-0,05
	Machine azimuth	°	0	0	0	0	0	0	0	0
	Convalida pilotaggio		0	0	0	0	0	0	0	0
	Forza di rotazione	j	0	0	0	0	0	0	0	0
	Tool Energy	j	0	0	0	0	0	0	0	0

b. α- value (alpha-value)

During drilling the rate of penetration (m per tool rotation) and torque (kN m) are measured. Using these data, the computer then calculates the α- value (penetration resistance). This dimensionless value is used as an indicator of the strength or density of the prevailing soil formation. It provides an indication that the required load bearing horizon of a pile is being reached and can, therefore, be used to optimise the pile length (as showed in Figure 1.21). Prior to starting the pile installation, an α- value record is determined and compared with borehole los in one or more trial borings. The working piles must be drilled using “Drilling Assistant” for ensuring the reproducibility of defined stop criteria (Bauer Maschinen GmbH, 2013).

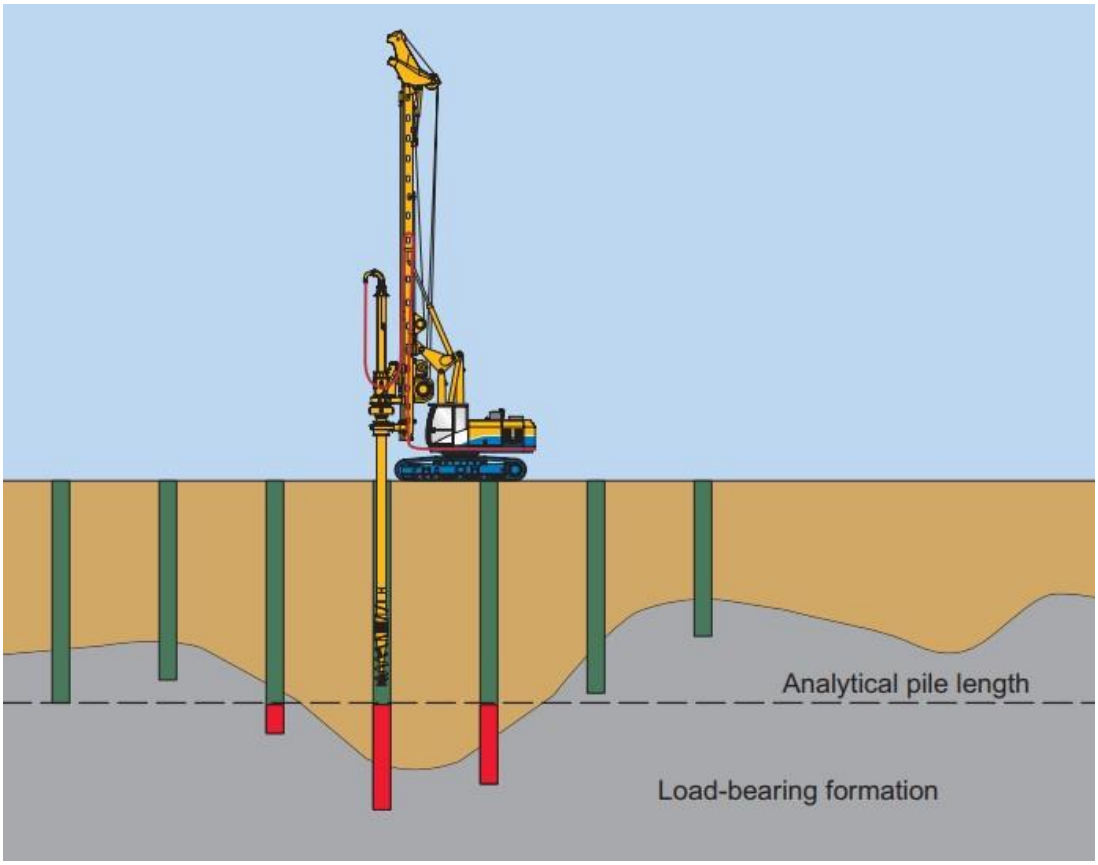

Figure 1.21. Self-exploratory system for flexible pile lengths which can be adapted to the geological conditions (Bauer Maschinen GmbH, 2013)

c. Advantages of using electronic "assistants"

That technology produce some benefits.

- Cost reduction for the customer

Knowing the type of soil in a given lot, given by the geological report, and confirming its composition for each single point of execution of the piles, thanks to the sensors applied to the drilling rig, the Company can calibrate the effective driving length of the piles based on the scope established by the designer.

- More security

The length of the piles, which directly affects their range, can be lower, thus leading to a reduction in the amount of work to be carried out or higher. If during the drilling the detected parameters do not coincide with what is hypothesized by the geological report, increasing the safety for the customer who would have the certainty about the effective door of the piles.

- Cost reduction for the construction company

The projects are drawn up applying prudence quotients well above the limits imposed by the regulations. During the drilling of each single pile, the drilling rig will detect the exact position of the clayey layer and, by means of the calculation SW, the capacity will be calculated instantly, thus making the pole of the length necessary to meet the required characteristics (qualitative improvement). It will therefore result that the poles will have on average a shorter length than the design ones, with an undoubted decrease in construction costs: less material used (iron and cement) and shorter construction time (therefore less wear of machinery and reduction of diesel consumption) - (both quantitative improvements).

- Lower environmental impact

Another important advantage is that related to the lower environmental impact (qualitative improvement), through a more measured and efficient use of resources and a reduction in the quantity of material and diesel, which would lead to a reduction in exhaust gas and CO2 emissions. Furthermore, shorter piles on average also mean a lower impact in the subsoil with all that follows: reduction of waste material to be disposed of (special waste), limited impact on groundwater where present, etc.

1.3 Foundation design process

Foundation design is the decision-making process of selecting the type of foundation elements to adopt, deciding where to place them in the ground, choosing their dimensions, and specifying how to build them. The foundation engineer also inspects or supervises the construction or installation of foundations and, in some cases, monitors their performance under actual structural loads (Salgado, 2006). Salgado suggest a natural sequence to the solution of a foundation engineering problem

1.3.1 Determination of the design loads

The structural loads are usually the product of the structural design, with the possible exception of extremely simple structures, for which the foundation engineer might need to estimate the loads to be supported by the foundations. Loads may be due to the self-weight of the structure (dead loads), the use or function of the structure (live loads), and other sources (water and earth pressures, wind, snow, wave action and seismic loads). Dead loads are due to the self-weight of the different materials that constitute the structure or building in a permanent way while live loads include the weight of people and objects that occupy the structure some,

most, or all of the time but are not permanently attached to it. It is important to have all the following information for each load to be applied on a foundation element: (1) magnitude, (2) load direction, (3) point of application (centered or eccentric with respect to the foundation element), and (4) nature of loads (dead, live, wind, snow, seismic, and so on).

Structural engineers calculate how these loads propagate throughout the structure, eventually resulting in the loads that must be carried by the foundations. These loads are provided to the geotechnical or foundation engineer by the structural engineer. Depending on the country, on the local practice, on the problem, and even on the engineers involved, varying degrees of interaction then takes place between the geotechnical and the structural engineer to converge on a final foundation design.

Table 1.5 shows typical loads for residential buildings with reinforced concrete (RC) structures and brick-wall fillings. Using the numbers of the table, if we take a high-rise residential building with thirty stories, a typical maximum column load for such a building would be 9000 kN (equivalent to 918 metric tons and 1010 tons). This load is lower if internal walls are built using the dry wall method, which are hollow walls essentially made of a light, gypsum-based plaster.

Table 1.9. Typical vertical loads for residential buildings with reinforced concrete frame and brick walls (Salgado, 2006)

Load type	Load per floor
Distributed load	12 kN/m^2
Minimum column load	100 kN
Average column load	200 kN
Maximum column load	300 kN

1.3.2 Subsurface investigation

When having the values of the structural loads to be supported, the engineer must also assess the load-bearing capacity of the soil or rock. For soil sites, this is usually done in either of two ways: to directly correlate foundation capacity to the results of certain in situ tests or to estimate soil properties from laboratory or in situ tests that can then be used in stability or deformation analyses for assessment of foundation capacity.

The in-situ tests that are most often used in foundation design are the standard penetration test (SPT) and the cone penetration test (CPT). In situ test are performed at the site where

construction will take place by loading the soil in some manner and simultaneously making related measurements that are a function of the initial soil properties.

Another way of estimating soil properties is by collecting both disturbed and undisturbed soil samples and testing them in the laboratory. The term undisturbed refers to the desirability of having the samples reflect the true state of the soil in situ. It is obviously impossible to obtain perfect undisturbed samples, but it is possible in certain soils to obtain samples that are reasonably undisturbed. This requires selecting a suitable soil sample recovery technique and cautiously applying this technique.

1.3.3 Selection of suitable types of foundation

Based on the information collected at the subsurface investigation stages, possible types of foundations are selected. This selection is based on considerations of constructability, cost, and performance. The optimal foundation type is the one that can be constructed or installed with the least difficulty and cost.

In the process of selecting possible foundation types, we rely on a number of different resources. Soil and rock mechanics help us both interpret site investigation results and make preliminary foundation capacity calculations. Constructability is of course closely linked with site conditions. As an example, shallow foundation may be too expensive or outright impractical if the groundwater table is very near the ground surface, as the walls of the excavations needed to construct them would likely cave in. as an additional example of constructability problem, driving piles into soil containing large boulders would not be possible. Some piles would reach their design depth, but many would be either blocked or damaged.

Codes of practice can be helpful in establishing the range of foundation load capacity to be expected for different types of terrain. Previous experience, whether personal experience or experience reported in the literature, is essential to cost-effective and timely solution of foundation problems.

1.3.4 Final selection, placement and proportioning of foundation elements

The core of the foundation design process is the selection, placement and proportioning of foundation elements. If a single type of foundation has not yet been chosen, calculations are made at this point to assess which type is likely to be most economical. Traditionally, one of the first design decisions has been to select either shallow or deep foundations. More recently, possibility has become available; piled rafts (or piled mats). A piled raft is a combination of the traditional mat foundation (a shallow foundation) with piles.

The first step in foundation load-carrying capacity calculation is to choose the depth at which to place the bases of the foundation elements. Once the depth of placement of the foundations is known, the foundation elements are proportioned for the given loads. For a footing, this means establishing the plan dimensions based on available soil base resistance and the slab thickness based on the structural capacity of the footing. For a pile, it means choosing an appropriate cross section. For prefabricated piles, this means selecting the cross-sectional dimensions; for cast-in-place piles, there is also the need to specify the material properties and any reinforcement of the pile. Cast-in-situ piles are most often constructed with concrete but grout is also used.

The next step is to consolidate all this information in an organized way into a set of specifications.

1.3.5 Construction

in the construction stage, the ideas contained in the specifications are converted into reality. The general contractor can often handle construction of the shallow foundations, but the installation of deep foundations requires the hiring of a specialty contractor.

Conclusion

At the end of this chapter, the aim was to present foundations, design methods of these foundations and the foundation design process. It can be said that concerning shallow foundations we can have of different types likes isolated footing, strap footing, combined footing and mat foundation. When designing shallow foundation, we must ensure that it will not collapse and the settlement will be within tolerable limits, if both requirements are not satisfied, we should choose deep foundation which can be classified base on the size, the material used or the installation technique. The last criteria permit us to distinguish replacement (or drilled) piles like CFA piles and displacement (or driven) piles like Franki piles. FDP piles which despite being executed in situ like a bored pile can be classified also as a displacement pile due to the fact that throughout its execution, it exists the soil consolidation around the pile, as a result of a horizontal displacement imposed by the drilling equipment. The use of FDP presents wide range of advantages for example it reduces soil removal, the installation process is without vibrations and it gives high bearing capacity. Load tests on pile can be used to compute the bearing capacity of a pile, which is obtain following the prescriptions given by some norms (likes Eurocode or NTC2018), or it’s correct installation according to the

maximum load exerted on the pile test. The bearing capacity of a pile can also be found during the construction stage (drilling phase) by recording the pile penetration resistance which permit to optimize the pile length. The foundation engineer must ensure the respect of the sequence which leads to the solution of a foundation engineering problem starting from the determination of the design loads to the construction stage.

CHAPTER 2: METHODOLOGY

Introduction

For each analysis, it is necessary to define a methodology of work. The methodology is the part where the work main steps are described and explained. It gives the procedure to follow to attain the aim of work. This chapter will consist on the presentation of the study area, the presentation of the geotechnical investigations and the studies done on the site in order to identify the soil and subsoil characteristics useful in the foundation design, Finally, design methods of pile foundation will be implemented using traditional technics, load tests and using pile installation characteristics.

2.1 General recognition of the site

The site recognition was done through a documentary research. This is aimed at providing the geographical location of the project area, the climatic conditions presenting the temperatures and precipitations, the demography and economic activities carried out in the region.

2.2 Site visit

The site visit and the in-situ investigations was done by the company GEOLAMBDA Engineering S.r.l. At the site, they made some in-situ investigations.

- 4 penetrometer tests.
- 7 continuous core drilling with execution of expeditious tests in the hole and sampling undisturbed of some soil samples subjected to laboratory tests.
- 1 geophysical spreading of type “MASW” to define the seismic action of the project.

The tests were scheduled on the basis of the current legislation relating to

- investigations on land and built as specified in the “Programming Recommendations and execution of geotechnical surveys” by the Italian Geotechnical Association (1977).
- Ministerial decree of 17 January 2018, Update of the “Technical standards for construction”, Ministry of Infrastructure and Transport.
- Circular 21 January 2019 n.7, Update of “Technical standards for construction”, Ministry of Infrastructure and Transport.

2.3 Collection of the data

The company GEOLAMBDA Engineering S.r.l. also defined the geological, seismic and geotechnical characteristics of the land for a correct dimensioning of the foundation structures in accordance with the D.M.17.01.2018.

2.3.1 Geological study

In this part some studies were carried out in order to have first the geological, geomorphological and hydrogeological framework of the site, in addition the hydrogeological and the piezometry characteristics of the site were studied, others pertinent points of the study are the seismic framework and the hydraulic hazard, the studies end with the constraints and fragility.

2.3.2 Seismic study

The subsoil category allows to determine the elastic response spectra that allow a correct structural design in relation to site-specific conditions, guaranteeing an adequate level of anti-seismic protection of buildings (O.P.C.M. 3274 and subsequent amendments; Ministerial Decree 17.01.2018).

To achieve the goal, a seismic profile is performed with the MASW methodology, through which the trend of the speed of the shear seismic waves (S waves) with depth is reconstructed. The one-dimensional seismic model (Vs-depth) constitutes in fact the main aspect both in the estimation of the seismic effects of the site and in the definition of the seismic action of the project, as it allows to know the incidence of the local litho-stratigraphic conditions in the modification of the basic seismic hazard.

2.3.2.1 Geophysical survey with the MASW methodology

a. Aim of the test

The MASW test, developed in 1999 by researchers from the Kansas Geological survey (Park CB et al., 1999), allows to determine in detail the trend of the velocity of the shear seismic waves (or S waves) as a function of the depth through the study of Rayleigh surface wave propagation.

b. Test principle

The MASW survey method is divided into “active” and “passive” (Zywicki D.J., 1999; Park C.B., Miller R.D., 2006; Roma V., 2006):

1) In the “active method” the surface waves are produced by an impulsive source arranged on the ground level and are recorded by a linear array composed of numerous receivers placed at a short distance (intergeophonic distance).
2) In the “passive method” the spreading has the same geometric characteristics of the active method but the receivers do not record the surface waves produced by a source impulsive, but the background noise (also called “microtremors”) produced by natural (wind) and anthropogenic (traffic, industrial activities) sources.

The two techniques investigate different spectral bands. While the active method allows to obtain a dispersion curve in the frequency range between 10 and 40 Hz and provides information on the most superficial part of the subsoil (up to about 20-30 m depth depending on the soil stiffness), the passive method allows to determine a dispersion curve in the frequency band between 4 and 20 Hz and provides information on the deeper layers (generally above 30 m).

The combination of the two techniques allows to obtain a complete spectrum in the frequency band between 4 and 40 Hz and allows a detailed reconstruction of the speed trend of the shear waves up to about 30-40 m depth (always depending on the stiffness of the layers).

The analysis of the surface waves is performed using the classical instrumentation for seismic refraction prospecting arranged on the ground according to a linear array of 24 geophones with spacing equal to 1.5 m (the geometric configuration adopted was dictated by both the logistical conditions and the need to best reconstruct the Rayleigh surface wave velocity spectrum).

To obtain a good resolution in terms of frequency, in addition to using 4.5 Hz geophones, a 24-bit seismograph was used.

During the execution of the active MASW test, an 8 kg club struck on a metal plate was used as an energization system. To increase the signal / noise ratio, we proceeded to the sum of several energizations (stacking process).

The source was placed at a distance between 6 and 12 m from the first geophone by carrying out several energizations in different points (“Optimum Field Parameters of an MASW Survey”, Park CB et al., 200; Dal Moro G., 2012).

At the end of the active survey, with the same geometric configuration, the recording of microtremors (passive MASW or ReMi) was carried out, acquiring a total of 10 noise recordings, each 30 s in length.

c. Equipment of the test

The main characteristics of the instrumentation used for the execution of the MASW test are summarized in Table 2.1.

Table 2.1. characteristics of the instrumentation used for the execution of the MASW test (GEOLAMBDA Engineering S.r.l., 2018)

n°	Instrumentation	Characteristics
1	Acquisition unit	GEOMETRICS "GEEO" 24-bit seismograph
24	Vertical geophones	"Geospace" with f0 = 4.5 Hz
1	Seismic cable	L=60 m
1	Source	Sledge hammer on metal plate

d. Operating mode

The experimental data, acquired in SEG-2 format, were transferred to a PC and converted into a compatible format (KGS format file) for interpretation through the use of a specific processing program (SurfSeis 5.0 of Kansas University, Park CB, 2016).

This program allows to process the acquired data both with the active and passive method. The analysis consists in the transformation of the recorded signals into a two-dimensional "phase velocity-frequency (c-f)" spectrum which analyses the propagation energy of the surface waves along the seismic line.

The two-dimensional spectra obtained from the recordings with the active and passive methods, processed in separate phases, are subsequently combined in order to obtain a unique spectrum.

In this graph it is possible to distinguish the "fundamental mode" of surface waves, as Rayleigh waves have a markedly dispersive character that differentiates them from other types of waves (reflected waves, refracted waves, multiple waves).

Furthermore, the combination of the two MASW methods allows to identify the "fundamental mode" of the surface waves in the frequency range between 4 and 40 Hz and to obtain both "superficial and "deep" information.

A "picking" is performed on the frequency spectrum by attributing to a certain number of points one or more phase velocities for a certain number of frequencies (see the dispersion curve shown in figure 2.2 of chapter 3).

These values are subsequently reported on a phase-period-velocity diagram for the analysis of the dispersion curve and the optimization of an interpretative model.

By varying the geometry of the starting model and the speed values of the S waves, the calculated dispersion curve is automatically modified until a good fit is achieved with the experimental values.

e. Expression of results

iii. Definition of the subsoil category according to NTC18

Starting from the one-dimensional seismic model reconstructed through the geophysical survey carried out, it is possible to calculate the value of the $V_{s,eq}$, which represents the equivalent speed of propagation of shear waves up to the depth of the seismic bedrock H (substrate with Vs > 800 m/s). For deposits with substrate depth H greater than 30 m, the equivalent speed of the shear waves is defined by the parameter Vs,30 obtained by setting H=30 m in the following equation (Ministerial Decree 17.01.2018 "Update of technical standards for constructions"):

$$V_{s,eq} = \frac{H}{\sum_{i=1}^{n} \frac{h_i}{V_{s,i}}} \qquad (2.1)$$

Where h_i and $V_{s,i}$ indicate the thickness (in m) and the speed of the shear waves of the i-th layer (up to the seismic bedrock or 30 m from the set height of the foundations), N the number of layers and H the depth of the substrate with Vs > 800 m/s.

iv. Elastic response spectrum according to the anti-seismic regulations

This section defines the elastic response spectra required by the anti-seismic legislation in force. The quantification of the local seismic response takes place through the use of subsoil categories that allow an estimate of the stratigraphic amplification, generated by the particular litho-mechanical conditions of the soils that make up the area in question (simplified approach – Chap. 3.2.2 Categories of subsoil and topographical conditions).

In the calculation of the seismic action, reference was made to what is contained in the Ministerial Decree 17.01.2018, in particular in chapters 2 and 3.

The hypotheses assumed in the definition of the elastic response spectra in acceleration result was:

- Seismic zone = 3 (D.C.R. Veneto 67 of 03/12/2003 – figure 4);
- Nominal life of the structure: VN = 50 years;
- Class of use = III;
- Reference period for the seismic action VR = 75 years (CU = 1.5);

• Maximum horizontal acceleration values (Table 2.2) and spectral parameters (Table 2.3) for the different limit states (interpolated values obtained from the weighted average with the 4 points of the acceleration grid that include the site under examination [ED50: Lat 45.373311 – Long 11.383403] as defined in Annex A and B of the Ministerial Decree 14.01.2008):

Table 2.2. Maximum horizontal acceleration for the different limit states (Ministerial Decree 14.01.2008)

	P_{VR}	T_R	a_g	F_O	T_{C^*}
		[years]	[g/10]		[s]
SLO	81%	45	0.425	2.533	0.2516
SLD	63%	75	0.552	2.511	0.2688
SLV	10%	712	1.447	2.470	0.2883
SLC	5%	1462	1.895	2.449	0.2908

• **Subsoil category = C**, **topographic category = T1** (S_T = 1.0) and viscosity damping coefficient = 5% which correspond to the following values:

Table 2.3. Spectral parameters for the different limit states (Ministerial Decree 14.01.2008)

	S_S	C_C	S	T_B	T_C	T_D
				[s]	[s]	[s]
SLO	1.50	1.66	1.50	0.14	0.42	1.77
SLD	1.50	1.62	1.50	0.15	0.44	1.82
SLV	1.49	1.58	1.49	0.15	0.46	2.18
SLC	1.42	1.58	1.42	0.15	0.46	2.36

v. Analysis of the liquefaction potential of foundation soils

The purpose is to define if the foundation soil is susceptible or not to liquefaction. Liquefaction is a phenomenon associated with the loss of shear strength or an accumulation of plastic deformations in saturated, predominantly sandy soils, stressed by dynamic actions (earthquakes) acting in undrained conditions.

The analysis of the susceptibility to liquefaction of a given site depends on:

• characteristics of the seismic action (intensity and duration);

• geotechnical properties of soils;

• lithological characteristics of the soils and depth of the aquifer.

The liquefaction of a deposit is therefore the result of the combined effect of two main categories of factors: soil conditions (predisposing factor) and seismicity (triggering factor)

Pursuant to NTC2018 (Chap. 7.11.3.4.2), the liquefaction check can be omitted if at least one of the following conditions occurs:

1. Maximum accelerations expected at ground level in the absence of artefacts (free field condition) < 0.10g;

2. Average seasonal depth of the water table greater than 15 m from the ground level;

3. Deposits consisting of clean sands with normalized penetrometer resistance $(N_1)_{60} > 30$ or $q_{cln} > 180$;

The input parameters used in calculating the liquefaction potential are summarized below:

- Maximum horizontal acceleration a_{max}= 0.215g ($a_{max} = a_g * S$ – SLV condition);
- Reference magnitude $M_w = 6.60$ (seismogenic zone 906 called "Garda-Veronese);
- CRR calculated using the simplified analysis based on the correlations proposed by Robertson and Wride (1998) based on the penetrometer resistance measured in the CPT tests performed. We study the CRR values relative to granular levels only (CRR_x_gran) characterized by a value of the factor IC < 2.6 (liquefiable soils);
- CSR calculated by the following formula

$CSR = {}^{\tau_{av}}/_{\sigma_{v0}} = 0.65(a_{max}/g)(\sigma_{v0}/\sigma'_{v0}).r_d$ (NCEER 1998); (2.2)

Project pitch = 2 m from ground floor;

The liquefaction of a medium occurs when:

$CSR \geq CRR$ (2.3).

2.3.3 Geotechnical study

As mentioned in the site visit, the geotechnical investigation campaign made use of:

❖ 4 penetrometer tests performed with a mechanical tip static penetrometer (CPT), pushed to a maximum depth of 11.5 m from the ground level;

❖ 7 continuous coring boreholes pushed to a maximum depth of 20 m (with some standard penetration tests (SPT) in the hole and undisturbed soil sampling, subsequently sent to the laboratory for the execution of 2 oedometer tests);

2.3.3.1 Cone penetration test (CPT)

a. Aim of the test

The Cone Penetration Test (CPT) is an invasive soil test that can identify soil strata type, soil properties, and strength parameters.

b. Test principle

The investigation using a mechanical tip static penetrometer consists of measuring the resistance to penetration of a conical tip of standard dimensions and characteristics, driven into

the ground at a constant speed. Some images of the penetrometer tests are presented in Annexe 2.

c. Equipment of the test

The equipment consists of a hydraulic thrust device which acts alternately on the tip and on a connected sleeve: the test is therefore discontinuous and the resistance measurements are performed and recorded every 20 cm of penetration.

d. Operating mode

A device (expanding ring) was installed on the rods to reduce the effect of ground friction and facilitate deepening with the same thrust available.

They are thus measured at constant intervals (20 cm):

- The R_p or resistance to advancement of the tip only;
- The $R_{l\,tot}$, or the overall resistance to advancement of the tip and sleeve of known dimensions.

The attached documentation (see chapter 3) includes both a copy of the readings performed directly by the penetrometer instrument, and the graphs according to the following pairs of values:

- R_p (or q_c) / depth;
- R_l / depth.

From the analysis of the results and through the ratio R_p / R_l it was possible to trace with a certain approximation the lithological nature of the soils crossed, using the method suggested by Schmertmann (1978) as a discriminant; the latter considers the ratio between the tip resistance and the lateral resistance by the ratio Fr as indicative of the lithology (Figure 2.1)

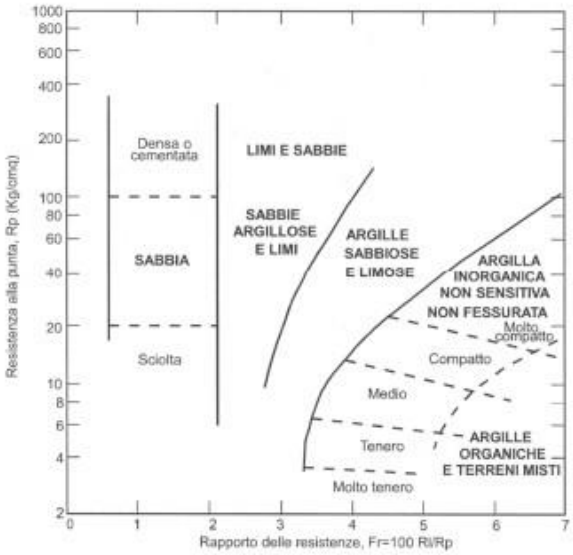

Figure 2.1. relation between the tip resistance and Fr (Schmetmann,1978)

However, it should be remembered that, although the CPT-type penetrometer survey provides reliable geotechnical data, the information on the lithological and granulometric nature of the soils derives substantially from empirical correlations.

e. Expression of results

In the interpretation of the results, the penetrometer tests were assimilated to rapid tests in conditions of prevented drainage and, in the definition of geotechnical behavior, a fundamental distinction was adopted between incoherent soils (shear resistance characterized only by the friction angle) and fine soils (shear resistance characterized above all by the existence of cohesive bonds).

As regards the definition of the geotechnical parameters, using the best known and most widespread correlations based on CPT data, the following was calculated:

- Angle of internal friction (φ) and of the deformation modulus I for incoherent soils;
- Undrained cohesion (Cu) and oedometric modulus (Ed) for cohesive soils.

The methods used for the calculation of the geotechnical parameters (the results of which were subsequently critically reviewed) are illustrated below.

CUTTING RESISTANCE ANGLE φ

To estimate this parameter, different methods were used in which the friction angle is calculated as a function of the resistance at the tip and the effective vertical tension, subsequently compared with each other; in particular:

CAQUOT method: $\emptyset = 9.8 + 4.96 \cdot \ln\left(\frac{q_c}{\sigma'_v}\right)$ (2.4)

KOPPEJAN method: $\emptyset = 5.8 + 5.21 \cdot \ln\left(\frac{q_c}{\sigma'_v}\right)$ (2.5)

DE BEER method: $\emptyset = 5.9 + 4.76 \cdot \ln\left(\frac{q_c}{\sigma'_v}\right)$ (2.6)

RELATIVE DENSITY D_R

Defines the degree of densification of the land crossed; the following methods were used:

HARMAN: this correlation is valid for all types of sand and involves evaluating the relative density as a function of the resistance at the tip and the effective vertical tension

$D_r = 34.36 \cdot \ln\left(\frac{q_c}{12.3 \cdot \sigma'^{0.7}_v}\right)$ (2.7)

In which:

σ'_v: effective vertical stress

q_c: tip resistance

SCHMERTMANN: this correlation is valid for all types of soil and involves evaluating the relative density as a function of the resistance at the tip and the effective vertical tension.

$D_r = -97.8 + 36.6 \cdot \ln q_c - 26.9 \cdot \ln \sigma'_v$ (2.8)

UNDRAINED SHEAR STRENGHT C_U

The empirical method proposed by Lunne and Eide was used (valid, obviously only for cohesive soils):

$C_U(Kg/cm^2) = (R_p - \sigma_v)/K$ (2.9)

With K = constant between 12 and 19 (as a function of plasticity)

YOUNG'S MODULUS E

Defines the value of young's modulus using the following empirical correlation (Schmertmann):

$E(Kg/cm^2) = 2.5 * R_p$ (2.10)

OEDOMETRIC MODULUS E_D

It was calculated through:

- The empirical correlation $R_p - C_u$ defined by the following relationship, valid as a first reference estimate for cohesive soils in general (from plastic silts to clays):
  $E_d(kg * cm^{-2}) = e^{3.12+1.08Cu}$ (2.11)
- The correlation of Mitchell & Gardner (1975):
  $E_d(kg/cmq) = \alpha R_p$ (2.12)

Where R_p is the resistance at the tip and α is a variable coefficient according to the type of soil.

NATURAL UNIT WEIGHT γ_n

A mean value of γ_n characteristic was assumed according to literature data for the type of soil observed.

2.3.3.2 Continuous core drilling

To correctly reconstruct the local geological and geotechnical model, seven (7) continuous core boreholes pushed to a maximum depth of 20 m with respect to the ground level were made, within which some standard penetration test (S.P.T) in advance, with open toe according to the ISSMFE standard.

The material, cored and placed in special cataloging boxes of 5 meters each, was described, evaluated and photographed. The reconstruct stratigraphy and photographic documentation are shown in chapter 3.

2.3.3.3 Standard penetration test

a. Aim of the test

The purpose of this test is not only to provides information from which soil strength can be estimated but also provides a physical sample that can be visually inspected or used for laboratory classification.

b. Test principle

The standard penetration test consists in the insertion, by beating with a standard mallet, of a thin-walled sampler recording the number of strokes necessary to produce the insertion, for three intervals of 15 cm each. From the test three values are obtained (N1, N2, N3):

c. Expression of results

The parameter $N_{SPT} = N_2 + N_3$ is assumed as the resistance to the penetration; the first noted value is discarded as it is affected by the disturbance on the bottom of the hole resulting from the execution of the survey.

Furthermore, when processing the data, it must be considered that the results obtained are influenced by the methods of execution of the test, in particular by the various driving devices and by the effective vertical tension of the soil at the depth of execution of the test. Taking these factors into account, the normalized value of N_{SPT}, that is $(N_1)_{60}$, was then calculated using the following expression:

$$(N_1)_{60} = C_N(ER/60) \cdot \lambda \cdot N_{SPT} \quad (2.13)$$

In which:

C_N = correction coefficient dependent on the value of σ'vo [Liao & Whitman, 1986];

σ'vo = effective pressure at the test execution height;

ER = average efficiency of the driving device expressed as a percentage (in the specific case: 60%);

λ = parameter that considers the energy loss for the length of the rods.

For the estimation of the geotechnical parameters, the correlations of De Mello (1971) and Shioi & Fukuni (1982) were used for the friction angle and the correlation of Schmertmann (1978) and Schultze and Menzebach for the calculation of the Young's modulus; the values obtained by carrying out the S.P.T. contributed to the development of the geotechnical model together with the results of the S.C.P.T. tests.

2.3.3.4 Evaluation of the geotechnical ultimate limit states (ULS) and exercise limit states (SLE)

In order to define the geotechnical reactions in the case of direct foundations, two geotechnical profiles were used, which constitute the extremes between those detected. In particular profile n° 1 which represents the vertical detected in the S1 survey located at the western end of the planned building and profile n°2, on the other hand, represents the vertical of the S4 survey located at the opposite extreme.

a. Geotechnical ultimate limit state (ULS): evaluation of the bearing capacity

Considering the stratigraphic and geotechnical articulation of the substrate soils, the geotechnical responses of the soils in correspondence with profile n°1 (western sector, best geotechnical characteristics) and of profile n°2 (eastern sector, worst geotechnical characteristics), assuming the following foundations:

- PROFILE 1: square-based plinth structure with zero eccentricity placed within Unit B and a joint (D) equal to 1.0 m.
- PROFILE 2: square-based plinth structure with zero eccentricity laid within the silty-sandy deposits of Unit A and a joint (D) equal to 1.0 m.

For the evaluation of the ultimate load, the Terzaghi trinomy expression (LOAD CAPACITY calculation program) was used, subsequently checked with other methods (Meyerhof, Brinch-Hansen):

$$q_d = cN_cS_c + \gamma_1 DN_qS_q + 0.5\gamma_2 BN_\gamma S_\gamma \quad (2.14)$$

Where:

$\gamma_{1,2}$ = average volume weight respectively above and below the laying surface

c = cohesion of the soil

D = laying depth of the foundation

B = foundation width (short side dimension)

N_c, N_q, N_γ = dimensionless coefficients linked respectively to the contribution of the cohesive soil, to the soil placed above the foundation plane and to the layers of zero cohesion

S_c, S_q, S_γ = dimensionless factors related to the shape of the foundation

The safety checks against the ultimate limit states were carried out considering the partial coefficients for the actions (A1), for the geotechnical parameters (M1) and for the resistances (R3), shown in tables 6.2. I, 6.2. II of the aforementioned DM 17.01.2018 (NT.C2018).

The ULS checks were carried out following APPROACH 2, consisting of the following combination A1 + M1 + R2 (the partial coefficients applied are γ_γ = 1; $\gamma_{c'}$ = 1; $\gamma_{tan\varphi'}$ = 1; γ_R = 2.3).

The resistance Rd of the geotechnical system setting is:

$$R_d = q_{lim} * (B * L)/\gamma_R. \quad (2.16)$$

According to the legislation, an adequate degree of safety is achieved when the relationship is verified:

$$R_d/E_d \geq 1 \quad (2.15)$$

The design values of the actions (E_d) will be calculated using the appropriate partial coefficients to be applied depending on the loads transmitted from the superstructure to the foundation.

b. Geotechnical serviceability limit states (SLS): assessment of breakdowns

During the verification phase, after having determined the distribution of the stresses (Newmark method) produced by an action (E_d) equal to the ground resistance (R_d) calculated with approach 2, the absolute settlements were estimated using the "Elasticity Theory" (or Terzaghi's simplified method, 1943) (QSB2 calculation program), whose compatibility with the elevated structure will be verified in the structural design phase.

2.4 Design of Full Displacement pile (FDP)

The design was done basing on the traditional technics (analytical formulation, cone penetration and standard penetration), basing on the load tests and basing on the informations on the pile installation.

2.4.1 Design from the analytical formulation

In this part we compute the limit load as a function of the pile geometry, the characteristics of the ground and the interface. The computation was made using the software Microsoft Excel.

We have assumed a pile length of 14.63 m and a diameter of 600 mm. the water table is at 2 m below the ground level and the unit weight of water is $\gamma_w = 9.8\, kN/m^3$.We used the stratigraphy of the soil given by the S1 and by the S4 survey .

The maximum axial load is considered composed by two contributions (as shown in equation 1.17): the base bearing capacity Q_b and the shaft contribution Q_s.

$$Q_{lim} = Q_b + Q_s = q_b \cdot A_b + q_s \cdot A_s \quad (2.17)$$

$A_b = \pi D^2/4$ and $A_s = \pi DL$

The ultimate tip resistance was computed considering drained conditions

$$q_b = c' N_c + \sigma'_{VL} N_q \quad (2.18)$$

where σ'_{VL} is the effective vertical stress at the base and N_q have been computed with the Berezantsev (1961) formulation using the original φ.

The limit unit shaft resistance in undrained conditions is:

$$q_s = \alpha \cdot c_u \quad (2.19)$$

Where α is the adhesion coefficient which depends on the pile type and soil consistency. Table 2.4 gives us the values of the adhesion coefficient.

Table 2.4. Values of the adhesion coefficients (Cola, lesson 10,2021)

Pile	c_u	α
Driven	$c_u \leq 25$	1.0
	$25 < c_u < 70$	$1-0.011(c_u-25)$
	$c_u \geq 70$	0.5
Drilled	$c_u \leq 25$	0.7
	$25 < c_u < 70$	$0.7-0.008(c_u-25)$
	$c_u \geq 70$	0.35

In drained conditions we computed the shaft resistance is:

$$q_s = K \cdot \sigma'_z \cdot \tan\delta \quad (2.20)$$

Table 2.5 was used to have the values of K and δ.

Table 2.5. Values of K and δ (Cola lesson 10, 2021)

Pile Type	k – Loose Soil	k – Dense Soil	δ
Driven in Steel	0.7	1.0	20°
Driven precast concrete	1.0	2.0	$3/4\phi_c$
Driven CIP concrete	1.0	3.0	ϕ_c
Drilled	1-sinϕ	K_o=1-sinϕ	ϕ_c
CFA	0.7	0.9	ϕ_c

2.4.2 Design from the empirical formulation

Here we used the results from the CPT and the SPT tests to compute the bearing capacity of the soil. We also assumed a pile length of 14.63 m and a diameter of 600 mm. The computation was made using the software Microsoft Excel.

2.4.2.1 Design from the CPT tests

We computed the bearing capacity using the data given by CPT C and CPT D

The ultimate tip resistance is

$$q_{bL} = c_p \cdot q_{c,p} \tag{2.21}$$

In CPT C $q_{c,p}$ is the average value of q_c from 11.00 m to 11.40 m depth.

In CPT D $q_{c,p}$ is the average value of q_c from 9.80 m to 11.40 m depth.

Since the material at the lowest depth in CPT C and in CPT D is sand the value of c_p used was 0.41 from Randolph (2003)..

The ultimate shaft resistance is

$$q_{sL} = c_s \cdot q_{s,p} \tag{2.22}$$

In CPT C and in CPT D $q_{s,p}$ is the average value of $q_{s,i}$ from 0.2 to 14.63 m depth.

The value of c_s chosen is 0.0057 from Aoki & al. (1978).

2.4.2.2 Design from the SPT tests

We computed the bearing capacity using the results of SPT S1 and SPT S4.

The ultimate tip resistance is)

$$q_{bL}/_{pa} = n_b \cdot N_b \tag{2.23}$$

In SPT S1 and SPT S4, the value of N_b used is 3.8.

Since the material at the tip depth is Silty sand the value chosen for n_b is 2.05 from Aoki & Velleso (1975).

The shaft resistance is

$$q_{si}/_{pa} = n_{si} \cdot N_{si} \quad (2.24)$$

In SPT S1 and SPT S2 we used n_b = 0.02 from Meyerhof (1976,1983) all over the pile length from.

According to NTC2018, the characteristic value of the bearing capacity is given by:

$$R_{c,k} = min\left\{\frac{(R_{c,m})_{mean}}{\xi_3}; \frac{(R_{c,m})_{min}}{\xi_4}\right\} \quad (2.25)$$

The values ofξ are given by Table 2.6

Table 2.6. Values of ξ for the characteristic resistance (Brezzi, lesson 12, 2022)

Numero di verticali indagate	1	2	3	4	5	7	≥ 10
ξ_3	1,70	1,65	1,60	1,55	1,50	1,45	1,40
ξ_4	1,70	1,55	1,48	1,42	1,34	1,28	1,21

2.4.3 Design from the load test

The tests concern three (3) FDP piles with a length of 14.00 m and a diameter of 600 mm, related to the construction work of a new LIDL store located near the provincial road 17 in Lonigo (VI). The tests were carried out according to:

- Ministerial Decree of 17 january 2018, Update of the "Technical standards for construction", Ministry of Infrastructure and Transport
- Circular 21 January 2019 n. 7, Update of "Technical standards for construction", Ministry of Infrastructure and Transport
- Agi Recommendations on Foundation Stakes (1984)
- CNR- official Bulletin N. 191, Procedures for the execution and interpretation of compression axial load tests on foundation piles (1999).

2.4.3.1 Aim of the test

The aim is to evaluate the bearing capacity after the pile realization based on the load tests realized one the piles mentioned above.

a. Test principle

The compression load on the pile was obtained with a hydraulic jack placed in contrast with a suitable structure consisting on two steel beams, constrained to the two piles adjacent to the loaded pile.

The measurement of the lowering of the pile was carried out by means of 3 displacement transducers (n°1, n°2 and n°3) positioned vertically on the top of the pile. The feedback is obtained with special supports sufficiently far from the pile so as not to be influenced by its lowering. The sensor was positioned on a metal plate at 120° from each other in order to monitor the lowering from the top of the pile by averaging the values of the readings taken on three points. The pressure measurement in the circuit was carried out by means of a transducer of digital pressure. The images of the execution of the loads tests on the three piles are presented in Annexe 1.

2.4.3.2 Operating mode

Two loads cycles were performed for each load test, with load steps of approximately 116.0 kN each until reaching the load of 464.0 kN (SLE) for the 1st cycle and 696.0 kN for the 2nd cycle. Each load step was maintained until the settlements stabilized.

The unloading phase was carried out in steps until complete unloading and reading residual settlements. The instruments used are presented in the annexes.

2.4.3.3 Expression of results

In our case we choose to use the 2nd cycle of load (table 2.7) because it reaches a value of the load higher than in the 1st cycle.

We computed the bearing capacity using hyperbolic method (Chin 1970).

Table 2.7. Results of the 2nd cycle of the load test on the three piles test.

Pile No 1			Pile No 2			Pile No 3		
Q	w	w/Q	Q	w	w/Q	Q	w	w/Q
(kN)	(mm)	(mm/kN)	(kN)	(mm)	(mm/kN)	(kN)	(mm)	(mm/kN)
0.0	0.00		0.10	0.00		0.0	0.00	
115.5	0.11	0.0010	116.90	0.27	0.0023	117.0	0.33	0.003
116.4	0.11	0.0009	116.40	0.27	0.0023	120.4	0.33	0.003
231.7	0.20	0.0009	229.40	0.41	0.0018	230.9	0.50	0.002
231.0	0.21	0.0009	232.80	0.42	0.0018	233.4	0.51	0.002
348.0	0.29	0.0008	349.40	0.54	0.0015	346.8	0.66	0.002
350.7	0.31	0.0009	349.20	0.54	0.0015	351.1	0.68	0.002
463.7	0.40	0.0009	462.40	0.65	0.0014	467.1	0.80	0.002
465.5	0.40	0.0009	462.40	0.67	0.0014	469.3	0.81	0.002
580.8	0.49	0.0008	579.40	0.82	0.0014	581.7	1.08	0.002
578.7	0.51	0.0009	582.40	0.86	0.0015	581.6	1.10	0.002
695.1	0.61	0.0009	695.80	1.07	0.0015	696.6	1.28	0.002
697.5	0.68	0.0010	696.20	1.35	0.0019	696.6	1.38	0.002
455.1	0.51	0.0011	462.20	1.15	0.0025	457.0	1.22	0.003
456.8	0.50	0.0011	464.30	1.14	0.0025	458.8	1.21	0.003
227.4	0.33	0.0015	235.20	0.90	0.0038	241.1	0.93	0.004
230.0	0.32	0.0014	238.70	0.89	0.004	240.6	0.93	0.004
0.0	0.08		0.00	0.32		0.0	0.23	
0.0	0.06		0.00	0.3		0.0	0.13	

The limit load of each pile was computed using the hyperbolic method (Chin 1970) which suggest to plot the data in a (w, w/Q) graph in order to have the intercept and the slope of the fitting line then using the following equation to compute the limit load

$$Q_{lim} = \frac{0.9}{n} \tag{2.26}$$

According to NTC2018 the characteristic value $R_{c,k}$ of bearing capacity for a pile in compression, is obtained from the following expression :

$$R_{c,k} = min\left\{\frac{(R_{c,m})_{mean}}{\xi_1}; \frac{(R_{c,m})_{min}}{\xi_2}\right\} \tag{2.27}$$

Since the number of tests is 3, $\xi_1 = 1.20$ and $\xi_2 = 1.05$ (from literature review).

2.4.4 Design based on the pile installation data

The purpose in this part is to obtain the bearing capacity just after the pile realization basing on the information on the installation parameters

Thanks to the 4.0 technology of the drilling rig and in particular of the Lutz system installed in it, it was possible for the company Negropal to retrieve the pile installation data in real time on drilling (Figure 2.2, Figure 2.3 and Figure 2.4)

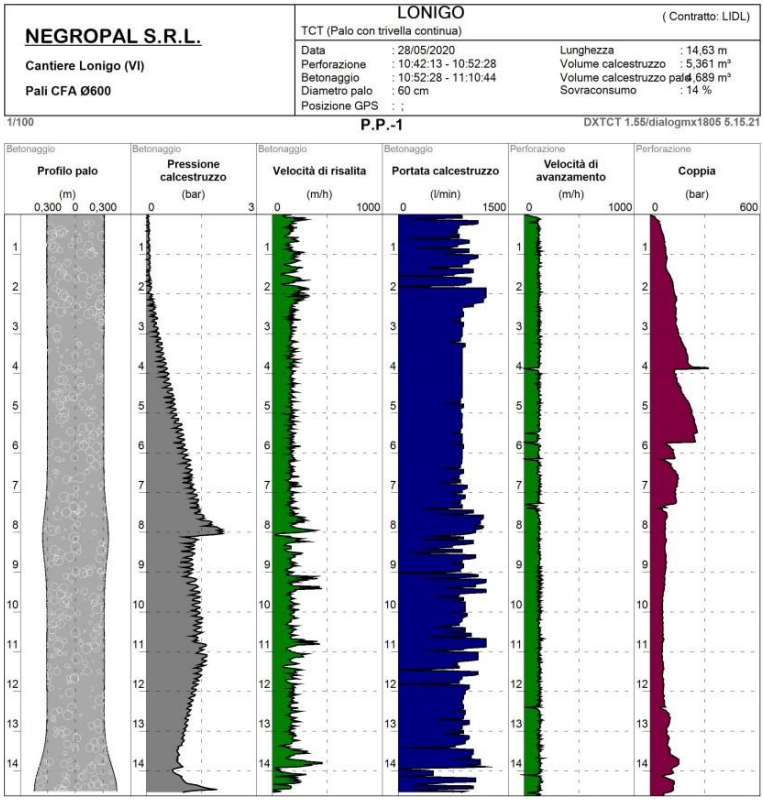

Figure 2.2. Sw Lutz graphic report on the pole n.1 made in the Lonigo construction site (Negropal, 2020)

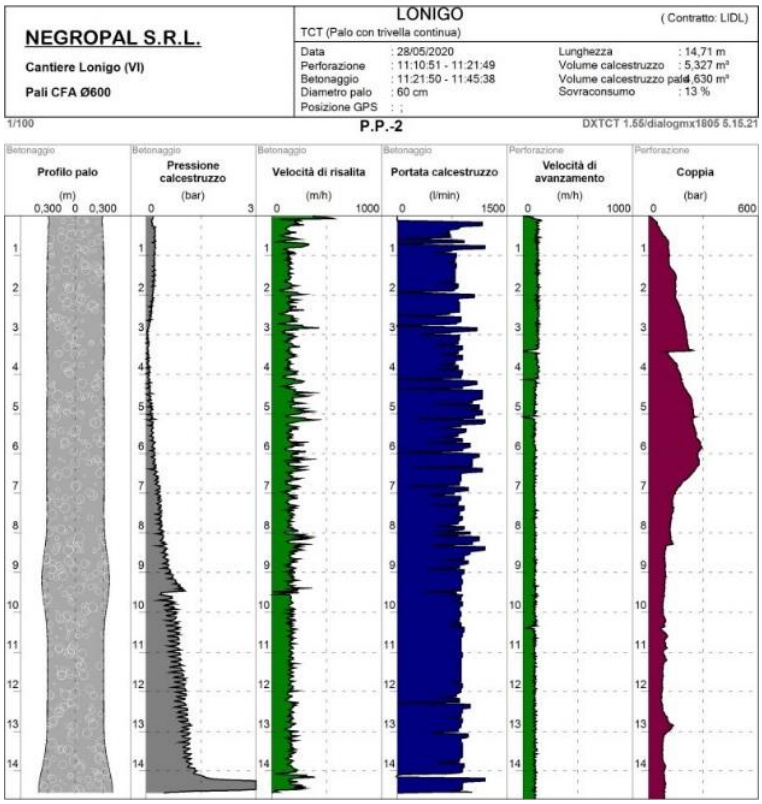

Figure 2.3. Sw Lutz graphic report on the pole n.2 made in the Lonigo construction site (Negropal, 2020)

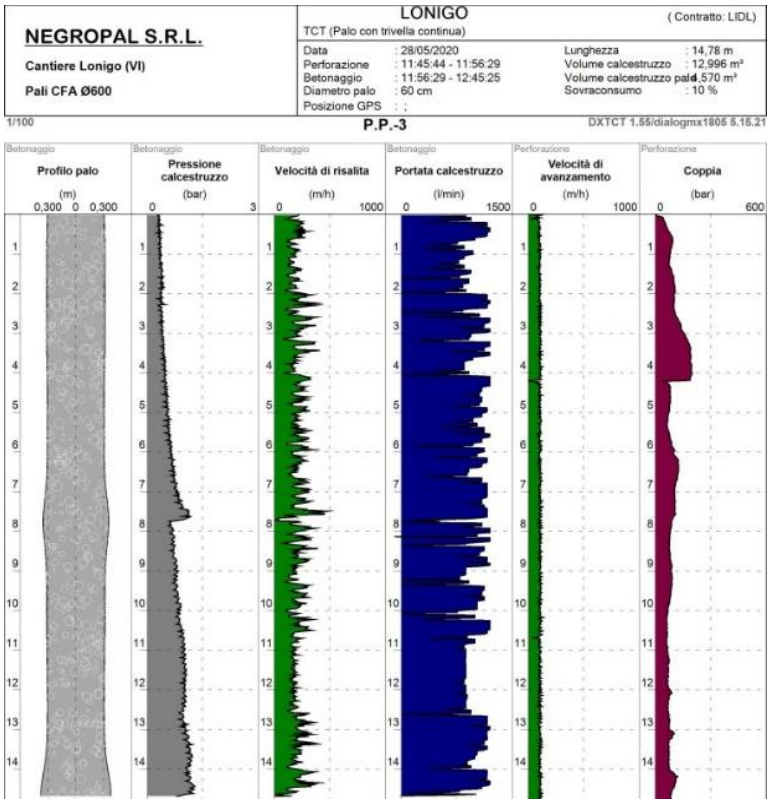

Figure 2.4. Sw Lutz graphic report on the pole n.3 made in the Lonigo construction site (Negropal, 2020)

The bearing capacity is computed using the alpha value recorded in the drilling phase of the construction. The alpha (α) value is computed with the expression below:

$$\alpha = \frac{torque}{penetration} \tag{2.28}$$

Where the torque is in [KNm] and the penetration in [m/tool rotation]

2.5 Conclusion

Having reach, the end of the chapter, the aim of our work was to present the procedure used to design three piles foundation of our commercial building. In order to do that we first define the physical and socio-economic characteristics of the study area then we presented the different on site investigations (continuous core drilling, CPT, SPT and MASW test) and study (geological, seismic and geotechnical) made by the company GEOLAMBDA Engineering S.r.l. We continued with the design procedure of a shallow foundation at ultimate and serviceability limit state and we ended with the evaluation of the bearing capacity of three full displacement piles before the piles realization basing on the traditional technics (using analytical formulation,

CPT results and SPT results) and after the pile realization basing on the load tests and on the informations on the pile installation.

CHAPTER 3: RESULTS PRESENTATION AND INTERPRETATION

Introduction

After having defined the methodology of our work, it is important for us to expose the results which are the culmination of the research and the basis of the discussion.

3.1 General presentation of the site

The documentary research has been made and the results of the physical characteristics and the socio-economic characteristics of the site were carried out.

3.1.1 Geographical location of the site

Officially, the Italian Republic or Republic of Italy is a country consisting of a peninsula delimited by the Alps and several islands surrounding it, whose territory largely coincides with the homonymous geographical region. Italy is located in the middle of Mediterranean Sea, in Southern Europe; it is also considered part of Western Europe. A unitary parliamentary republic with Rome as its capital and largest city, the country covers a total area of 301.230 km² (116.310 sq. mi) and shares land borders with France, Switzerland, Austria, Slovenia, as well as the enclaved microstates of Vatican City and San Marino. Vicenza is a city in north-eastern Italy as we can see in Figure 3.1, it is in the Veneto region at the northern base of Monte Berico, where it straddles the Bacchiglione River. Vicenza is approximately 60 kilometres (37 mi) west of Venice and 200 kilometres (120 mi) east of Milan.

Figure 3.1. Localization of Vicenza in Italy (https://en.wikipedia.org/wiki/Vicenza, 2021)

3.1.2 The climate

The climate in Vicenza can be understand looking at Figure 3.2.

Month	Jan	Feb	Mar	Apr	May	Jun	Jul	Aug	Sep	Oct	Nov	Dec	Year
Record high °C (°F)	15.9 (60.6)	21.7 (71.1)	26.8 (80.2)	30.0 (86.0)	34.8 (94.6)	37.4 (99.3)	37.4 (99.3)	38.2 (100.8)	33.2 (91.8)	29.4 (84.9)	24.4 (75.9)	17.8 (64.0)	38.2 (100.8)
Average high °C (°F)	7.0 (44.6)	9.3 (48.7)	13.5 (56.3)	17.3 (63.1)	22.8 (73.0)	26.2 (79.2)	29.1 (84.4)	28.7 (83.7)	24.3 (75.7)	18.4 (65.1)	11.8 (53.2)	7.5 (45.5)	18.0 (64.4)
Daily mean °C (°F)	3.0 (37.4)	4.6 (40.3)	8.4 (47.1)	12.1 (53.8)	17.4 (63.3)	20.8 (69.4)	23.4 (74.1)	22.9 (73.2)	18.9 (66.0)	13.5 (56.3)	7.5 (45.5)	3.5 (38.3)	13.0 (55.4)
Average low °C (°F)	−1 (30)	−0.1 (31.8)	3.3 (37.9)	7.0 (44.6)	11.9 (53.4)	15.5 (59.9)	17.7 (63.9)	17.2 (63.0)	13.5 (56.3)	8.5 (47.3)	3.1 (37.6)	−0.4 (31.3)	8.0 (46.4)
Record low °C (°F)	−20 (−4)	−18.6 (−1.5)	−10 (14)	−3.2 (26.2)	−0.8 (30.6)	2.6 (36.7)	9.5 (49.1)	8.0 (46.4)	3.8 (38.8)	−3.6 (25.5)	−8 (18)	−13 (9)	−20.0 (−4.0)
Average precipitation mm (inches)	76.5 (3.01)	67.9 (2.67)	76.9 (3.03)	97.3 (3.83)	100.0 (3.94)	104.3 (4.11)	74.0 (2.91)	79.5 (3.13)	92.7 (3.65)	115.5 (4.55)	93.7 (3.69)	81.5 (3.21)	1,059.8 (41.73)
Average precipitation days (≥ 1.0 mm)	7.0	5.0	6.4	9.5	10.0	9.3	6.8	6.7	6.1	7.5	7.1	6.4	87.8
Average relative humidity (%)	81	77	73	74	72	73	72	73	74	78	80	82	76

Figure 3.2. Climate data for Vicenza (servizio meteorologico retrieved 19 May 2015)

3.1.3 The demography

In 2010, 83.5% of the population was Italian. From 1876 to 1976 it has been calculated that over 1,000,000 people from the province of Vicenza have emigrated, with more than 3,000,000 people of Vicentino descent living around the world (most common migration currents included Brazil, the United States, Canada, Australia, Germany, France, Belgium and Switzerland) escaping the devastation left by poverty, war and sickness. Today, almost 100,000 Vicenza citizens live and work abroad. Today, the city has morphed from a land of emigration to a land of immigration. The largest immigrant group comes from the United States (about 9,000 people, partly due to the presence of the military base). Other ethnic minorities come from other European nations (the largest being Serbia, Romania and Moldova), South Asian (the largest being Bangladesh and Pakistan), sub-Saharan Africa and North Africa (largest is from Morocco). The city is predominantly Roman Catholic, but due to immigration, it now has some Orthodox Christian, Muslim and Sikh followers.

3.1.4 The economy

The surrounding country is predominantly agricultural. Major products are wine, wheat, corn, olive oil (in the Barbarano area) and cherries and asparagus are a particularity of Bassano. There are also quarries of marble, sulphur, copper, and silver mines, and beds of lignite and kaolin; mineral springs also abound, the most famous being those of Recoaro.

Massive industrial areas surround the city and extend extensively in the western and eastern hinterland, with numerous steel and textile factories located in the Montecchio

Maggiore, Chiampo and Sovizzo area in the west and Camisano Vicentino and Torri di Quartesolo in the east, areas characterised by a disorganised and extensive cementifaction.

Elite sectors are the jewellery and clothing factories. Important vicentino clothing firms include: Diesel, Pal Zileri, Marzotto, Bottega Veneta, Marlboro Classics etc. The Gold Exposition is world-famous and it takes place in Vicenza twice a year (January and September).

3.2 Presentation of the study area

Here are the results of the activities made by the company GEOLAMBDA Engineering S.r.l during the site visit.

3.2.1 Results of the site observation

The following figure (Photo 3.1) shows the study area in question, located on the southern edge of the capital, along the S.P. 500.

Photo 3.1. Location of the intervention area (Google Earth).

3.2.2 Results of the site investigations

The location of the investigations (Figure 3.3) and different section views (Figure 3.4 and Figure 3.5) are showed in the following:

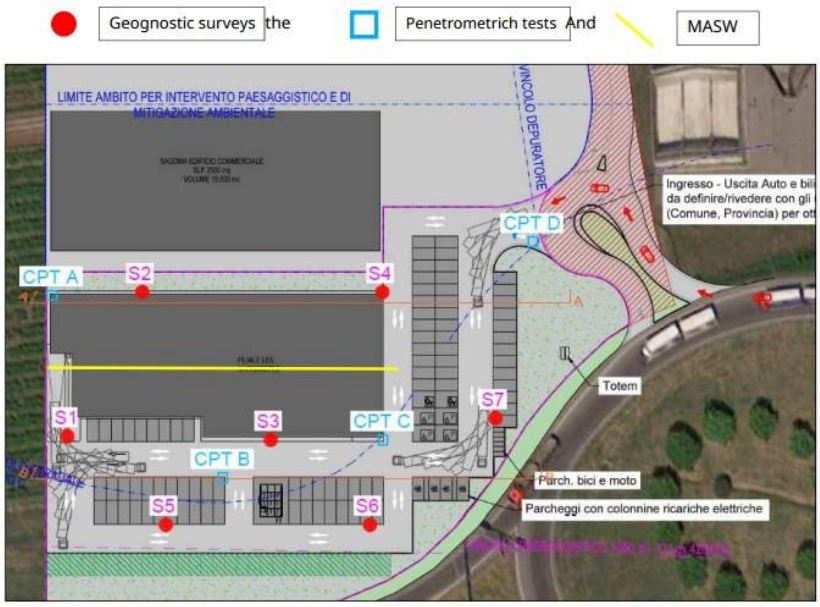

Figure 3.3. Location of the investigations (GEOLAMBDA Engineering S.r.l.,2018)

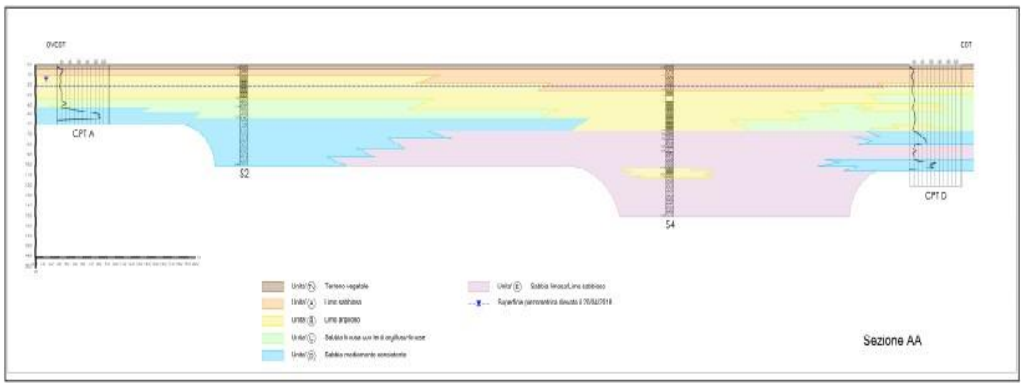

Figure 3.4. Section AA (GEOLAMBDA Engineering S.r.l.,2018)

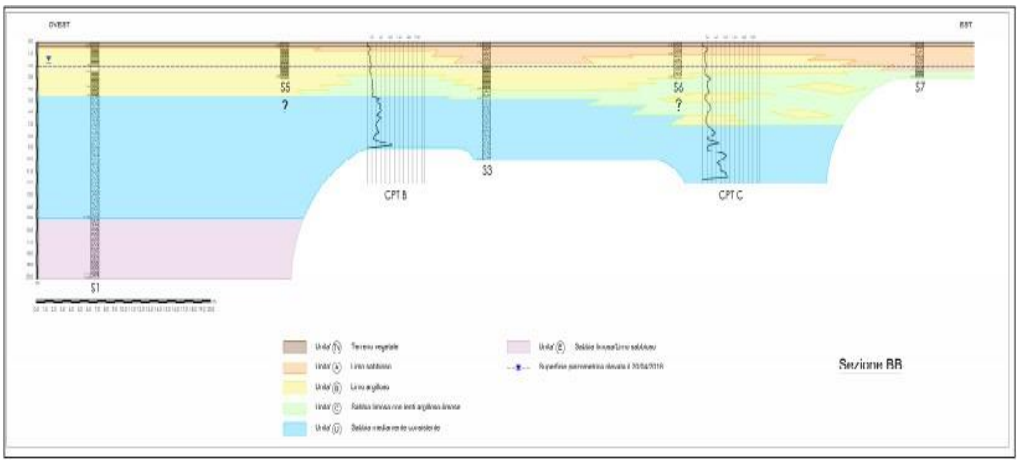

Figure3.5. Section BB (GEOLAMBDA Engineering S.r.l.,2018)

3.2.2.1 Tip and shaft resistance from the penetrometer tests

The results of the tip resistance, lateral resistance and lithological trend from CPT A are showed in Figure 3.6 and Figure 3.7.

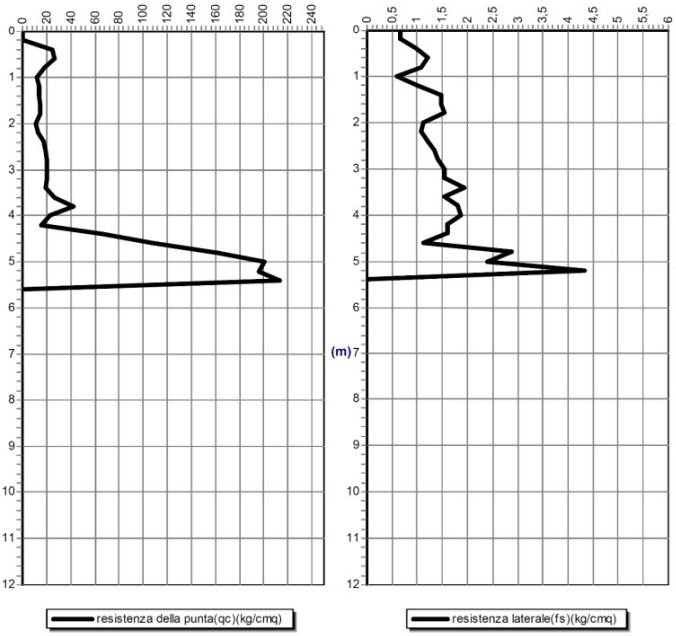

Depth of the water table from the ground level (m): 2

Figure 3.6. Graphs of the tip and the lateral resistance from CPT A (GEOLAMBDA Engineering S.r.l.,2018)

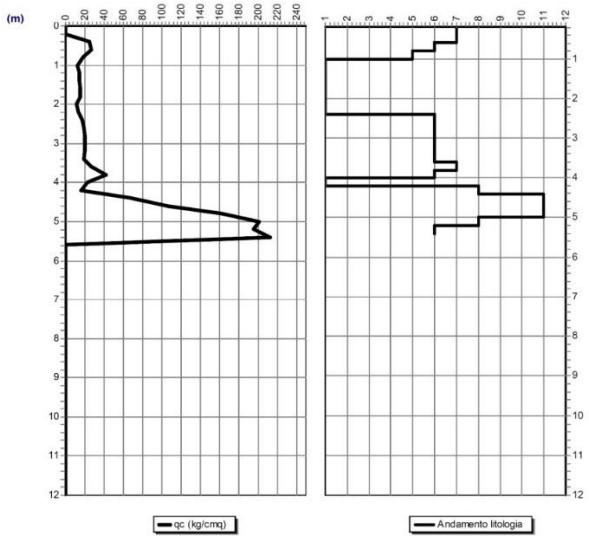

SCHMERTMANN (1978): 1= organic clay-2= very soft silver-3= soft silver-4= medium thick silver-5= thick silver-6= very thick silver-7= sandy/silty silver-8= sand and silt-9= loose sand-10= medium thickened sand-11= thickened sand-12= cemented sand.

Figure 3.7. Tip resistance – lithological trend from CPT A (GEOLAMBDA Engineering S.r.l.,2018)

The results of the tip resistance, lateral resistance and lithological trend from CPT B are showed in Figure 3.8 and Figure 3.9.

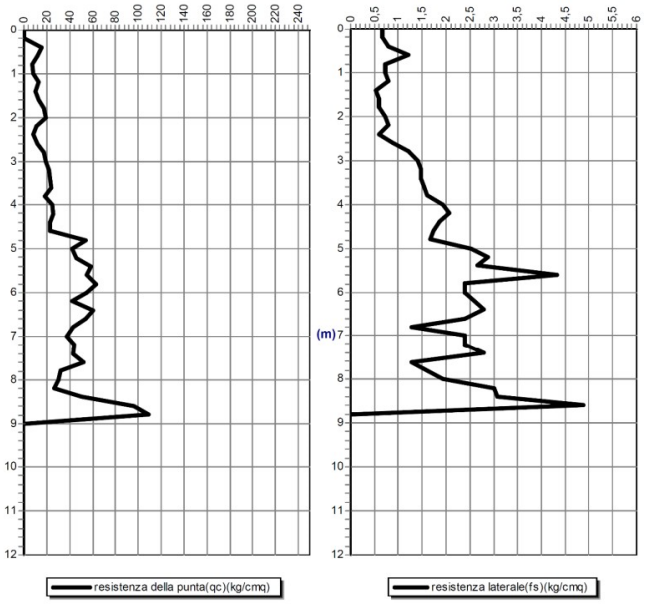

Depth of the water table from the ground level (m): 2

Figure 3.8. Graphs of the tip and the lateral resistance from CPT B (GEOLAMBDA Engineering S.r.l.,2018)

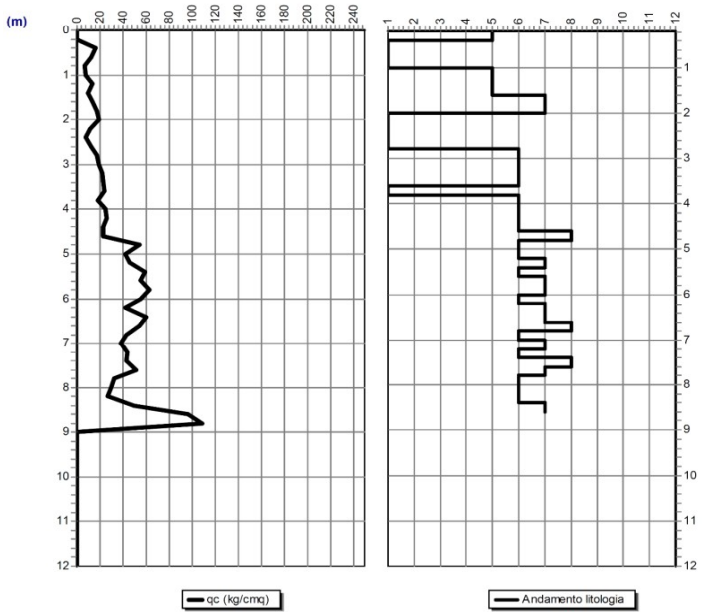

SCHMERTMANN (1978): 1= organic clay-2= very soft silver-3= soft silver-4= medium thick silver-5= thick silver-6= very thick silver-7= sandy/silty silver-8= sand and silt-9= loose sand-10= medium thickened sand-11= thickened sand-12= cemented sand.

Figure 3.9. Tip resistance – lithological trend from CPT B (GEOLAMBDA Engineering S.r.l.,2018)

The results of the tip resistance, lateral resistance and lithological trend from CPT C are showed in Figure 3.10 and Figure 3.11.

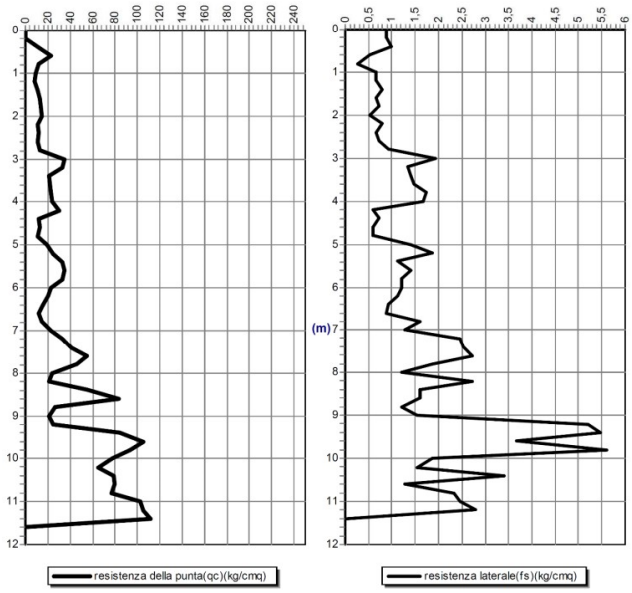

Depth of the water table from the ground level (m): 2

Figure 3.10. Graphs of the tip and the lateral resistance from CPT C (GEOLAMBDA Engineering S.r.l.,2018)

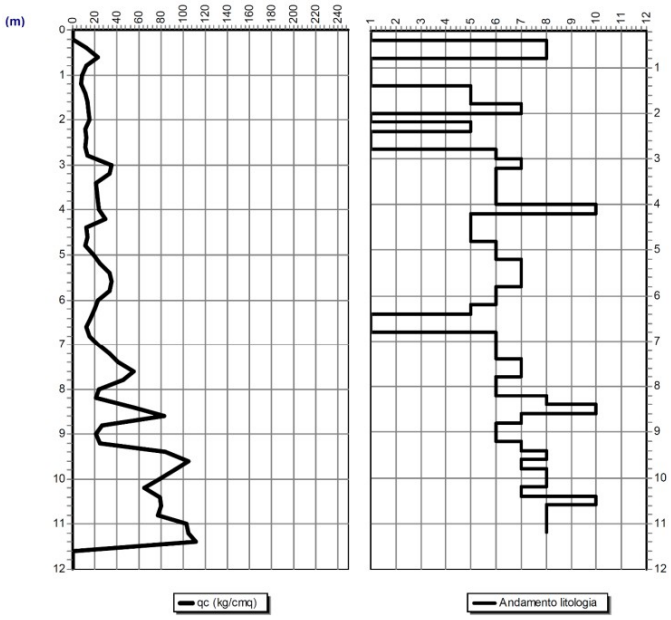

SCHMERTMANN (1978): 1= organic clay-2= very soft silver-3= soft silver-4= medium thick silver-5= thick silver-6= very thick silver-7= sandy/silty silver-8= sand and silt-9= loose sand-10= medium thickened sand-11= thickened sand-12= cemented sand.

Figure 3.11. Tip resistance – lithological trend from CPT C (GEOLAMBDA Engineering S.r.l.,2018)

The results of the tip resistance, lateral resistance and lithological trend from CPT D are showed in Figure 3.12 and Figure 3.13.

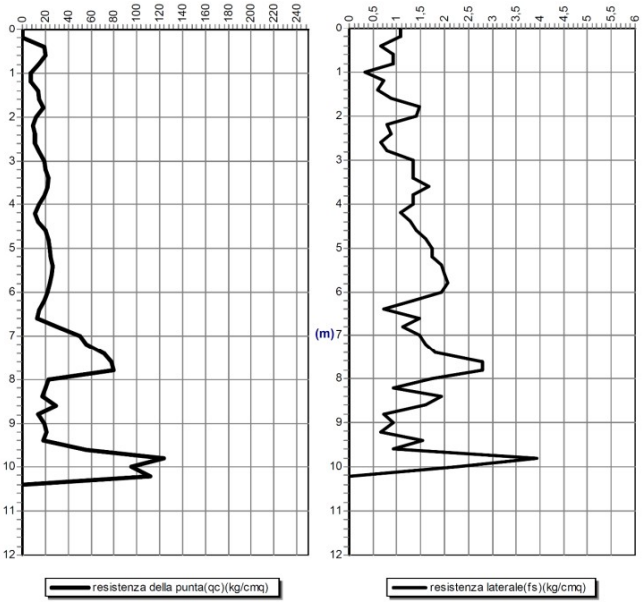

Depth of the water table from the ground level (m): 2

Figure 3.12. Graphs of the tip and the lateral resistance from CPT D (GEOLAMBDA Engineering S.r.l.,2018)

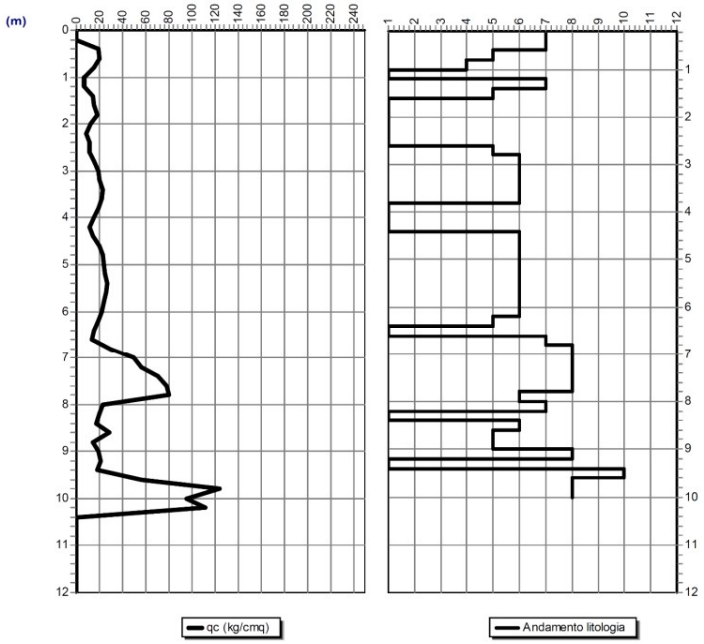

SCHMERTMANN (1978): 1= organic clay-2= very soft silver-3= soft silver-4= medium thick silver-5= thick silver-6= very thick silver-7= sandy/silty silver-8= sand and silt-9= loose sand-10= medium thickened sand-11= thickened sand-12= cemented sand.

Figure 3.13. Tip resistance – lithological trend from CPT D (GEOLAMBDA Engineering S.r.l.,2018)

3.2.2.2 Results of the continuous core drilling

The material, cored and placed in special cataloging boxes of 5 meters each, was described, evaluated and photographed.

a. Stratigraphy and photography from S1 survey

The stratigraphy of the subsoil (Figure 3.14) and the photography of the samples (Photo 3.2, Photo 3.3 and Photo 3.4) from S1 survey is presented below.

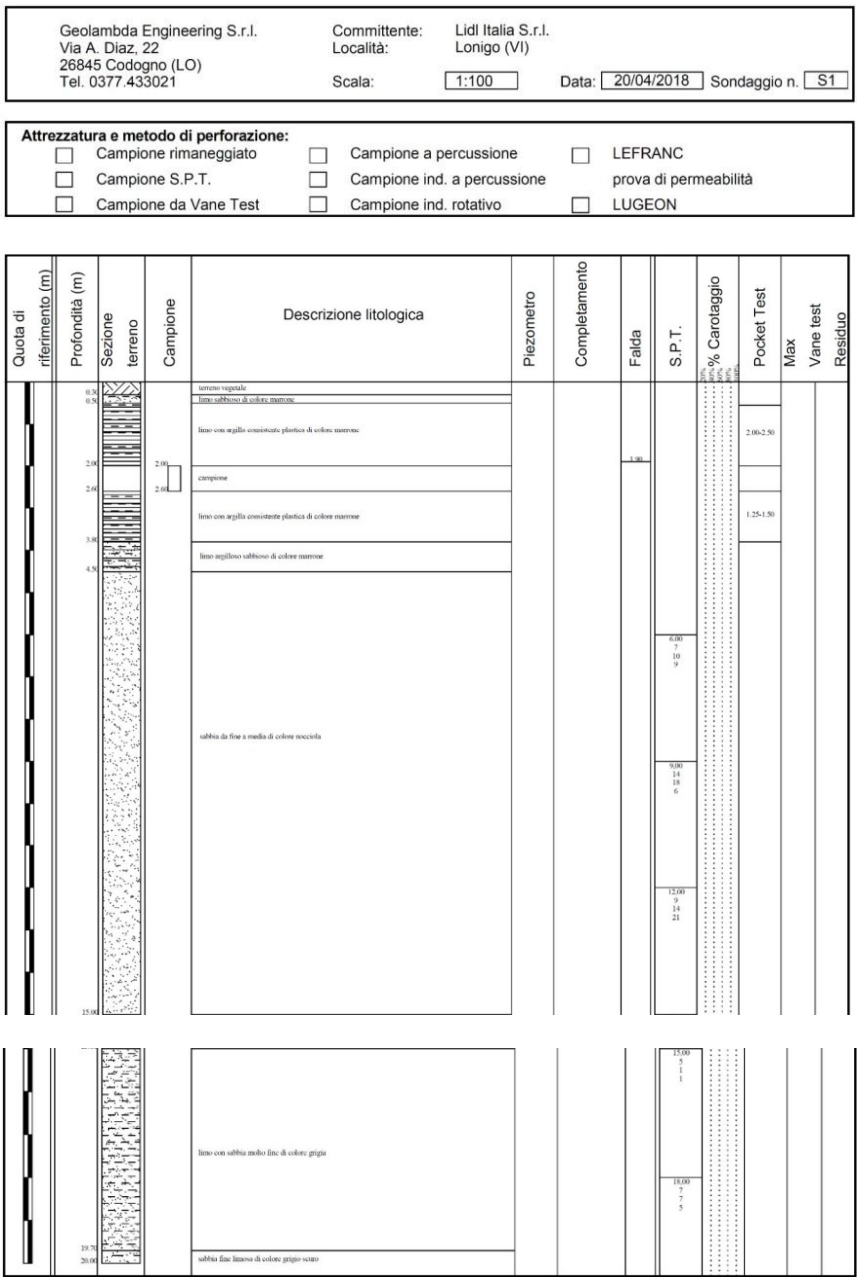

Figure 3.14. Stratigraphy of the soil given by survey S1 (GEOLAMBDA Engineering S.r.l.,2018)

Photo 3.2. S1 survey Samples from 0 to 5 m (GEOLAMBDA Engineering S.r.l.,2018)

Photo 3.3. S1 survey Samples from 5 to 10 m (GEOLAMBDA Engineering S.r.l.,2018)

Photo 3.4. S1 survey Samples from 10 to 15 m (GEOLAMBDA Engineering S.r.l.,2018)

b. Stratigraphy and photography from S2 survey

The stratigraphy of the subsoil (Figure 3.15) and the photography of the samples (Photo 3.5 and Photo 3.6)) from S2 survey is presented below.

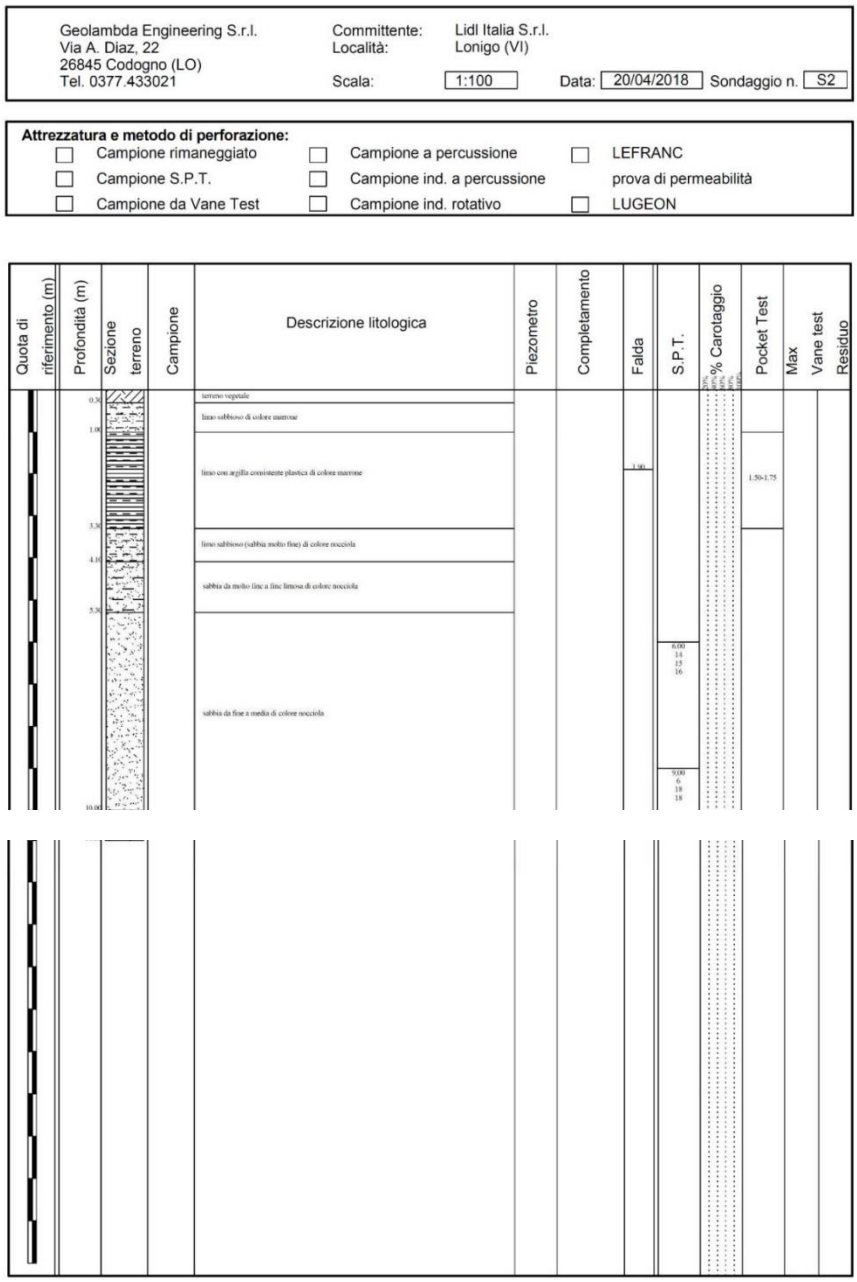

Figure 3.15. Stratigraphy of the soil given by survey S2 (GEOLAMBDA Engineering S.r.l.,2018)

Photo 3.5. S2 Survey samples from 0 to 5 m (GEOLAMBDA Engineering S.r.l.,2018)

Photo 3.6. S2 Survey samples from 5 to 10 m (GEOLAMBDA Engineering S.r.l.,2018)

c. Stratigraphy and photography from S3 survey

The stratigraphy of the subsoil (Figure 3.16) and the photography of the samples (Photo 3.7, and Photo 3.8) from S3 survey is presented below.

Photo 3.7. S3 Survey samples from 0 to 5 m (GEOLAMBDA Engineering S.r.l.,2018)

Photo 3.8. S3 Survey samples from 5 to 10 m (GEOLAMBDA Engineering S.r.l.,2018)

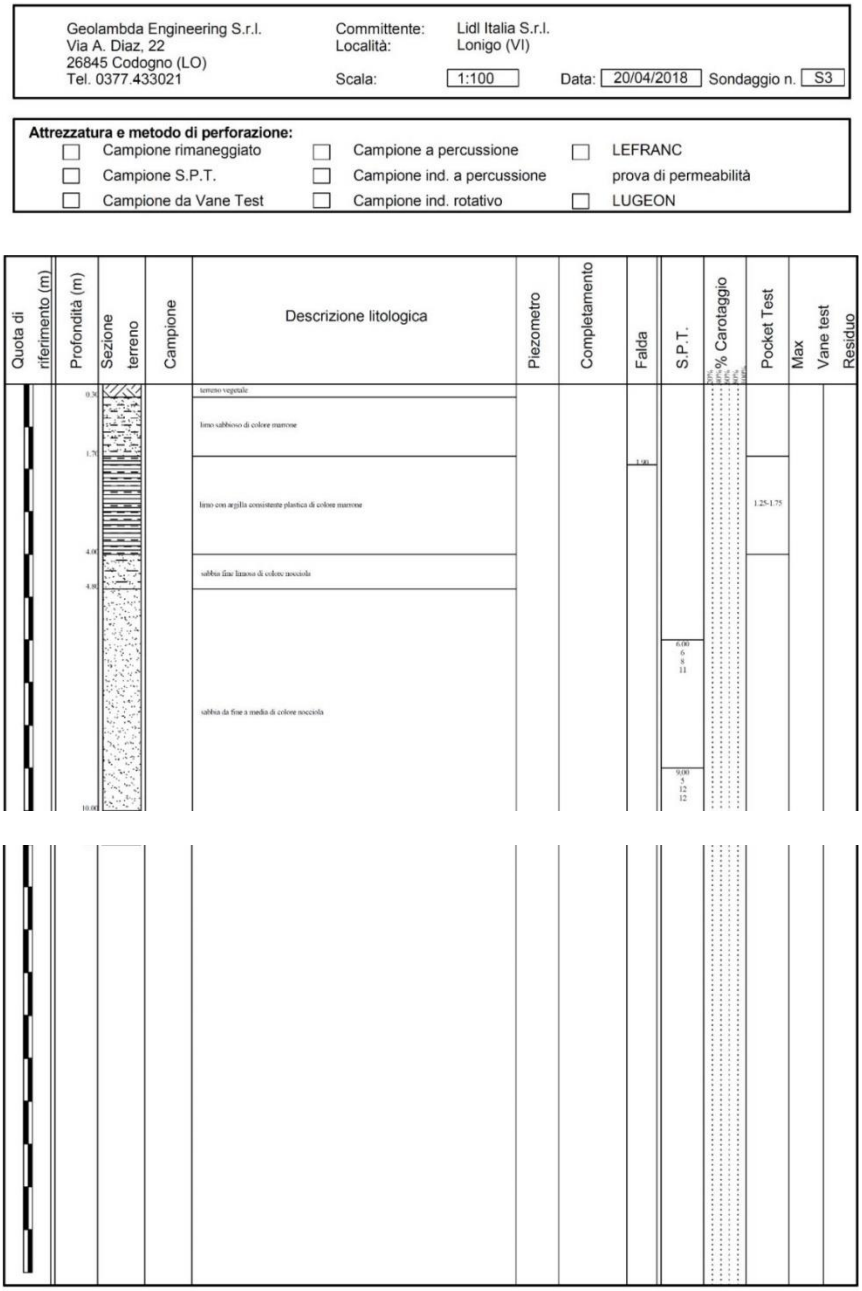

Figure 3.16. Stratigraphy of the soil given by survey S3 (GEOLAMBDA Engineering S.r.l.,2018)

d. Stratigraphy and photography from S4 survey

The stratigraphy of the subsoil (Figure 3.17) and the photography of the samples (Photo 3.9, Photo 3.10 and Photo 3.11) from S4 survey is presented below.

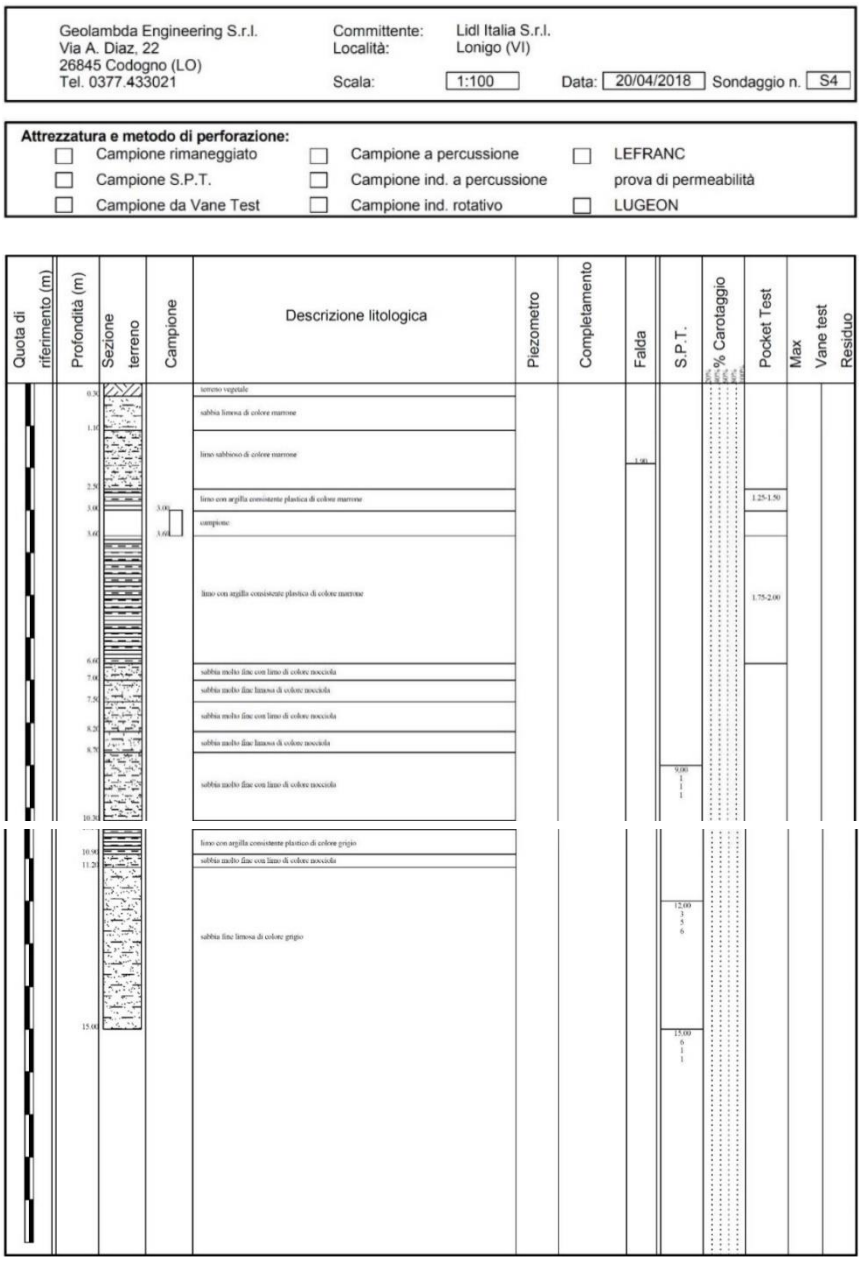

Figure 3.17. Stratigraphy of the soil given by survey S4 (GEOLAMBDA Engineering S.r.l.,2018)

Photo 3.9. S4 Survey samples from 0 to 5 m (GEOLAMBDA Engineering S.r.l.,2018)

Photo 3.10. S4 Survey samples from 5 to 10 m (GEOLAMBDA Engineering S.r.l.,2018)

Photo 3.11. S4 Survey samples from 10 to 15 m (GEOLAMBDA Engineering S.r.l.,2018)

e. Stratigraphy and photography from S5 survey

The stratigraphy of the subsoil (Figure 3.18) and the photography of the samples (Photo 3.12) from S5 survey is presented below.

Photo 3.12. S5 Survey samples from 0 to 3 m (GEOLAMBDA Engineering S.r.l.,2018)

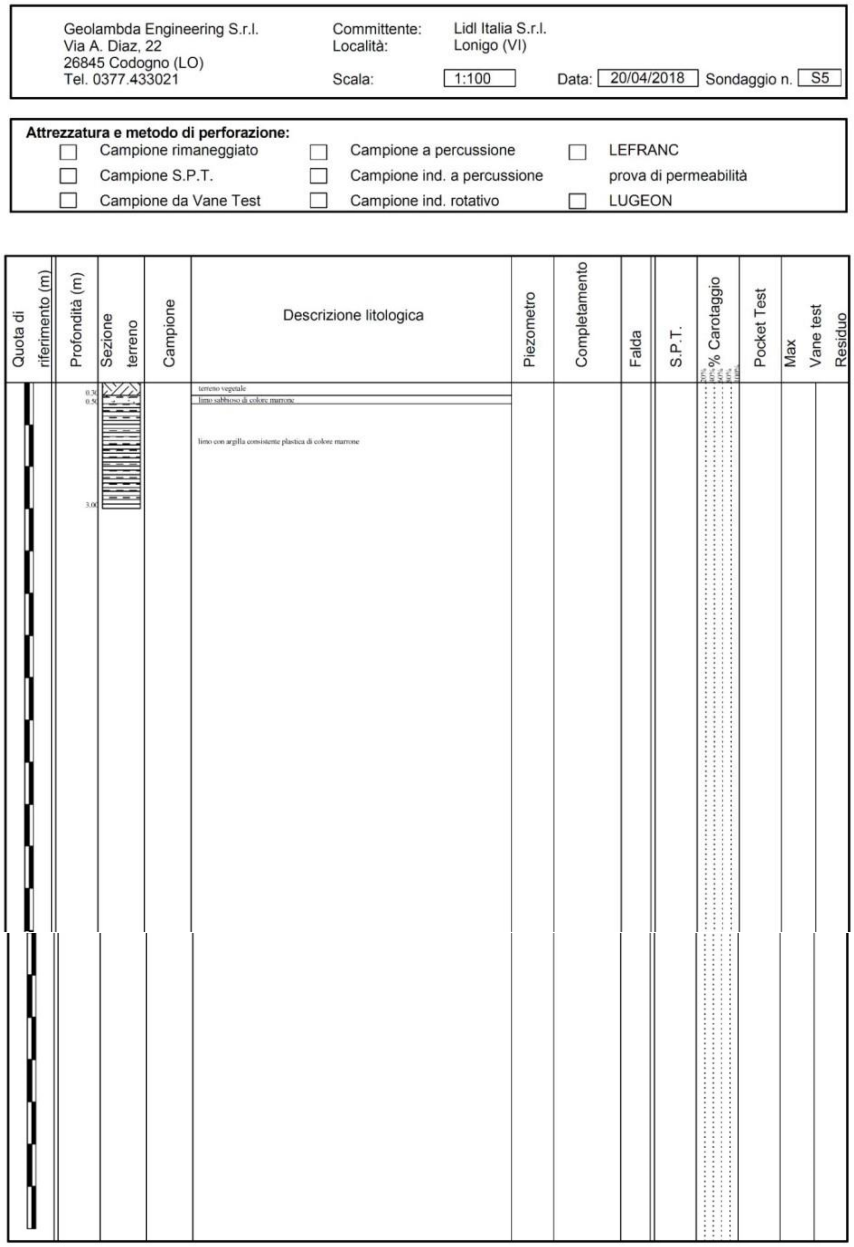

Figure 3.18. Stratigraphy of the soil given by survey S5 (GEOLAMBDA Engineering S.r.l.,2018)

f. Stratigraphy and photography from S6 survey

The stratigraphy of the subsoil (Figure 3.19) and the photography of the samples (Photo 3.13) from S6 survey is presented below.

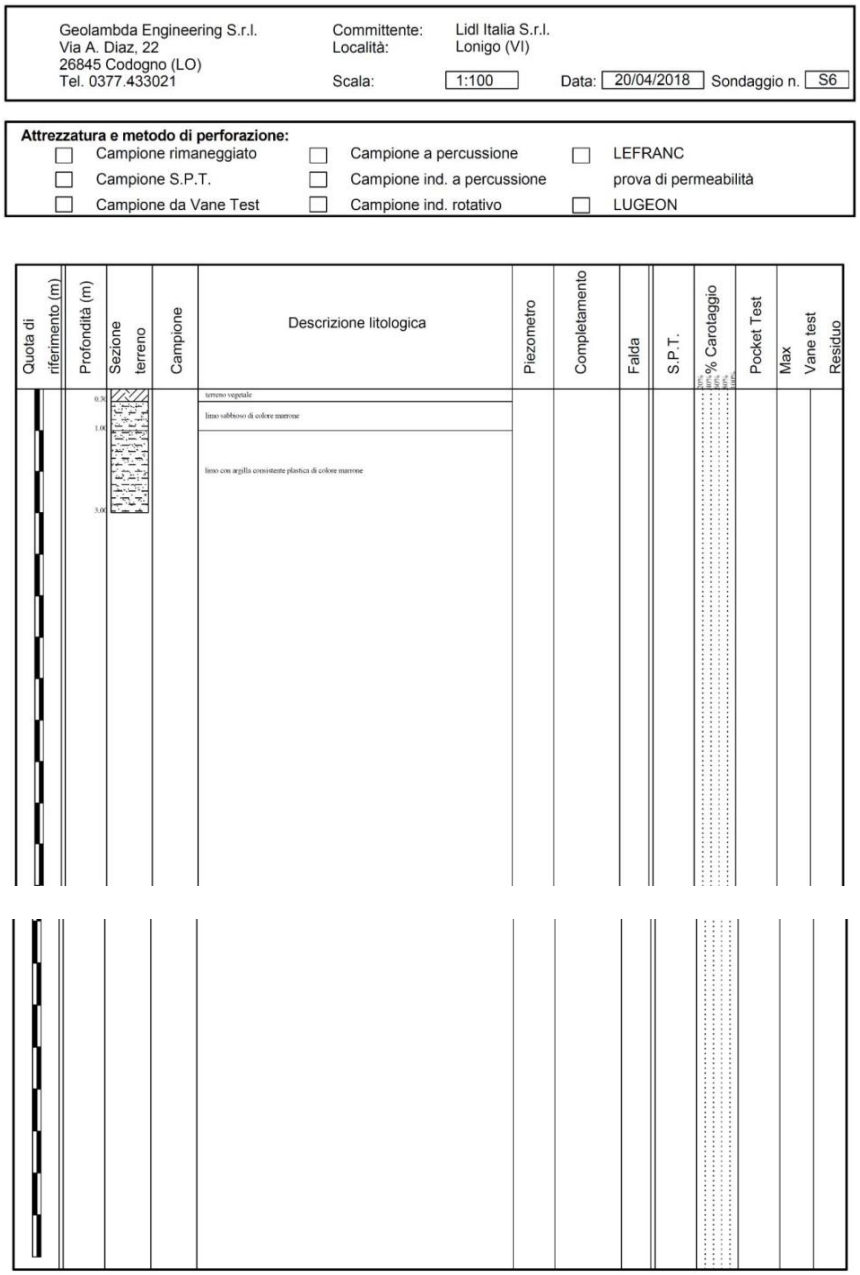

Figure 3.19. Stratigraphy of the soil given by survey S6 (GEOLAMBDA Engineering S.r.l.,2018)

Photo 3.13. S6 Survey samples from 0 to 3 m (GEOLAMBDA Engineering S.r.l.,2018)

g. Stratigraphy and photography from S7 survey

The stratigraphy of the subsoil (Figure 3.20) and the photography of the samples (Photo 3.14) from S7 survey is presented below.

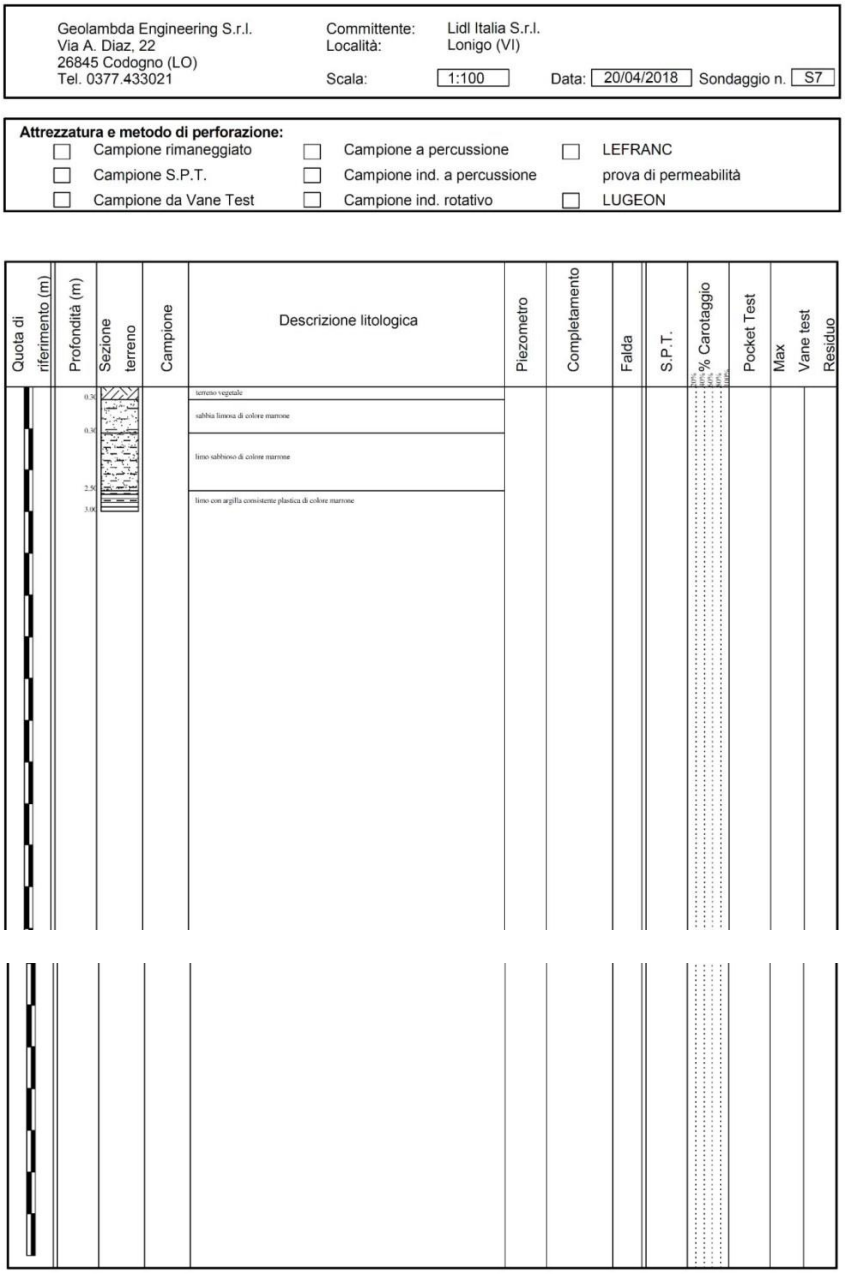

Figure 3.20. Stratigraphy of the soil given by survey S7 (GEOLAMBDA Engineering S.r.l.,2018)

Photo 3.14. S7 Survey samples from 0 to 3 m (GEOLAMBDA Engineering S.r.l.,2018)

3.2.2.3 Photography of the MASW test

The Photo 3.15 shows the execution of the MASW test

Photo 3.15. View of the MASW spreading carried out (GEOLAMBDA Engineering S.r.l.,2018)

3.3 Project presentation

This part consists in the presentation of the geological, seismic and geotechnical results of the study land.

3.3.1 Geological results

3.3.1.1 Geological, geomorphological and hydrogeological framework

The Municipality of Lonigo is part of the southern sector of the Province of Vicenza, extending over a mainly flat strip of land, downstream from the reliefs hills of the Colli Berici ridge, on the left bank of the Adige river. For a correct identification of the outcropping units,

an excerpt is reproduced in Figure 3.21 of the "Geological Map of Italy" – Sheet 49 "Verona", which shows the presence of Holocene alluvial continental deposits (Holocene Unit "al-2").

According to what is indicated in the geological study of the PAT, the substrate consists of the prevalence of poorly consolidated soils (silts and clays) with subordinate intercalations of sandy-gravelly and with poor to mediocre geotechnical characteristics.

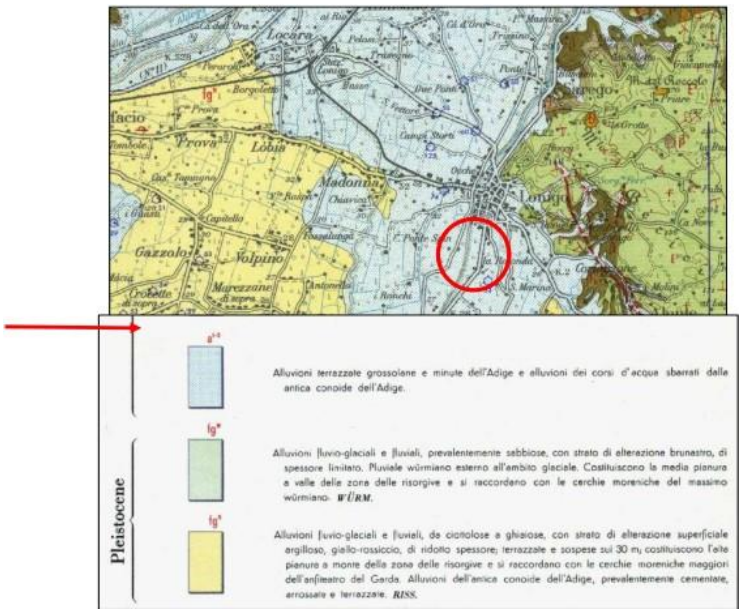

Figure 3.21. Extract from the "Geological Map of Italy" (scale 1:100,000) – Sheet 49 "Verona"

3.3.1.2 Hydrogeological characteristics and piezometry

Within the plain sector analysed, the subsoil consists of a mattress alluvial of a predominantly sandy nature, in which the aquifers are alternated with waterproof successions. In general, the aquifer complex is of the "multi-layer" type.

During the on-site investigations, a groundwater subsidence of approximately 2 m respect to the current ground plan, in accordance with what is indicated in the geological report of P.A.T. which suggests, on the vertical of the area, the presence of a water table with limited depths, with a direction of flow towards the southern quadrants.

3.3.1.3 Seismic framework

As regards the seismic classification, according to the D.C.R. Veneto 67 of 03/12/2003, the intervention area belongs to the seismic zone 3 (as indicated in Figure 3.22).

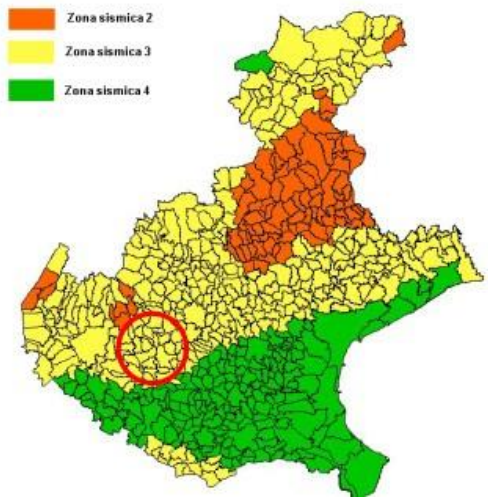

Figure 3.22. Seismic classification of the municipalities of Veneto (D.C.R. Veneto 67 of 03/12/2003).

3.3.1.4 Hydraulic hazard

With regard to the hydraulic hazard of the area, it should be noted that, according to the hydrogeological plan (PAI) of the competent Basin Authority (Brenta-Bacchiglione river), the intervention area is not affected by any kind of danger due to flooding from the lattice hydrographic (as shown in Figure 3.23).

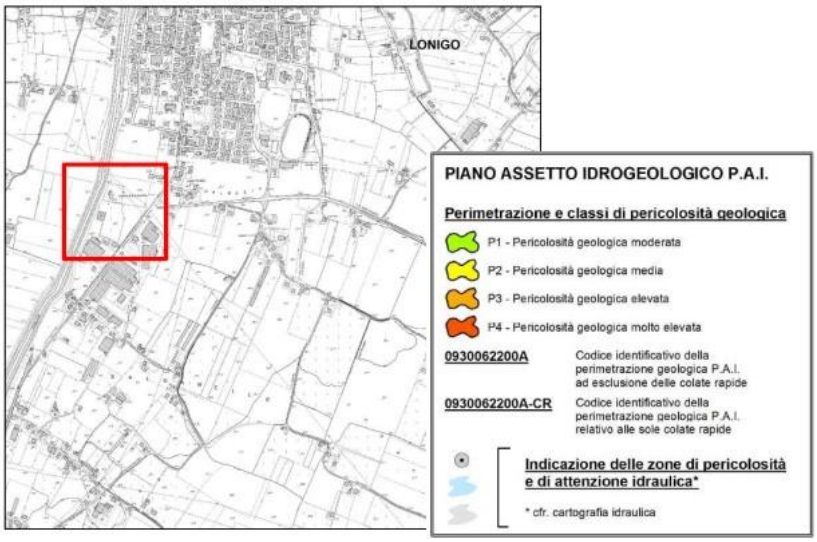

Figure 3.23. Extract from the "Hydraulic Hazard Map" (from the PAI of the Authority of Basin of the Brenta-Bacchiglione River)

3.3.1.5 Constraints and fragility

As regards the constraints and limits on the use of the territory, an excerpt is given in Figure 3.24 of the "Charter of Fragilities" derived from the P.A.T., which shows how the area is

suitable for condition, where the conditioning elements are clearly connected to geotechnical characteristics of the land and, above all, the hydrogeological and hydraulic conditions ("taken from the "P.A.T."). As shown in Figure 3.25 ("Map of invariants" of the P.A.T.), there is no geological constraint in the area.

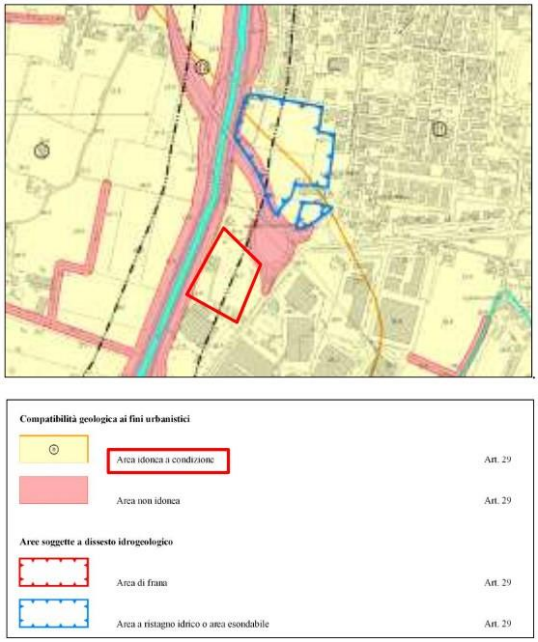

Figure 3.24. Map of fragilities (from: "Territory Planning Plan" P.A.T., Geological report, Municipalities of Lonigo, October 2014).

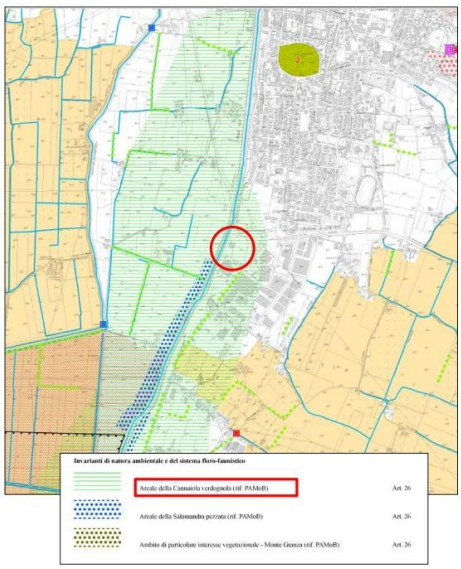

Figure 3.25. Map of the invariants (from: "Territory Planning Plan" P.A.T., Geological report, Municipalities of Lonigo, October 2014).

3.3.2 Seismic results

This part describes the results of the study on the seismic aspects of the area under examination, defining the category of subsoil in accordance with the NTC18 in order to determine the geological characteristics of the site capable of modifying the characteristics of the seismic motion on the surface (modifications of the basic seismic hazard - local amplifications).

3.3.2.1 MASW methodology results

The dispersion curve is presented in Figure 3.26

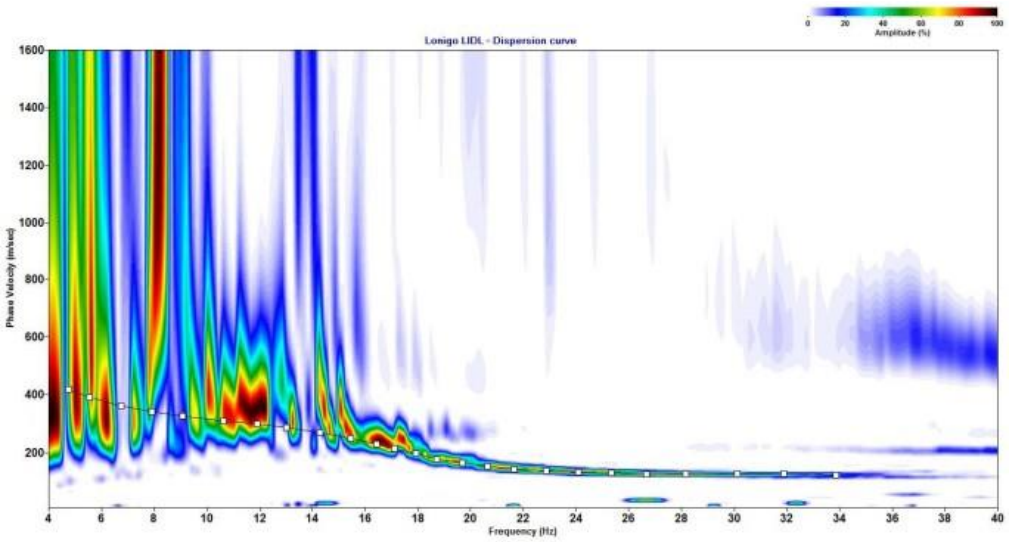

Figure 3.26. Two-dimensional c-f spectrum and picking of the dispersion curve used for the inversion procedure (GEOLAMBDA Engineering S.r.l.,2018)

The analysis of the two-dimensional spectrum c-f allows in this way to reconstruct a one -dimensional seismic model of the subsoil (see Table 3.1), which is constituted by the trend of the speed of the shear waves Vs as a function of depth.

Table 3.1. One-dimensional seismic model (GEOLAMBDA Engineering S.r.l.,2018)

MASW 1			
Layer	Thickness [m]	Vs [m/s]	Depth
1	0.7	**176**	0.7
2	0.9	**121**	1.6
3	1.1	**145**	2.8
4	1.4	**258**	4.2
5	1.8	**272**	5.9
6	2.2	**286**	8.1
7	2.8	**387**	10.9
8	3.5	**377**	14.4
9	4.3	**333**	18.7
10	5.4	**429**	24.1
11	6.7	**368**	30.8
12	7.2	**25**	38.0

From the inversion of the dispersion curve (relating to the "fundamental mode" of the Rayleigh surface waves) we obtain the following average speed model of the shear seismic waves with depth (as shown in Figure 3.27), representative of the investigated area:

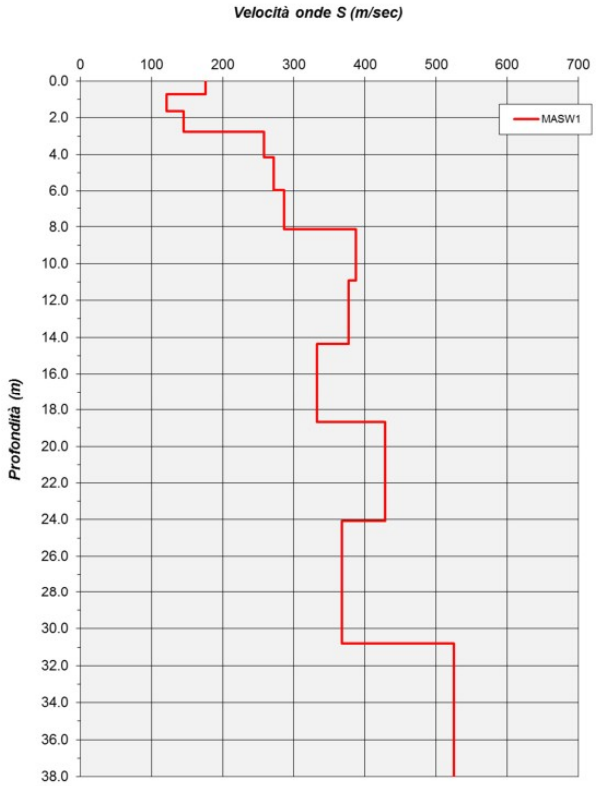

Figure 3.27. average speed model of the shear seismic waves with depth (GEOLAMBDA Engineering S.r.l.,2018)

3.3.2.2 Subsoil category results

Since the seismic bedrock is located beyond 30 m from the foundation plane, according to NTC18 the value of $V_{s,eq}$ coincides with the value of $V_{s,30}$.

Using the formula of equation 2.1, the values of the equivalent shear waves speed are obtained in Table 3.2 (the execution plan of the seismic spreading has been assumed as the calculation level [q. r.]) and the subsoil categories is presented in Table 3.3:

Table 3.2. Subsoil category in function of depth (GEOLAMBDA Engineering S.r.l.,2018)

Depth of laying the foundations from q. r.	Vs, eq = Vs, 30 [m/s]	Subsoil category
1.0 m	321.9	**C**
1.5 m	333.2	**C**

Table 3.3. Categories of subsoil (Ministerial Decree 17.01.2018).

Category	Description
A	Outcrop rock masses or very rigid soils characterized by shear wave speed values higher than 800 m / s, possibly including on the surface soils with poorer mechanical characteristics with a maximum thickness of 3 m
B	Soft rocks and very thickened coarse-grained soil deposits or very consistent fine-grained soils, characterized by an improvement in mechanical properties with depth and by equivalent velocity values between 360 m / s and 800 m / s.
C	Deposits of medium-thickened coarse-grained soils or medium-consistent fine-grained soils with substrate depths greater than 30 m, characterized by an improvement in mechanical properties with depth and equivalent velocity values between 180 m / s and 360 m / s.
D	Deposits of poorly thickened coarse-grained soils or poorly consistent fine-grained soils, with substrate depths greater than 30 m, characterized by an improvement in mechanical properties with depth and equivalent velocity values between 100 and 180 m / s.
E	Soils with characteristics and equivalent velocity values attributable to those defined for categories C or D, with substrate depth not exceeding 30 m.

3.3.2.3 Elastic response spectrum results

Figure 3.28 shows the elastic response spectra required by the anti-seismic legislation for the life-saving limit state SLV and for the limit state of prevention of SLC collapse (formulas reported in paragraph 3.2.3.2.1).

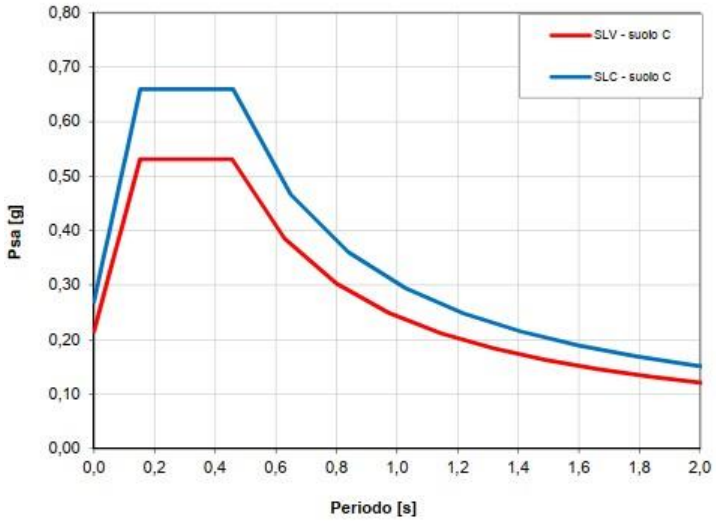

Figure 3.28. Elastic response spectra (GEOLAMBDA Engineering S.r.l.,2018)

3.3.2.4 Liquefaction susceptibility results

Since the exclusion conditions provided by the NTC18 were not met, the liquefaction potential of the land making up the area under consideration was assessed.

The results are plotted in figure 3.29 which shows a very low / negligible risk in relation to potential liquefaction phenomena for the investigated foundation soils.

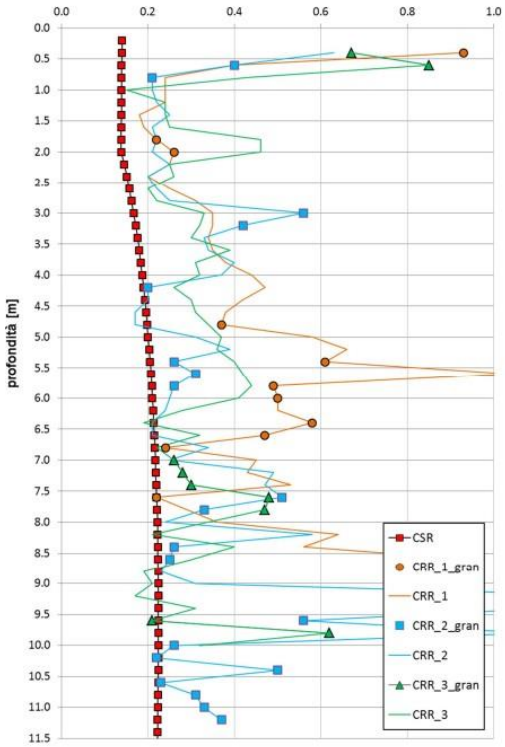

Figure 3.29. Analysis of the liquefaction potential of foundation soils (GEOLAMBDA Engineering S.r.l.,2018)

3.3.3 Geotechnical results

Here are presented the results of the geotechnical investigations.

3.3.3.1 Results of the CPT tests

The readings from the CPT tests are presented in Table 3.4.

Table 3.4. Readings from the CPT (GEOLAMBDA Engineering S.r.l.,2018)

CPT P. A			CPT P. B			CPT P. C			CPT P. D			Unit geotechnical
Prof.	Rp	Rl tot	Prof.	Rp	Rl tot	Prof.	Rp	Rl tot	Prof.	Rp	Rl tot	
m	kg / cm²	kg / cm²	m	kg / cm²	kg / cm²	m	kg / cm²	kg / cm²	m	kg / cm²	kg / cm²	
0.2	-		0.2	-		0.2	-		0.2	-		Ground vegetable
0.4	25	35	0.4	16	26	0.4	12	25	0.4	19	35	
0.6	27	42	0.6	12	24	0.6	23	38	0.6	20	30	Unit A
0.8	18	36	0.8	7	25	0.8	12	20	0.8	15	29	
1.0	12	28	1.0	8	19	1.0	9	13	1.0	7	21	
1.2	14	23	1.2	13	24	1.2	8	18	1.2	7	12	
1.4	14	29	1.4	10	22	1.4	11	21	1.4	14	25	
1.6	15	37	1.6	13	21	1.6	13	25	1.6	15	24	
1.8	15	37	1.8	17	26	1.8	14	24	1.8	18	31	
2.0	11	34	2.0	19	28	2.0	15	26	2.0	12	34	
2.2	13	30	2.2	11	22	2.2	11	19	2.2	9	30	Unit B
2.4	17	33	2.4	8	20	2.4	12	24	2.4	11	23	
2.6	19	37	2.6	12	21	2.6	11	21	2.6	11	24	
2.8	20	40	2.8	17	30	2.8	13	24	2.8	15	25	
3.0	20	41	3.0	19	37	3.0	35	49	3.0	19	31	
3.2	20	43	3.2	22	43	3.2	33	62	3.2	20	40	
3.4	19	42	3.4	23	45	3.4	21	41	3.4	23	43	
3.6	27	56	3.6	24	46	3.6	22	43	3.6	22	42	
3.8	42	65	3.8	18	41	3.8	23	45	3.8	19	44	
4.0	23	50	4.0	25	49	4.0	24	50	4.0	15	35	
4.2	16	44	4.2	26	55	4.2	30	55	4.2	11	31	
4.4	67	91	4.4	23	54	4.4	12	21	4.4	14	30	
4.6	107	131	4.6	23	51	4.6	13	24	4.6	20	39	
4.8	162	179	4.8	54	80	4.8	11	20	4.8	23	44	
5.0	201	244	5.0	42	67	5.0	19	28	5.0	24	48	Unit C
5.2	196	232	5.2	46	84	5.2	25	46	5.2	25	51	
5.4	213	278	5.4	59	102	5.4	33	61	5.4	27	53	
5.6			5.6	55	95	5.6	35	52	5.6	26	55	
5.8			5.8	63	128	5.8	33	54	5.8	24	54	
6.0			6.0	55	91	6.0	23	41	6.0	22	53	
6.2			6.2	42	78	6.2	20	38	6.2	19	48	
6.4			6.4	60	99	6.4	16	33	6.4	15	35	
6.6			6.6	54	96	6.6	12	26	6.6	13	24	
6.8			6.8	43	79	6.8	15	28	6.8	30	52	
7.0			7.0	38	57	7.0	23	47	7.0	50	67	Unit D
7.2			7.2	44	80	7.2	33	52	7.2	56	78	
7.4			7.4	43	79	7.4	41	78	7.4	71	95	
7.6			7.6	52	94	7.6	55	93	7.6	78	105	
7.8			7.8	32	51	7.8	46	87	7.8	80	122	
8.0			8.0	30	54	8.0	24	52	8.0	23	65	
8.2			8.2	27	56	8.2	21	39	8.2	20	46	
8.4			8.4	50	95	8.4	55	96	8.4	17	31	
8.6			8.6	96	142	8.6	83	107	8.6	29	58	Unit E
8.8			8.8	109	182	8.8	27	51	8.8	14	38	
9.0			9.0			9.0	21	39	9.0	19	30	
9.2			9.2			9.2	25	48	9.2	21	35	
9.4			9.4			9.4	84	162	9.4	18	28	
9.6			9.6			9.6	105	187	9.6	56	79	
9.8			9.8			9.8	93	148	9.8	124	138	
10.0			10.0			10.0	78	162	10.0	95	154	
10.2			10.2			10.2	65	93	10.2	112	146	
10.4			10.4			10.4	79	102	10.4			Unit D
10.6			10.6			10.6	80	131	10.6			
10.8			10.8			10.8	77	96	10.8			
11.0			11.0			11.0	103	138	11.0			
11.2			11.2			11.2	105	142	11.2			
11.4			11.4			11.4	112	154	11.4			

3.3.3.2 Results of the SPT test

The following tables (Table 3.5, Table 3.6, Table 3.7 and Table 3.8) are the calculated (and critically corrected) resistance values $(N_1)_{60}$ for the various boreholes and graph of the values of $(N_1)_{60}$ as a function of depth (Figure 3.30)

Table 3.5. Results of the S.P.T. performed in borehole S1 and calculated values of (N1) 60 (GEOLAMBDA Engineering S.r.l.,2018)

Survey S1						
Depth from p.c.	N_1	N_2	N_3	N_{SPT}	$(N_1)_{60}$	Lithology
From 6.00 to 6.45 m	7	10	9	19	19	Fine to medium sand
From 9.00 to 9.45 m	14	18	6	24	23	Fine to medium sand
From 12.00 to 12.45 m	9	14	21	35	32	Fine to medium sand
From 15.00 to 15.45 m	5	1	1	2	2	Silt with sand
From 18.00 to 18.45 m	7	7	5	12	9	Silt with sand

Table 3.6. Results of the S.P.T. performed in borehole S2 and calculated values of (N1) 60 (GEOLAMBDA Engineering S.r.l.,2018)

Survey S2						
Depth from p.c.	N_1	N_2	N_3	N_{SPT}	$(N_1)_{60}$	Lithology
From 6.00 to 6.45 m	14	15	16	31	31	Fine to medium sand
From 9.00 to 9.45 m	6	18	18	36	31	Fine to medium sand

Table 3.7. Results of the S.P.T. performed in borehole S3 and calculated values of (N1) 60 (GEOLAMBDA Engineering S.r.l.,2018)

Survey S3						
Depth from p.c.	N_1	N_2	N_3	N_{SPT}	$(N_1)_{60}$	Lithology
From 6.00 to 6.45 m	6	8	11	19	19	Fine to medium sand
From 9.00 to 9.45 m	5	12	12	24	23	Fine to medium sand

Table 3.8. Results of the S.P.T. performed in borehole S4 and calculated values of (N1) 60 (GEOLAMBDA Engineering S.r.l.,2018)

Survey S4						
Depth from p.c.	N_1	N_2	N_3	N_{SPT}	$(N_1)_{60}$	Lithology
From 9.00 to 9.45 m	1	1	1	2	2	Fine sand with silt
From 12.00 to 12.45 m	3	5	6	11	10	Fine silty sand
From 15.00 to 15.45 m	6	1	1	2	2	Fine silty sand

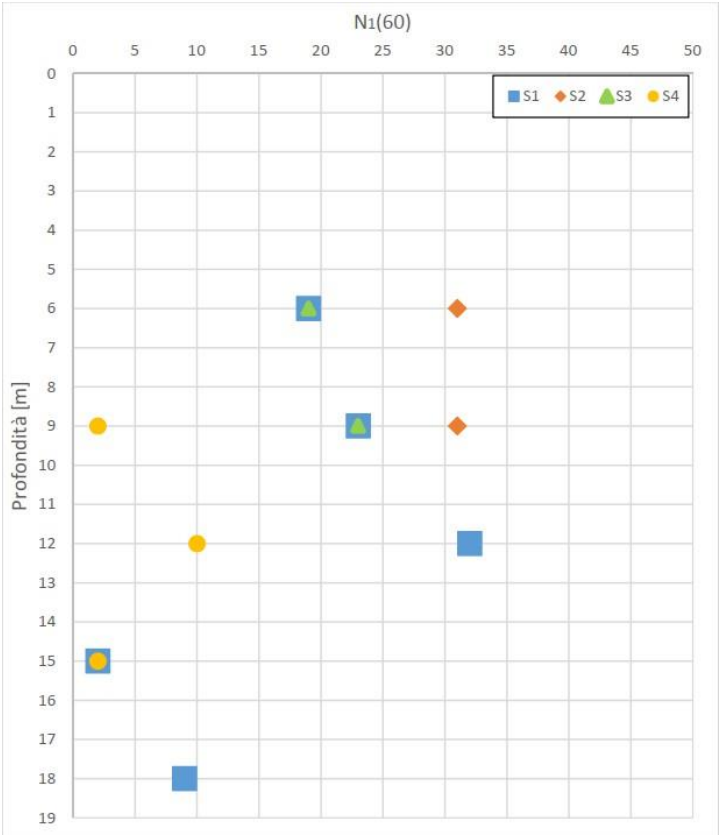

Figure 3.30. Values of $(N_1)_{60}$ determined during the survey as a function of depth (GEOLAMBDA Engineering S.r.l.,2018)

In the reconstruction of the stratigraphy and of the local geotechnical model, the following aspects emerged:

1) The substrate of the planned structures consists of geotechnical units that have different characteristics;
2) During the execution of the on-site tests, underground water was detected at a depth of approximately 2 m compared to the current ground level (the possible piezometric oscillations are not known).

Based on the tests performed, the following geotechnical model was reconstructed (Table 3.9), representative of the area under examination and the starting point for subsequent processing.

Table 3.9. Representation of the geotechnical reference model (GEOLAMBDA Engineering S.r.l.,2018)

Unit A	Under a vegetal and alteration horizon, a deposit develops characterized by a widespread silty-sandy matrix, for which a friction angle Φ = 21° - 23° and a deformation modulus E = 30 – 50 kg/cm² have been calculated. The thickness of Unit A varies up to a maximum of approximately 0.2 m in correspondence of the borehole S1.
Unit B	It is a silty-clayey deposit on average consistent with moderate geotechnical properties; on the basis of the penetrometer resistances and the results of the tests carried out in the laboratory (aimed at estimating the oedometric modulus), a cohesion Cu = 0.5-0.6 kg/cm² and oedometric modulus Ed = 40 – 50 kg/cm² were calculated.
Unit C	It is a silty sand deposit of low density and poor geotechnical properties (Φ = 24° - 25°; E = 50 – 70 kg/cm²), discontinuous in the subsoil of the building under construction, as shown in the sections of annex 3. Inside the deposit there are horizons of worse geotechnical characteristics (similar to the overlying unit B), probably conditioned by a greater silty-clayey fraction.
Unit D	Developed starting from the base of unit C or directly in contact with unit B, unit D is an incoherent deposit (prevailing sand) medium thickened and with discrete geotechnical properties, in the definition of which both the penetrometric results were used, both the SPT tests; a friction Φ = 28° - 30° and a deformation modulus E = 180 – 200 kg/cm² were calculated. Even in this case, it is a discontinuous deposit in the area in question, which overlaps or partially replaces the deposit of worse characteristics of unit E
Unit E	At variable depths between a minimum of approximately 6.6 m (S4, in the eastern sector of the building in the project where it completely replaces units C and D) and 15 m (S1, in the western sector) a silty-sand deposit develops with poor geotechnical characteristics (Φ = 23° - 25°; E = 70 – 90 kg/cm²)

3.3.3.3 Bearing capacity and settlement of the foundation soil

The geotechnical profiles used for the shallow foundations are presented in Figure 3.31 and Figure 3.32

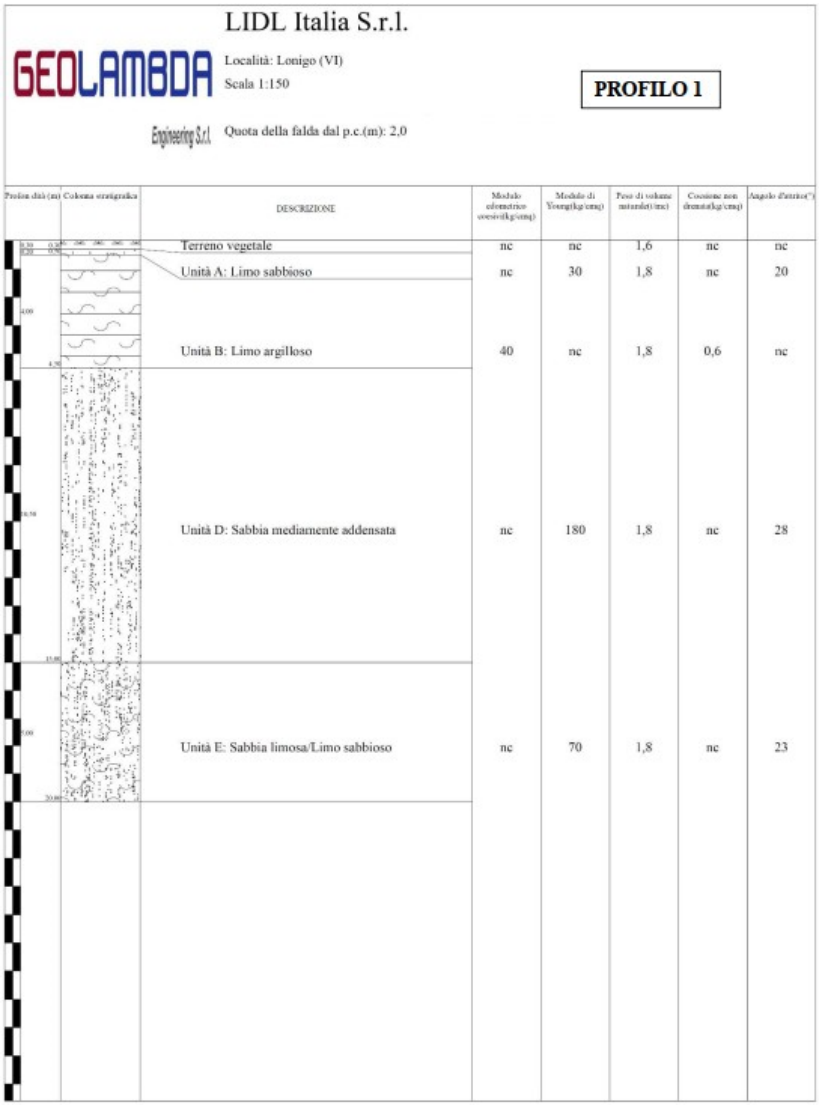

Figure 3.31. Profile n°1 (GEOLAMBDA Engineering S.r.l.,2018)

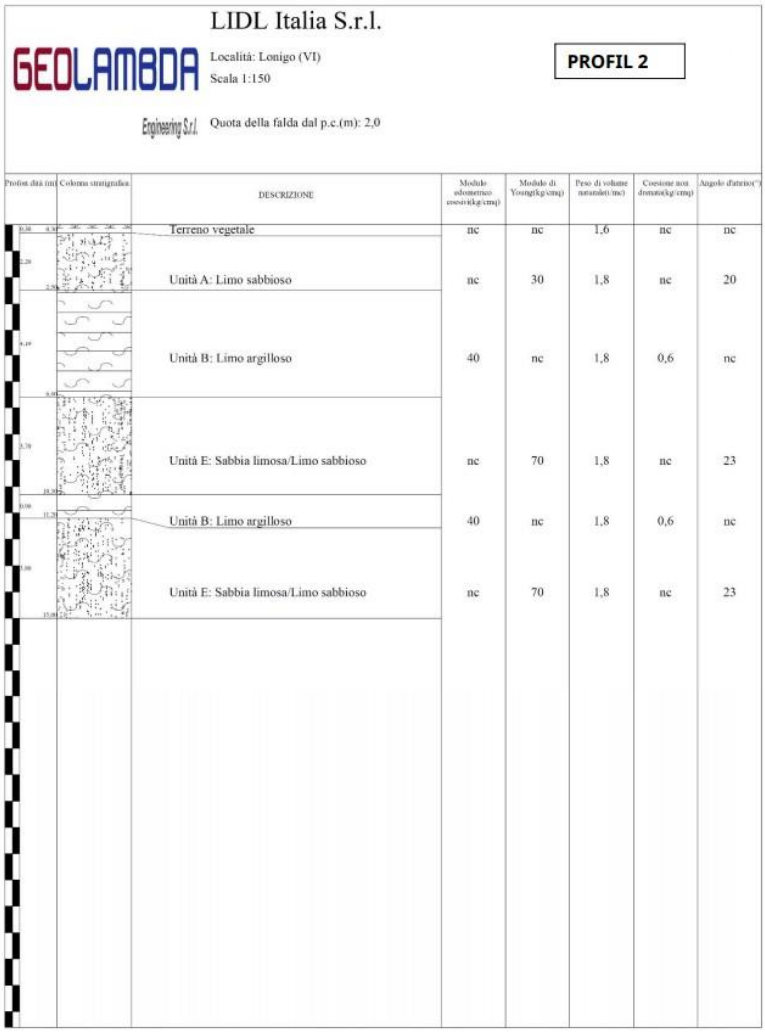

Figure 3.32. Profile n°2 (GEOLAMBDA Engineering S.r.l.,2018)

a. Bearing capacity of the foundation soil

Using the geotechnical responses of the soil in correspondence with profile n°1 (best geotechnical characteristics), the results of the bearing capacities are presented in Table 3.10:

Table 3.10. results of the bearing capacity calculation using profile 1 (GEOLAMBDA Engineering S.r.l.,2018)

FOUNDATION PLINTH - PROFILE 1								
B [cm]	L [cm]	q_{lim} [kg* cm^{-2}]	q_{lim} [kPa]	γ_R	q_{lim}/γ_R [kg*cm^{-2}]	q_{lim}/γ_R [kPa]	R_d [kg*10^3]/ml	R_d [kN]/ml
200	200	4.62	453.07	2.3	2.01	196.99	80.35	787.94
300	300	4.62	453.07	2.3	2.01	196.99	180.78	1772.87
400	400	4.62	453.07	2.3	2.01	196.99	321.39	311.77

Using the geotechnical responses of the soil in correspondence with profile n°2 (best geotechnical characteristics), the results of the bearing capacities are presented in Table 3.11:

Table 3.11. results of the bearing capacity calculation using profile 2 (GEOLAMBDA Engineering S.r.l.,2018)

FOUNDATION PLINTH - PROFILE 2								
B [cm]	L [cm]	q_{lim} [kg* cm^{-2}]	q_{lim} [kPa]	γ_R	q_{lim}/γ_R [kg*cm^{-2}]	q_{lim}/γ_R [kPa]	R_d [kg*10^3]/ml	R_d [kN]/ml
200	200	1.98	194.17	2.3	0.86	84.42	34.43	337.69
300	300	2.22	217.71	2.3	0.97	94.66	86.87	851.90
400	400	2.42	237.32	2.3	1.05	103.18	168.35	1650.93

b. Settlements of the foundation soil

Using the geotechnical responses of the soil in correspondence with profile n°1 (best geotechnical characteristics), the results of the settlements are presented in Table 3.12.

Table 3.12. results of the settlement calculation using scenario 1 (GEOLAMBDA Engineering S.r.l.,2018)

FOUNDATION PLINTH - SCENARIO 1						
B [cm]	L [cm]	q_{lim}/γ_R [kg*cm^{-2}]	q_{lim}/γ_R [kPa]	E_d[kg*10^3]/ml	E_d[kN]/ml	Failure S (mm)
200	200	2.01	196.99	80.35	787.94	75-80
300	300	2.01	196.99	180.78	1772.87	100-110
400	400	2.01	196.99	321.39	3151.77	120-130

Using the geotechnical responses of the soil in correspondence with profile n°2 (best geotechnical characteristics), the results of the settlements are presented in Table 3.13.

Table 3.13. results of the settlement calculation using scenario 2 (GEOLAMBDA Engineering S.r.l.,2018)

FOUNDATION PLINTH - SCENARIO 2						
B [cm]	L [cm]	q_{lim}/γ_R [kg*cm^{-2}]	q_{lim}/γ_R [kPa]	E_d[kg*10^3]/ml	E_d[kN]/ml	Failure S (mm)
200	200	0.86	84.42	34.43	337.69	35-37
300	300	0.97	94.66	86.87	851.90	45-47
400	400	1.05	103.18	168.35	1650.93	62-64

From the calculations carried out in both scenarios, values higher than the limits suggested by traditional geotechnics (25-30 mm) are deduced if actions (E_d) corresponding to the ground resistances (R_d) calculated as ULS GEO in approach 2 are applied.

Even with the same foundation geometry and structural stresses on the entire building site, there will also be differential settlements resulting from the uneven lateral-vertical distribution of the geotechnical units, to be appropriately considered in the structure design.

However, it should be remembered that for the determination of the geotechnical SLS an interaction between geotechnical evaluations and structural design needs is necessary: the settlements, in fact, are function of both the geometry of the foundation and the applied loads (design actions) while the maximum acceptable deformation of the superstructure can only be defined in the structural design. The information on settlements, therefore, is not to be considered a definitive evaluation on geotechnical SLS, but rather an essential first approach for their determination.

To limit subsidence and improve the geotechnical response to structural stresses, the solution could lie in the adoption of adequately sized foundation piles: even in this case, however, due to the articulated geotechnical and stratigraphic model and not knowing precisely the exact lateral-vertical distribution of the geotechnical units, it is advisable to adopt the worst profile among those detected as a precaution.

3.4 Design of the FDP pile

For the foundation structure to be much more stable and able to resist the structural load from the upper structure, the choice of and FDP pile of length 14.63 m and a diameter of 600 mm was done as regards to the stratigraphy of our subsoil and the ability of FDP pile to have high bearing capacity greater than CFA technology and the other bored piles of same diameter.in this part we showed the results of the design procedure using respectively analytical method, empirical method, static load test and we finished by presenting our design based on the pile installation data.

3.4.1 Analytical formulation results

In this part we presented the results of the tip and of the lateral resistance using ground characteristics from survey S1 (Table 3.14) and S4 (Table 3.15).

Table 3.14. Stratigraphy of the soil given by the S1 survey

layer	type	top (m)	bottom (m)	thickness	$\gamma\,(t/m^3)$	$\gamma\,(kN/m^3)$	$\gamma_{sat}\,(kN/m^3)$	$\gamma'\,(kN/m^3)$	$C_u\,(kg/cm^2)$	$C_u(kPa)$	$\emptyset(°)$	$\emptyset(radian)$
1	Vegetal land	0	0.3	0.3	1.6	15.69064	15.69064	5.89064				0
2	Sandy Silt	0.3	0.5	0.2	1.8	17.65197	17.65197	7.85197			20	0.34906585
3	Clayey Silt	0.5	4.5	4	1.8	17.65197	17.65197	7.85197	0.6	58.8399		0
4	Medium thickened sand	4.5	15	10.5	1.8	17.65197	17.65197	7.85197			28	0.488692191
5	Silty Sand/ Sandy Silt	15	20	5	1.8	17.65197	17.65197	7.85197			23	0.401425728

Table 3.15. Stratigraphy of the soil given by the S4 survey

layer	type	top (m)	bottom (m)	thickness	$\gamma\ (t/m^3)$	$\gamma\ (kN/m^3)$	$\gamma_{sat}\ (kN/m^3)$	$\gamma'\ (kN/m^3)$	$C_u\ (kg/cm^2)$	$C_u(kPa)$	$\emptyset(°)$	$\emptyset(radian)$
1	Vegetal land	0	0.3	0.3	1.6	15.69064	15.69064	5.89064	-			0
2	Sandy silt	0.3	2.5	2.2	1.8	17.65197	17.65197	7.85197			20	0.34906585
3	Clayey silt	2.5	6.6	4.1	1.8	17.65197	17.65197	7.85197	0.6	58.8399		0
4	Silty Sand/ Sandy Silt	6.6	10.3	3.7	1.8	17.65197	17.65197	7.85197			23	0.401425728
5	Clayey silt	10.3	11.2	0.9	1.8	17.65197	17.65197	7.85197	0.6	58.8399		0
6	Silty Sand/ Sandy Silt	11.2	15	3.8	1.8	17.65197	17.65197	7.85197			23	0.401425728

We first start by computing the tip bearing capacity of our pile and the analyze was done in drained conditions since we observed the occurrence of sandy material at the pile tip. The N_q factor was computed using the Berezantsev approach and we choose to use a friction angle equal to the original one because we consider that our pile installation conditions is situated between driven and drilled situations. We consider driven conditions since we have a densification of the lateral soil during the pile execution inducing and increase of the friction resistance and we also considered drilled because the pile execution is done similarly as CFA piles since we have a combined action of torque and axial thrust. The values of the effective stress and the N_q factor from survey S1 and S4 are given in Table 3.16 and Table 3.17.

Table 3.16. Effective stress and Nq value from survey S1

Layer	2	4	5
σ'_{VL}	3.53	132.08	171.34
Nq		15	

Table 3.17. Effective stress and N_q value from survey S4

Layer	2	4	6
σ'_{VL}	33.93	95.18	132.08
Nq			10

After having computed the effective stress at each depth and the Nq value at the tip of the pile, we computed the tip bearing capacity considering drained conditions. The values can be seen in Tables 3.18 and 3.19.

Table 3.18. Tip bearing capacity from survey S1

Layer	**2**	**3**	**4**	**5**
$q_{b,ult}$ (kN/m²)	0	0	1981.26	0
Q_b (kN)	**0**	**0**	**560.19**	**0**
Ab (m²) =	0.28			

Table 3.19. Tip bearing capacity from survey S4

Layer	2	3	4	5	6
$q_{b,ult}$ (kN/m²)	0	0	0	0	1320.84
Q_b (kN)	0	0	0	0	**373.46**
Ab (m²) =	0.28				

We continued by computing the lateral resistance of our pile by considering drained and undrained conditions since the water table is located at a depth of 2 m below the ground level. At this stage we first obtained the values of parameters entering in the shaft resistance evaluation as we can see in Tables 3.20 and 3.21.

Table 3.20. Shaft resistance parameters from survey S1

Layer	2	4	5
K	0.66	0.53	0.61
δ	0.35	0.49	0.40
σ'_z	3.53	132.08	171.34

Layer	3
C_u	58.84
α	0.67

Table 3.21. Shaft resistance parameters from survey S4

Layer	2	4	6
K	0.66	0.61	0.61
δ	0.35	0.40	0.40

Layer	3
C_u	58.84
α	0.43

Knowing the values of the lateral resistance parameters we computed the value of the shaft resistance by associating to each layer the corresponding thickness as shown in Tables 3.22 and 3.23

Table 3.22. Shaft resistance at different layer from survey S1

Layer	2	3	4	5	
q_{sli} (kN/m²)	0.85	39.60	37.26	44.31	
A_{sLi} (m²)	0.94	7.54	19.09	0.00	
Qs (kN)	**0.80**	**298.54**	**711.45**	**0.00**	
L	0.5	4	10.13	0	14.63

Table 3.23. Shaft resistance at different layer from survey S4

Layer	2	3	4	5	6	
q_{sli} (kN/m²)	8.12676678	25.2588393	24.6153067	25.2588393	34.15946	
A_{sLi} (m²)	4.71238898	7.72831793	6.97433569	1.69646003	6.46539768	
Qs (kN)	**38.2964862**	**195.208341**	**171.675412**	**42.8506114**	**220.854493**	
L	2.5	4.1	3.7	0.9	3.43	14.63

3.4.2 Results of the empirical formulation

The computation of the bearing capacity and of the lateral resistance was made through the use of the data given by CPT and SPT tests at various depth

3.4.2.1 Bearing capacity from CPT tests

In our studied area four (4) CPT tests was made named as CPT A, CPT B, CPT C, CPT D. due to the fact that CPT C and CPT D were more deeper going from 0.2 m to 11.4 m and 0.2 to 10.2 m respectively we were more confident using their results and so we skiped to use the data given by the other CPT tests.

We first started by computing the tip resistance of our pile and since our retain CPT tests were not deep enough to reach the depth of our pile which was 14 m depth, we assumed that for CPT C we can used at the pile tip the average value of the cone resistance from 11.00 to 11.40 m which gave to us a value of 106.67 kg/cm^2 and for CPT D we used for the pile tip the average value of the cone resistance from 9.80 to 10.20 m which gave to us a value of 110.33 kg/cm^2. With those values, we computed the tip resistances of our pile as we can see in Table 3.24.

Table 3.24. Tip resistance from CPT C and CPT D

	cpt C	cpt D
L (m)	11.4	10.2
D (m)	0.6	0.6
L-4D	9	7.8
L+D	12	10.8
q_c (kg/cm²)	106.67	110.33
material	Sand	Sand
c_p	0.41	0.41
q_{bL} (kg/cm²)	43.73	45.24
q_{bL} (kpa)	4288.77	4436.20

Then we continued by computing the lateral resistance of our pile and since our tests were not deep enough we first assumed that the lateral resistance at 14.63 m depth is the average value from 9.60 to 11.40 m depth which gave us 135.30 kg/cm² for CPT C and the average value from 9.60 to 10.2 m depth which gave us 129.25 kg/cm² for CPT D.

To compute the lateral resistance we used the average value from 0.2 to 14.63 m which gave us 26.08 kg/cm² for CPT C and 21.52kg/cm² for CPT D. Those last values were used to compute the lateral resistance respectively for CPT C and for CPT D as we can see in Table 3.25.

Table 3.25. Lateral resistance from CPT C and CPT D

cpt C				
material	**q_{si} (kg/cm²)**	**c_s**	**q_{si} (kg/cm²)**	**q_{si} (kpa)**
sand	26.08	0.01	0.15	14.58
cpt D				
material	**q_{si} (kg/cm²)**	**c_s**	**q_{si} (kg/cm²)**	**q_{si} (kpa)**
sand	21.52	0.01	0.12	12.03

3.4.2.2 Bearing capacity from SPT tests

In our case study seven (7) continuous core drilling were made within wich four (4) SPT tests. In this part; we usd the data given by the SPT tests to design our FDP pile.

Only two (2) SPT tests within the four (4) that was made were deeper enough to reach a value greater than 14.63 m which is our pile length. The datas given by the other two SPT tests were not consider reliable and were skipped. So the SPT from survey S1 and the SPT from survey S4 was used to design our FDP pile.

When designing the tip resistance, we assumed to have a blowcount a bit larger than the one in the range of 15.00 to 15.45 m because our pile depth is at 14.63 m and we observed the decreasing with depth of the blowcount. We also considered from the stratigraphies to have silty sand as material at the tip of our pile which gave to us a value of $n_b = 2.05$.

For the shaft resistance according to Meyerhof (1976,1983), n_{si} is 0.02 for full displacement pile.

Those values permit us to compute the tip bearing capacity and the lateral resistance of our pile as shown in Tables 3.26 and 3.27.

Table 3.26. Tip resistances from SPT tests in surveys S1 and S4

	Survey S1	**Survey S4**
L (m)	18.45	15.45
D (m)	0.6	0.6
L-1.5D	17.55	14.55
L+1.5D	19.35	16.35
N_b	3.8	3.8
material	Sandy silt	Sandy silt
n_b	2.05	2.05
q_{bL}/p_a	7.79	7.79
q_{bL} (kpa)	779	779

Table 3.27. Shaft resistances from SPT tests in surveys S1 and S4

Survey S1	N_{si}	19	23	32	2	9
	material	medium Sand	medium Sand	medium Sand	Silty Sand	Silty Sand
	n_{si}	0.02	0.02	0.02	0.02	0.02
	q_{si}/p_a	0.38	0.46	0.64	0.04	0.18
	q_{si} (kpa)	38	46	64	4	18
	L	9.45	5.18	0		
Survey S4	N_{si}	2	10	2		
	material	Silty Sand/ Sa	Silty Sand/ Sa	Silty Sand/ Sandy Silt		
	n_{si}	0.02	0.02	0.02		
	q_{si}/p_a	0.04	0.2	0.04		
	q_{si} (kpa)	4	20	4		

3.4.3 Summary of the design methods used

We computed the total resistance by adding the product of the tip resistance with the cross-sectional area of the pile to the product of the shaft resistance with the corresponding length. The total bearing capacities obtained from the methods above are showed on Table 3.28, Table 3.29, Table 3.30, Table 3.31, Table 3.32 and table 3.33.

Table 3.28. Total resistance from survey S1

Survey S1			
Depth (m)	**Tip bearing capacity**	**Shaft bearing capacity**	**Total bearing capacity**
	qbi (kpa)	**Qsi (kN)**	**Q (kN)**
0.5	0.00	0.80	0.80
4.5	0.00	298.54	298.54
14.63	1981.26	711.45	1271.64
	0.00	0.00	0.00
Characteristique resistance (kN)			**1570.97**

Table 3.29. Total resistance from survey S4

Survey S4			
Depth (m)	**Tip bearing capacity**	**Shaft bearing capacity**	**Total bearing capacity**
	q_{bi} (kpa)	**Q_{si} (kN)**	**Q (kN)**
2.5	0.00	38.30	38.30
6.6	0.00	195.21	195.21
10.3	0.00	171.68	171.68
11.2	0.00	42.85	42.85
14.63	1320.84	220.85	594.31
15		0.00	373.46
Characteristique resistance (kN)			**1415.80**

Table 3.30. Total resistance from CPT C

cpt C		
Tip bearing capacity	**Shaft bearing capacity**	**Characteristique resistance**
kpa	**kpa**	**kN**
4288.77	14.58	**1614.65**

Table 3.31. Total resistance from CPT D

cpt D		
Tip bearing capacity	**Shaft bearing capacity**	**Characteristique resistance**
kpa	**kpa**	**kN**
4436.20	12.03	**1586.03**

Table 3.32. Total resistance from SPT S1

	Spt S1				
L	depth (m)	N	Tip resistance (kpa)	Shaft resistance (kpa)	Total resistance (kN)
6.45	From 6.00 to 6.45	19	0	38	462.00
3	From 9.00 to 9.45	23	0	46	260.12
5.18	From 12.00 to 12.45	32	0	64	624.90
0	From 15.00 to 15.45	2	779	4	220.26
14.63	**Characteristique resistance (kN)**				**1567.28**

Table 3.33. Total resistance from SPT S2

	Spt S4				
L	depth (m)	N	Tip resistance (kpa)	Shaft resistance (kpa)	Total resistance (kN)
9.45	From 9.00 to 9.45	2	0	4	71.25
5.18	From 12.00 to 12.45	10	0	20	195.28
0	From 15.00 to 15.45	2	779	4	220.26
14.63	**Charateristique resistance (kN)**				**486.79**

The results are in general coherent because the values seem to be very close except the bearing capacity from SPT S2 which is far lower than the others and so was not consider reliable and was not included in the computation of the characteristic resistance. The Table 3.34 shows the beating capacities used in the computation of the characteristic resistance.

Table 3.34. Summary of the total resistance from the design methods

R_c		R_c		R_c	
Survey S1	**Survey S2**	**Spt S1**		**Cpt C**	**Cpt D**
1570.97	1415.80	1567.28		1614.65	1586.03

From the above we computed the minimum and the average value of the bearing capacities which is showed in Table 3.35

Table 3.35. Average and minimum value of the total resistance

$R_{c,mean}$ =	1033.97	kN
$R_{c,min}$ =	1056.57	kN

According to NTC18, knowing the average and minimum values of the bearing capacity and knowing the number of tests used which is five (5) in our case because we used two (2) analytical formulations, two (2) CPT tests, and two (2) SPT tests, we can know the parameter ξ_3 = 1.5 and ξ_4 = 1.34 entering in the computation of the characteristic resistance. So the characteristic resistance is:

$R_{c,k}$ =	**1033.97 kN**

3.4.4 Design from the load tests

In this part, we will present the load-settlement relationship derives from the execution of three (3) compression load tests on three (3) pile tests and we will present the bearing capacity evaluated with Chin (1970) method. The location of the load test is present in the Figure 3.33

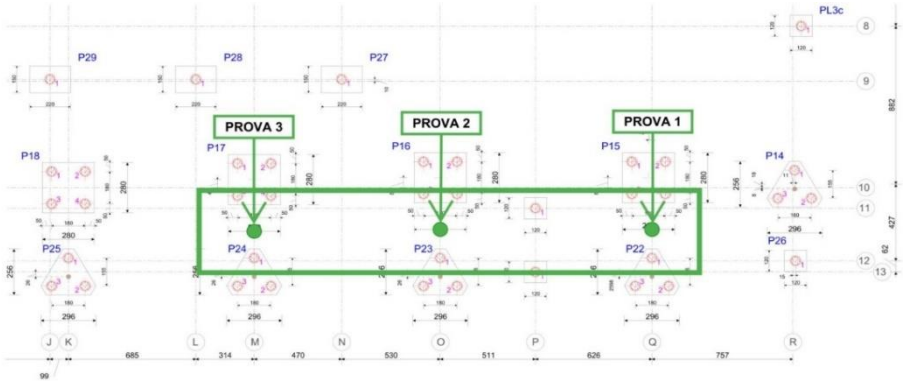

Figure 3.33. Test location (Rosa Marcello & al., 2020)

The results of the data elaboration on the FDP piles using the first and the second cycle of loading are presented in Figure 3.34, Figure 3.35 and Figure 3.36.

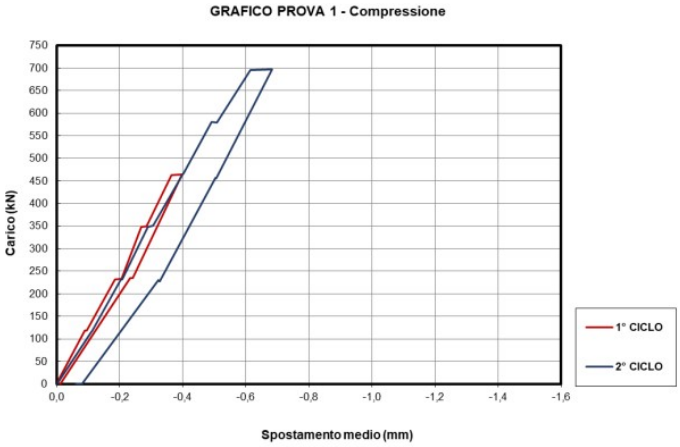

Figure 3.34. Average displacement of pile n°1 due to the exerted load (Rosa Marcello & al., 2020)

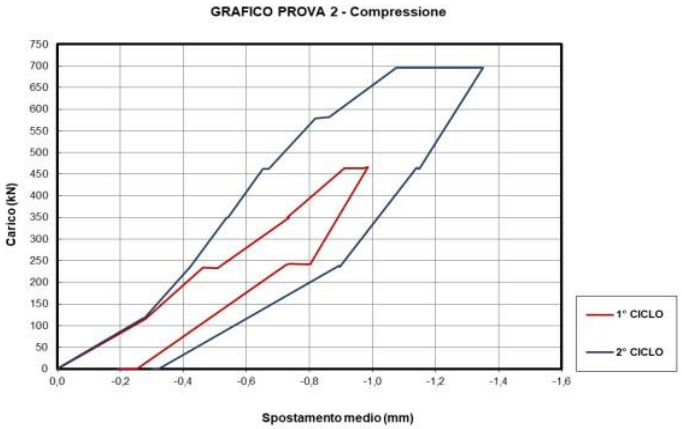

Figure 3.35. Average displacement of pile n°2 due to the exerted load (Rosa Marcello & al., 2020)

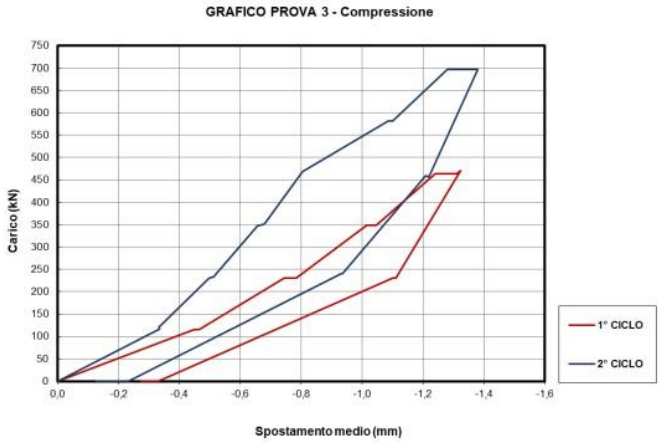

Figure 3.36. Average displacement of pile n°3 due to the exerted load (Rosa Marcello & al., 2020)

Generally, the load for evaluating the bearing capacity reach higher value (about thousands of kilonewtons), but these loads were not reached in this case. The maximum load did not even reach 1000 kN. We can say that the company did not want to risk damage to damage the piles that are included in the construction and are not prototype.

We applied the interpolation method to interpret, but we already know that those tests are proof load tests and are used more to check the effectiveness of the pile than to design them and the tests just study the first elastic response of the system.

We first started by using the last five loads of the loading phase with the corresponding settlements to plot the load settlement relation as showed in Figure 3.37 and Figure 3.38.

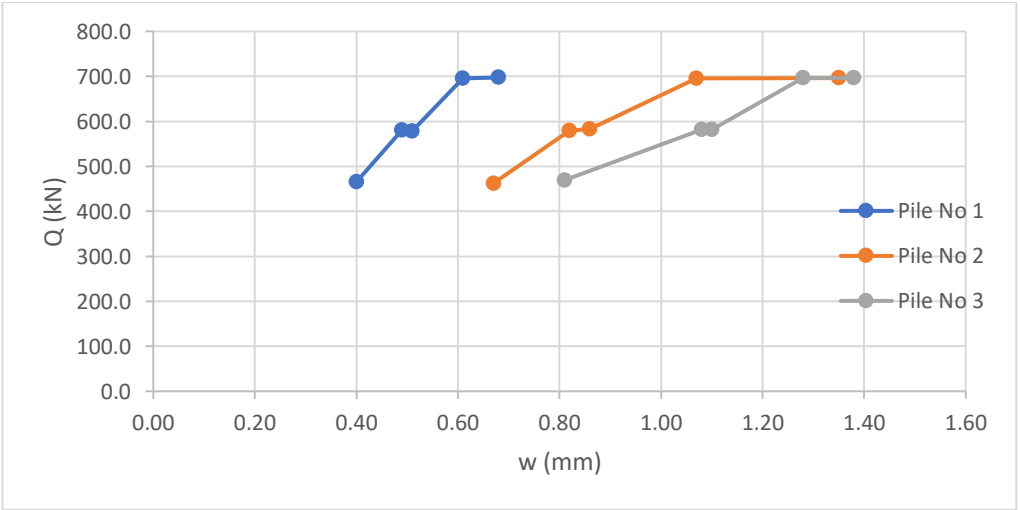

Figure 3.37. Load vs settlement curve for the three piles test

We interpolated the data in order to obtain the intercept on the vertical axis and the inclination over the horizontal (Table 3.36)

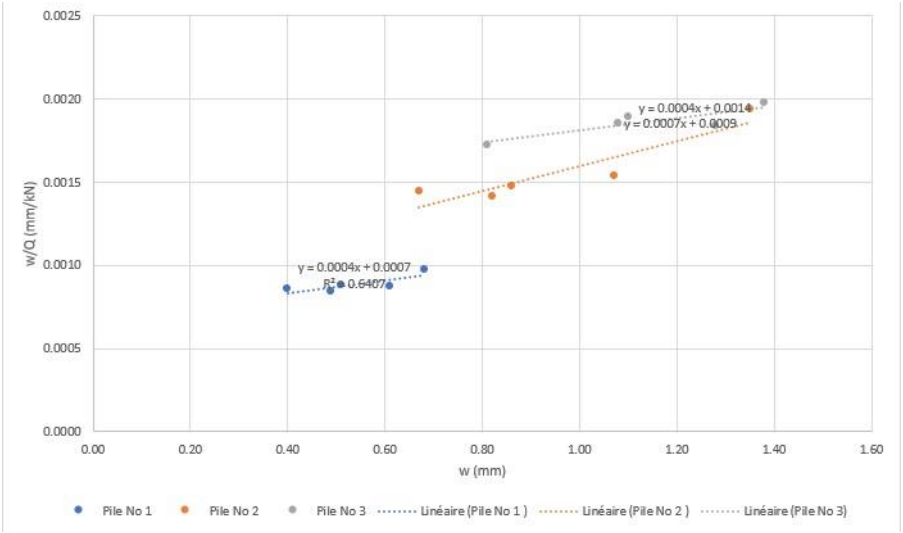

Figure 3.38. Settlement vs settlement/load plot from the 2nd cycle of load test

Table 3.36. Limit loads using hyperbolic method for each pile

Test	1	2	3	
m =	0.0007	0.0009	0.001	mm/kN
n =	0.0004	0.0007	0.0004	kN^{-1}
R^2 =	0.03	0.0378	0.7317	
Q_{lim} =	2250.00	1285.71	2250	kN

Since the number of tests is 3, according to NTC 2018, $\xi_1 = 1.2$ and $\xi_2 = 1.05$. With the results of the average and minimum limit loads we can compute the characteristic resistance as shown in Table 3.37.

Table 3.37. Characteristic value of the bearing capacity from load test

R_m1 =	2250.00	kN
R_m2 =	1285.71	kN
R_m3 =	2250	kN
$(R_m)_{media}$ =	1928.57	kN
$(R_m)_{min}$ =	1285.71	kN
$(R_m)_{media}/\xi_1$ =	1607.14	kN
$(R_m)_{min}/\xi_2$ =	1224.49	kN
$R_{c,k}$ =	1224.49	kN

The maximum load that was reached for our load test were around 700 kN which is lower compare to the values of the literature for a design test. The leads generally used for prototype piles used for designing a pile usually reach thousands of kilonewtons, so we cannot consider

as reliable the results given by this load tests for our design. In any case, these results are not so far from the previous ones, and can be considered the demonstration that the realized piles show bearing capacities coherent with those of design.

3.4.5 Design from the pile installation data

In this part we aim to use the drilling data obtained during the pile's execution to compute the bearing capacity of an FDP pile.

During the pile execution they can record, thanks to the Lutz system installed on the drilling machine, real time data that permit us to evaluate the penetration resistance of a FDP pile. The pile penetration resistance or alpha (α) value is a parameter which indicates the soil density. Consequently, the greater this parameter, the harder will it become to drill the soil. The main goal for the use of this parameter is to optimize the pile length due to the fact that, if during the drilling process a value greater than α is obtained, the reached depth will be enough for the desired loading capacity.

This parameter is directly related to the cone resistance obtained from the CPT test which in case of resistance increase, the α value will increase as well.

From the data recorded by the Lutz software, we computed the values of alpha (Table 3.38, Table 3.39 and Table 3.40) for the three pile tests and we plot those values through depth (Figure 3.39, Figure 3.40 and Figure 3.41).

Table 3.38. Extract of the alpha value for pile no 1 (Negropal, 2020)

pile no 1			
Depth	No lives	Couple	alpha
m	m / rad	kNm	
0	0	3	
0	0	5	
0	0	5	
0	0	5	
0	0	9.817	
0	0	9.817	
0	0	9.817	
0.024	0.0045	4.8333	170.943019
0.048	0.0238	24.5556	164.207778
0.069	0.0402	27	106.895111
0.09	0.0459	29.6667	102.867145
0.114	0.0515	33.2222	102.669463
0.134	0.0367	39	169.129231
0.155	0.0355	44.5556	199.753352
0.176	0.0225	51.5556	364.68127
0.196	0.0071	47.8333	

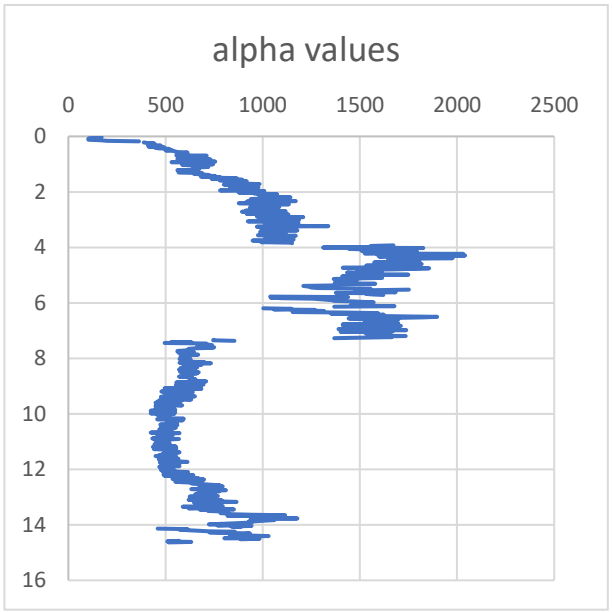

Figure 3.39. Alpha values from the drilling of pile n°1

From the figure above, we can see that from 0 to 4 m depth the alpha value is increasing so the soil is becoming more and more harder. From 4 to 7 m depth we record greater values of alpha so the soil is denser and that depth. From 7 up to 14.63 m we record lesser values of alpha so the soil is softer at that level.

Table 3.39. Extract of the alpha value for pile no 2 (Negropal, 2020)

pile no 2			
Depth	No lives	Couple	alpha
m	m / rad	kNm	
0	0	5	
0	0	5	
0	0	5	
0	0	5	
0	0	5	
0	0	5	
0	0	5	
0	0	4.9441	
0	0	4.9441	
0	0	4.9441	
0.02	0.0014	5	3571.42857
0.04	0.0459	14.4167	314.089325
0.06	0.0408	21.3846	524.132353
0.081	0.0684	23.4	342.105263
0.104	0.1022	30.875	302.103718
0.125	0.0895	35	391.061453
0.146	0.0631	40.375	639.857369
0.167	0.0484	47	971.07438

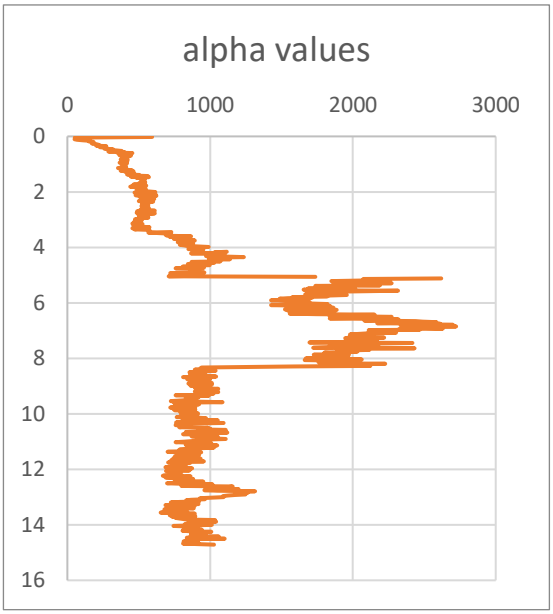

Figure 3.40. alpha values from the drilling of pile no 2

From the figure above, similarly to what observed in the firs pile, we can see that from 0 to 5 m depth, the penetration resistance is increasing so the soil is becoming harder. From 5 to 8.2 m depth the alpha values are higher the soil has more strength at those depths. From 8.2 to 14.71 m the soil has less strength but higher than the initial level.

Table 3.40. Extract of the alpha value for pile no 3 (Negropal, 2020)

pile no 3			
Depth	No lives	Couple	alpha
m	m / rad	kNm	
0	0	5	
0	0	5	
0	0	5	
0	0	5	
0	0	5	
0	0	5	
0	0	5	
0.02	0	5	
0.042	0.0286	13	454.545455
0.062	0.0329	33.75	1025.83587
0.082	0.0242	42.1	1739.66942
0.102	0.0028	42.0392	15014
0.122	0.0153	43.6364	2852.05229
0.143	0.0144	46.6667	3240.74306
0.163	0.0143	47.2727	3305.78322

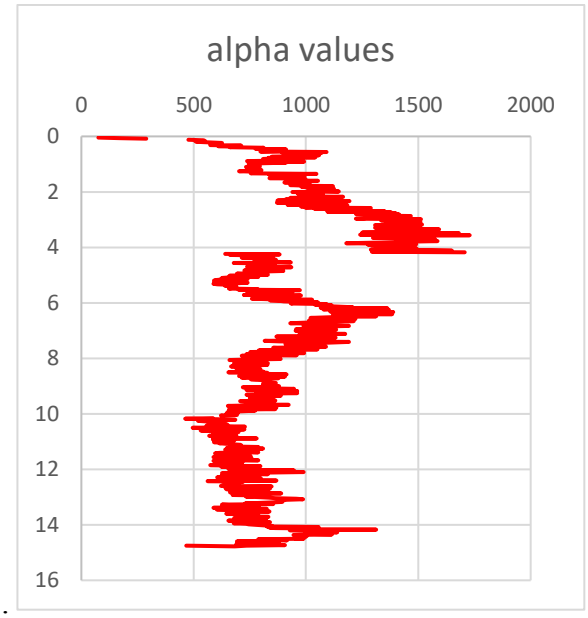

Figure 3.41. alpha values from the drilling of pile no 3

From the above we can say that from 0 to 4 m depth, the strength of the soil is increasing since the alpha values are increasing. From 4 to 5 m depth, the strength of the soil decreases. From 5 to 6.5 m the strength of the soil increases. From 6.5 to 14.78 m the strength of the soil decreases. This last result is slightly different form the first two, but confirm the heterogeneity of the layers of soil observed interpreting the various tests performed.

In order for us to end our analysis, we need to compare the penetration resistance for the three piles (presented in Figure 3.42) obtain using the drilling machine with the data given to us by the various CPT tests (Figure 3.43 and Figure 3.44), boreholes and SPT tests.

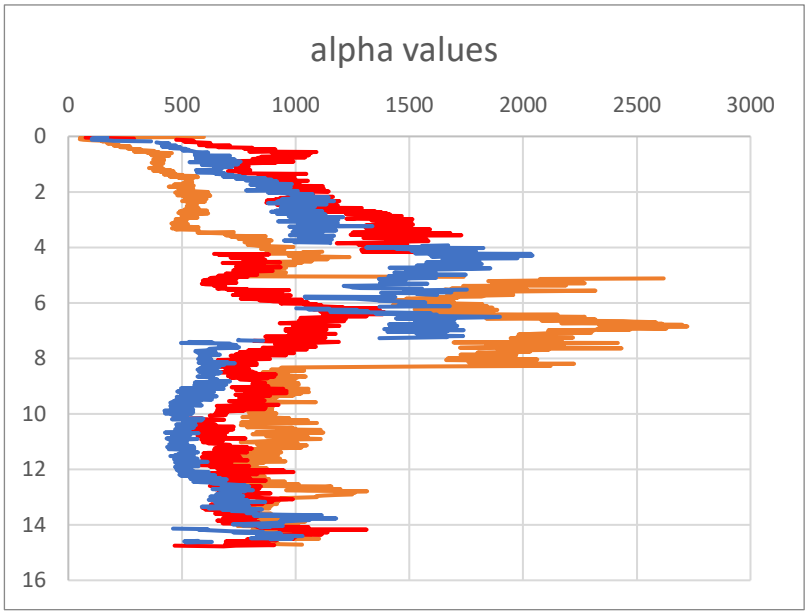

Figure 3.42. Penetration resistance of three FDP piles (in blue pile 1, in orange pile 2, in red pile 3)

Looking Figure 3.42, we can recognize some common parts of the alpha profile, and some other that show bigger differences. Anyway, the general trend of the three results may indicate details in accordance one another. In all the graphs, the first meter of depth shows a linear increase of alpha; after this, a second thin layer of softer material is evident until around 2 m of depth. From this point, for piles 1 and 2 a constant trend of 2 meters is evident, while pile 3 highlight an increase. Between 3 and 4 m, piles 2 and 3 suggest the presence of a harder layer. From 4 to 8 m of depth all the results suggest the presence of two different type of soil: pile 1 and 2 indicate the presence of a harder soil, with a thin layer positioned around 6-7 m of depth. Contrarily, pile 3 shows a softer material from 4 to 6 m, and a stronger until 8 m. After the position of 8 m, all the results show similar trend, indicating a homogeneous type of soil, with some heterogeneity around the tip of the piles. From a general point of view, the interpretation of the alpha trend is not so easy. Two piles underline similar trends, while the third shows some differences, probably due to the heterogeneity of the material present in that area. It has to be noted that also the traditional tests, such as CPT, SPT and core surveys indicated a not homogeneous stratigraphy of the area.

If now we try to compare these observations with the results of the traditional techniques, we can try to correlate the evidences noted with the reliable stratigraphy of the site, trying to determine if the alpha value can be used for evaluating the type of soils present, thus allowing in future to a bearing capacity calculation based on the pile installation itself.

From CPT C (Figure 3.43), the stratigraphy of the soil is composed of silty sand down to 1.0 m, of silty clay from 1.0 to 2.8 m, of silty sand from 2.8 to 4.2 m, of silty clay from 4.2 to 4.8 m, of silty sand from 4.8 to 6.2 m, of silty clay from 6.2 to 6.8 m, of silty sand from 6.8 to 7.2 m, then of medium sand down to 11.4 m.

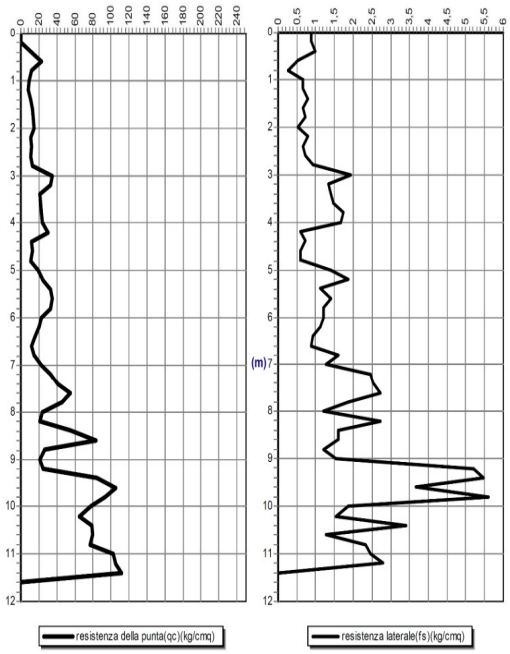

Figure 3.43. Tip and lateral resistance from CPT C (GEOLAMBDA Engineering S.r.l.,2018)

The resistance showed by CPT C can be considered similar to the trend of the alpha values, in the sense of the trend of alpha, more with respect to the value itself. The first 8 meters of soil indicate, looking the alpha values, an alternance of layer stronger and softer, of various type. This is coherent with the alternance individuated by the CPT C of silty sand and silty clay in that position. After the depth of 8 m, the CPT individuates a stronger material, defined as medium dense sand. Even if alpha is constant in that part of soil, individuating an almost homogeneous material, all the 3 piles show a reduction of alpha, underlying the difficulty of this parameter to catch that type of soil.

From CPT D (Figure 3.44) the stratigraphy of the soil is composed of silty sand down to 0.8 m, of silty clay from 0.8 to 3.2 m, of silty sand from 3.2 to 3.6 m, of silty clay from 3.6 to 4.4 m, of silty sand from 4.4 to 6.0 m, of silty clay from 6.0 to 6.6 m, of medium sand from 6.6 to 7.8 m, of silty sand from 7.8 to 9.4 m, then of medium sand from 9.4 to 10.2 m. The stratigraphy is coherent with the previous CPT, so the comments about the comparison between these results and alpha values are similar to the ones written above. In this CPT there is the presence of a silty sand layer that interrupts the medium sand layer that starts at 7 m of depth.

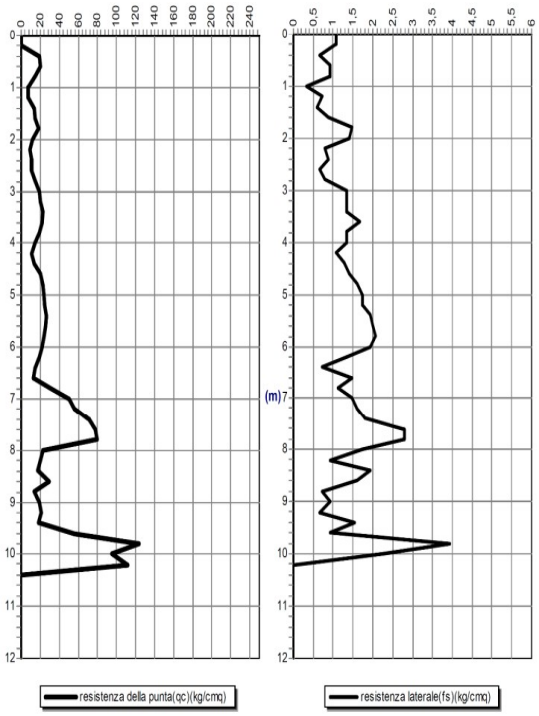

Figure 3.44. CPT D (GEOLAMBDA Engineering S.r.l.,2018)

If now we consider the survey S1, we remember that the stratigraphy of the soil is made up of sandy silt up to 0.5 m, of clayey silt from 0.5 to 4.5 m, of medium sand from 4.5 to 15 m, then of silty sand/sandy silt down to 20 m.

When we compare the stratigraphy from survey S1 with the alpha values of the piles, we can individuate the layer of sandy silt which is near the ground level as belonging to the two graphs. The other layer of medium sand does not correspond with the stratigraphy given by the alpha values.

From survey S4, the stratigraphy of the soil is composed of sandy silt up to 2.5 m, of clayey silt from 2.5 to 6.6 m, of silty sand/sandy silt from 6.6 to 10.3 m, of clayey silt from 10.3 to 11.2 m, then of silty sand/sandy silt from 11.2 to 15 m.

When we compare the stratigraphy from survey S4 with the alpha values we cannot find a correspondence between soil layers because layers from survey S4 are too large to correspond to the one from the alpha values.

Finally, looking the SPT S1, the stratigraphy of the soil is made up of fine to medium sand from 6.0 to 12.45 m, then of silty sand from 15.0 to 18.5 m.

When we compare the SPT S1 with the alpha value we can individuate the medium sand but between 6.0 m and 8.0 m above this we cannot have a medium sand layer which corresponds to the alpha values.

From SPT S4, the stratigraphy of the soil is made up of fine sand with silt from 9.0 to 9.5 m, then of fine silty sand from 12.0 to 15.45 m.

When comparing the alpha value with the stratigraphy of soil from SPT S4, we can say that the layer of sandy silt and the layer of fine silty sand can correspond with the stratigraphy given by the alpha value.

It has to be noted that the SPT results are less detailed respect to the CPT ones, thus the comparison between the alpha values and the SPT is considered less reliable. The comparison between the CPT and the alpha values shows some congruencies, especially in terms of individuation of the various layers. Less reliable is the correlation of alpha with the type of soil.

3.5 Conclusion

The goal of the chapter was to compare different methods aiming at designing a deep foundation. In order to do this, the case study that was chosen was located at the municipality of Lonigo. Before the dimensioning phase of work, we first of all collect information about the subsoil characteristics through geological, seismic and geotechnical study. After we have showed that an isolated footing was not appropriate for our building since the settlement induced by the load was not within tolerable limits according to the current legislation in the country (25-30 mm), we selected as deep foundations Full Displacement Piles the design of the piles was first done base on the traditional technics (analytical formulation, CPT, SPT) and based on load tests, we found that the results were not so far each from another and so the design give common sense. Then we computed the penetration resistance of the piles called alpha, which permit us to have an idea on the strength of the soil, and compare the behavior of the alpha with the results of the CPT, SPT and surveys, we found that with the CPT we can recognize some layers of soil like silty sand and silty clay, with SPT the comparison is less reliable since the SPT data are less detailed than the CPT one and also the correlation of alpha with the type of soil is less reliable.

General conclusion

Pile foundations are generally oversize due to the fact that in most cases, the geological and the geotechnical report are incomplete. Since it is possible to record, thanks to the 4.0 technology installed in the current drilling rigs, installation parameters in real time on drilling, the idea is to combine those parameters with the geological and geotechnical report in order to determine the effective capacity of each single pile during the construction phase.

The main objective of this work was to evaluate the bearing capacity of pile foundation of a commercial building just after the pile realization basing on the information on the installation parameters. In order to achieve the objective, a review on foundations was carried out along with the study of shallow foundations, deep foundations and the foundation design procedure. This was followed by the presentation of the research methodology used in order to conduct the study. Finally, following the methodology the results obtain from the methodology was presented and interpreted.

However, the methodology used in this study consisted of making a general site recognition, the presentation of the on-site investigations made, the geological, seismic and geotechnical study performed, the design procedure of an isolated footing and finally the methods used for the design of three Full Displacement Pile foundations which was based on traditional technics (analytical formulations, CPT, SPT), load tests and on information on the pile installation parameters. The design methods were implemented using the software MS EXCEL.

Two main parts constituted this research; the first part focused on the state of art on foundations. It consists on the presentation of shallow foundations and the method for their design, the presentation of deep foundations, their installation techniques and some design methods and we ended this part with the foundation design process. The second parts consist of the comparison between various design methods of a FDP pile among which analytical formulation, CPT, SPT, load test and basing on the pile installation data.

Concerning the different results obtained the conclusions (observations) derived from the study are:

- The substrate consists of the prevalence of poorly consolidated soils (silts and clays) with subordinate intercalations of sandy-gravelly and with poor to mediocre geotechnical characteristics.

- The investigated foundations show a very low / negligible risk in relation to potential liquefaction phenomena.
- The substrate of the planned structures consists of geotechnical units that have different characteristics and the underground water table was detected at 2 m depth from the ground level.
- The selected isolated footings were not satisfying serviceability limit states since values higher than the limits suggested by traditional geotechnics (25-30 mm) was deduced for actions corresponding to the ground resistances.
- The design of the Full Displacement Piles basing on the traditional technics is coherent since the value of the characteristic resistance obtain using analytical formulations, CPT and SPT was not far from the characteristic resistance obtain from the load tests.
- The penetration resistance (alpha values) obtained during the installation of the three Full Displacement Piles shows some similarities with the CPT in terms of individuations of various layers of soils like the layers of silty sand and silty clay.
- The alpha values and the SPT were less correspondents.
- The correlations between the alpha values and the type of soil obtain from the surveys was less reliable.

As perspectives we suggested for the future computations of the alpha values to take into account:

- The speed of rotation of the drilling tool.
- The downward thrust force of the drilling machine.
- The penetration depth at which is localize the drilling tool.

BIBLIOGRAPHY

Bauer Maschinen GmbH. (2013). *Full Displacement Pile System Process and Equipment*. Schrobenhausen. 16 p.

Brown & Co. (2007). *GEOTECHNICAL ENGINEERING CIRCULAR NO.8.Maryland*.

Dr. Braja Das & Dr. Nagaratman Sivakkugan. (2018). *Principles of Foundation Engineering*. United Kingdom: Taylor & Francis.

Dr. Eng. Lorenzo Brezzi. (n.d.). *BASIC FOUNDATION ENGINEERING*.

Eng. Rosa & Co. (2020). *LOAD TESTS ON FOUNDATION PILES. LONIGO (IV)*. 17 p.

GEOLAMBDA Engineering. (2018). *Project of a new commercial building in the Municipality of LONIGO (SP 500): GEOLOGICAL AND GEOTECHNICALREPORT. LONIGO*.

Leticia da Conceiçaio Melo Moniz. (2014). *Foundations and Soil Treatment using the Full Displacement Piles*. Lisbon, Portugal: Av. Rovisco Pais 1.

MUNI BUDHU. (2012). *SOIL MECHANICS AND FOUNDATIONS*. New York: Wayne Anderson.

NEGROPAL. (2020). *P.P.-1*. LONIGO.

NEGROPAL. (2020). *P.P.-2*. LONIGO.

NEGROPAL. (2020). *P.P.-3*. LONIGO.

NEGROPAL. (2021). *"Dynamic pile" Project for the construction of FDP (Full Displacement Pile) piles with dynamic sizing*. LONIGO.

Peter Faust. (2009). *Design and Construction of Drilled Full Displacement Piles using the Penetration Resistance Method*. Burlingame.

Prof. Carlo Viggiani & Co. (2012). *Piles and Pile Foundations*. London & New York: Taylor & Francis.

R.F. Craig. (2004). *Craig's Soil Mechanics*. New York: Taylor & Francis.

RODRIGO SALGADO. (2006). *The Engineering of Foundations*.

Cola S. (2021). Foundation course: "*Lesson on Eurocode*", "*Lesson on Vertical bearing capacity of piles*", "*Lesson on Load tests on piles*"

Park CB & Co. (2000). "*Optimum Field Parameters of an MASW Survey*"

Ministerial Decree of 17 January 2018, Update of the "*Technical standards for construction*", Ministry of infrastructure and Transport.

Ministerial Decree of 14 January 2008

Circular of 21 January 2019 n.7, Update of "*Technical standards for construction*", Ministry of infrastructure and Transport.

Programming Recommendations and execution of geotechnical surveys by the Italian Geotechnical Association (1977)

O.P.C.M. 3274 and subsequent amendments; Ministerial Decree of 17.01.2018

NTC2018

Skempton (1957). *Skempton's values of Nc*.

www.euroguide.org/soil-mechanics/influence-charts-for-vertical-stress-increments.html page consulted on 5th September 2022

www.nationalpilecroppers.com page consulted on the 4th April 2021

www.foundationblogspot.com page consulted on 24th April 2021

https://en.wikipedia.org/wiki/Vicenza page consulted on 10th September 2022

ANNEXES

ANNEXE 1 Images of the execution of the load tests

Illustration of test n.1

Test n.1- detail of jack and sensor positioning

Illustration of test n.2

Test n.2- detail of jack and sensor positioning

Illustration of test n.3

Test n.3- detail of jack and sensor positioning

ANNEXE 2 Images of some penetrometer tests

Static penetrometer test CPT A

Static penetrometer test CPT B